Summary Report

Development of the Large Lake Statistical Water Balance Model for Constructing a New Historical Record of the Great Lakes Water Balance

Submitted to:

The International Watersheds Initiative

of the

International Joint Commission

Submitted by:

NOAA Great Lakes Environmental Research Laboratory

and

University of Michigan

Cooperative Institute for Great Lakes Research

Lead authors:

Joeseph Smith (CIGLR)

Andrew Gronewold (NOAA-GLERL)

SEPTEMBER 2018

Contact: drew.gronewold@noaa.gov or joeseph@umich.edu

Contents

Executive Summary 3
1 – Introduction 4
2 – Water balance model 5
2.1 – Channel flows and diversions 8
3 – Data and the Bayesian network 9
3.1 – Data 9
3.2 – Bayesian network 10
3.2.1 – Prior distributions 10
3.2.2 – Likelihood functions 11
4 – Inference software 12
5 – Results 12
5.1 – Water balance closure assessment 13
5.2 – Intercomparison of L2SWBM configurations 14
5.3 – Verification of channel flow estimates 14
5.4 – Comparison of residual and component net basin supplies 15
6. Acknowledgments 15
References 15
Appendix 17
A. Stakeholder input 17
B. Implications of uncertainty in coordinated channel flows and diversions 21
B.1: Ogoki, Long Lac Diversion into Lake Superior 21
B.2: St. Marys River 22
B.3: Chicago Diversion 22
B.4: St. Clair River 23
B.5: Detroit River 23
B.6: Niagara River and Welland Canal 24
B.7: St. Lawrence River 26
C. Water balance component prior distributions 27
D. Graphical summary of new historical record 34

Executive Summary

This report describes the development of a new historical record of water balance components (over-lake precipitation, over-lake evaporation, lateral tributary runoff, channel flows, diversions, and changes in storage) for each of the Laurentian Great Lakes — Superior, Michigan-Huron, Erie, and Ontario, as well as St. Clair — from 1950 through 2015. To produce this new historical record, we programmed a water balance model into a Bayesian Network. Data for populating the network (via prior distributions and likelihood functions) were derived from water balance estimates developed separately from this project. Importantly, those independent estimates do not include a representation of uncertainty nor do they close the water balance for any of the Great Lakes; our approach directly reconciles both of these shortcomings.

This work supports the International St. Lawrence River Board of Control, the International Lake Superior Board of Control, and the International Niagara Board of Control (Great Lakes Boards of Control) in coordination with the Great Lakes — St. Lawrence River Adaptive Management Committee (GLAM). L2SWBM code and model-generated data are available on the following National Oceanic and Atmospheric Administration Great Lakes Environmental Research Laboratory (NOAA-GLERL) webpage:

https://www.glerl.noaa.gov/data/WaterBalanceModel/

1 – Introduction

Figure 1: The Laurentian Great Lakes and their basin (light brown region) including location of major cities, interbasin diversions, and connecting channels.

This report describes the development of a new historical record of monthly water balance components (lateral tributary runoff, over-lake evaporation, over-lake precipitation, connecting channel flows, diversions, and changes in storage) for each of the Laurentian Great Lakes — Superior, Michigan-Huron, Erie, and Ontario — as well as St. Clair (figure 1) from 1950 through 2015. We developed this new record using the Large Lake Statistical Water Balance Model (L2SWBM). The L2SWBM is a Bayesian Network that, through an explicit acknowledgment of bias and uncertainty, reconciles discrepancies between model- and measurement-based estimates of each component, while closing the Great Lakes water balance. Through a partnership between the National Oceanic and Atmospheric Administration's Great Lakes Environmental Research Laboratory (NOAA GLERL) and the University of Michigan's Cooperative Institute for Great Lakes Research (CIGLR), we developed a prototype L2SWBM for Lakes Superior and Michigan-Huron for the period of 2005 through 2014 (Gronewold et al. 2016) prior to this study to explain the record 2-year rise in water levels across both lakes between 2013 and 2014. The current study, therefore, focused on expanding the L2SWBM to all of the Great Lakes in addition to generating a longer historical record.

We envision the new historical record and the L2SWBM supporting the responsibilities of the International St. Lawrence River Board of Control, International Lake Superior Board of

Control and International Niagara Board of Control (Great Lakes Boards of Control) as prescribed by the Great Lakes — St. Lawrence River Adaptive Management Committee (GLAM). The GLAM directive from the International Joint Commission (IJC) identifies the need to monitor historical changes in the Great Lakes hydrologic system, and how those changes, if any, should be reflected in future regulation plans. We expect the newly-developed water balance estimates to provide a much more robust basis, relative to previous estimates, for decision making, not only because they include an expression of uncertainty but also because they provide a full explanation for changes in water levels across multiple time horizons.

We organized this report into five sections. We describe the core water balance model in section 2. In section 3 we present the data and L2SWBM structures we used to inform and draw inferences. Section 4 provides a summary of the software we used to perform inference of water balance components and generate a new historical record. We present results in section 5. We supply an appendix which includes plots of the new historical record for all of the Great Lakes as well as additional supporting information.

2 – Water balance model

With the L2SWBM, our goal was to produce new estimates of water balance components that express uncertainty, reconcile biases of multiple independent component estimates, and close the water balance over multiple time periods for all of the Great Lakes. While the prototype version of the L2SWBM achieved these goals for Lakes Superior and Michigan-Huron, its formulation led to an excessive computational expense, especially given the prototype's limited spatial and temporal domain. To reduce the number of required computations, we revised the L2SWBM to compute the water balance of each lake over fixed-length rolling windows (for more details, see Smith and Gronewold, 2018). Below, we describe revisions to the water balance model that make it more practical for all of the Great Lakes, and for developing a historical record from 1950 through 2015 of monthly water balance component estimates.

For all of the Great Lakes (and Lake St. Clair) we analyzed the water balance through rolling windows of length w (in months). We defined the changes in water elevation ($\Delta H_{l,j,w}$) for each lake l and over each rolling window as the difference between the lakewide-average surface water elevation at the beginning of month $j \epsilon [1, T - w + 1]$ and the lakewide-average surface water elevation at the beginning of month $j + w$. We note that, when referencing model components outside of the rolling window context, we index each month with the subscript $\epsilon [1, T]$, where $T = 792$, the total number of months in our analysis.

For Lakes Superior, Michigan-Huron, Erie, and Ontario, monthly-total water balance components are linked to changes in water elevation over w months (in millimeters) for each lake via a single-bucket WBM:

$$\Delta H_{l,j,w} = H_{l,j+w} - H_{l,j} = \sum_{i=j}^{j+w-1} \left(P_{l,i} - E_{l,i} + R_{l,i} + I_{l,i} - Q_{l,i} + D_{l,i} + \varepsilon_{l,i}\right) \quad (1)$$

where (all in mm over each lake surface area) P is over-lake precipitation, E is over-lake evaporation, R is lateral tributary runoff into the lake, I is inflow from an upstream connecting channel, Q is outflow into a downstream connecting channel through the lake's outlet (head of connecting channel), D represents diversions of water into or (expressed as a negative value) out of the lake basin, and ε is a process error term accounting for thermal expansion, glacial isostatic rebound, groundwater fluxes, and other sources of variability in monthly water levels not explained by water balance components $P, E, R, I, Q,$ or D alone. Additional details of our approach to modelling $I, Q,$ and D are in section 2.1.

We then related observations of water elevation (or level) change $y_{l,\Delta H,j,w}$ to the true, but unobserved water level change $\Delta H_{l,j,w}$ via likelihood functions in the Bayesian network:

$$y_{l,H,j+w} - y_{l,H,j} = y_{l,\Delta H,j,w} \sim \mathrm{N}(\Delta H_{l,j,w}, \tau_{l,\Delta H,w})$$

where the precision of water level measurements on a given lake and for a given rolling window $\tau_{l,\Delta H,w}$ is given a vague $Gamma(0.01,0.01)$ prior. Precision is an alternative expression of variance (σ^2) employed in the modeling framework such that $\tau = 1/\sigma^2$.

Our model for Lake St. Clair (STC) is slightly different because its surface area is small relative to the other Great Lakes and because there is significant uncertainty in historical estimates of its water balance. First, we modeled Lake St. Clair's water balance in units of m^3/s because its water balance is dominated by channel inflows and outflows, both of which are typically modeled in units of m^3/s. Second, rather than inferring estimates of Lake St. Clair precipitation, evaporation, and runoff individually, we inferred the Net Basin Supply (*NBS' = P' – E' + R',* where the 'prime' notation indicates that a variable is in m^3/s, rather than in mm). We therefore modeled the water balance for Lake St. Clair using the following equations:

$$y_{STC,H,t+1} - y_{STC,H,t} = y_{STC,\Delta H,t}$$

$$y'_{STC,\Delta H,t} = \frac{y_{STC,\Delta H,t} * A_{STC}}{86400 * d_t * 1000}$$

$$y'_{STC,\Delta H,j,w} = \sum_{i=j}^{j+w-1} y'_{STC,\Delta H,i}$$

$$y'_{STC,\Delta H,j,w} \sim \mathrm{N}(\Delta H'_{STC,j,w}, \tau'_{STC,\Delta H,w})$$

$$\Delta H'_{STC,j,w} = \sum_{i=j}^{j+w-1} \left(NBS'_{STC,i} + I'_{STC,i} - Q'_{STC,i} + \varepsilon'_{STC,i}\right) \quad (2)$$

where 86400 is the number of seconds in a day, d_t is the number of days in month t, and A_{STC} is the Lake St. Clair's surface area (in meters), derived from NOAA GLERL's 1-km digital maps

(table 3, Schwab and Sellers, 1996). We model $\tau_{STC,\Delta H,w}$ with a vague Ga(0.01,0.01) prior, following the same procedure we used for the other lakes.

In our expression for uncertainty in the overall water balance (equations 1 and 2), we model ε in two different ways. The first model for ε is:

$$\varepsilon_{l,t} = 0$$
$$\varepsilon'_{STC,t} = 0$$

in which all uncertainty in the water balance (for each month *t* in the historical record) is distributed in water balance component uncertainty and observation error. The second model is:

$$\varepsilon_{l,t} = \varepsilon_{l,c(t)}$$
$$\varepsilon'_{STC,t} = \varepsilon'_{STC,c(t)}$$

which prescribes unique process errors for each calendar month (c(t)) with vague, zero-mean, normal priors:

$$\pi(\varepsilon_{l,c(t)}) \sim \mathrm{N}(\mu = 0, \tau = 0.01) \quad (3)$$
$$\pi\left(\varepsilon'_{STC,c(t)}\right) \sim \mathrm{N}(\mu = 0, \tau = 0.053) \quad (4)$$

where precisions for Lakes Superior, Michigan-Huron, Erie, and Ontario (equation 3), and for Lake St. Clair (equation 4) are equivalent to a standard deviation of 10 mm. We discuss the role of prior probability distributions in a Bayesian model in section 3.2.

To better understand the relative benefits and implications of different model configurations, we conducted a model intercomparison experiment. Each experimental configuration had a different combination of length of rolling window windows ($w = 6$ or $w = 12$), and formulation of process error (table 1). We assessed each configuration by how well it closed the water balance for all lakes, and how inferred water balance components compared between models (details in section 5).

Table 1: Summary of the four L2SWBM configurations we tested, each utilizing one of two different rolling windows (columns), and one of two different process error structures. Configuration labels identify the rolling window length (6 or 12), and whether process errors are equal to zero ('N'one) or 'F'ixed by calendar month.

	$\boldsymbol{w = 6}$	$\boldsymbol{w = 12}$
$\boldsymbol{\varepsilon_{l,t} = \varepsilon'_{l,t} = 0}$	6N	12N
$\boldsymbol{\varepsilon_{l,t} = \varepsilon_{l,c(t)}, \varepsilon'_{l,t} = \varepsilon'_{l,c(t)}}$	6F	12F

2.1 – Channel flows and diversions

To ensure we obtained a single estimate of flow for each connecting channel, we replace parameter I in the water balance model of each lake (equations 1 and 2) with parameter Q from the immediate upstream lake. For example (table 2), the flow through the St. Marys River is represented as Q_{SUP} in the water balance models for both Lake Superior (as a negative contribution) and Michigan-Huron (as a positive contribution). Similarly, to ensure we obtained a single estimate of flow through the Welland Canal, we replaced D_{ONT} with $-D_{ERI}$ in the water balance model for Lake Ontario. In Appendix B, we document additional details of coordinated channel flow and diversion estimates.

Table 2: Association between variables I, Q, and D and channels, rivers, and diversions, for each lake model. Each row represents a lake model, and each column indicates how variables I, Q, and D are identified in that model.

Lake	***I***	***Q***	***D***
Superior (SUP)	None	St. Marys River	Ogoki-Long Lac (+)
Michigan-Huron (MHU)	St. Marys River	St. Clair River	Chicago (-)
St. Clair (STC)	St. Clair River	Detroit River	None
Erie (ERI)	Detroit River	Niagara River	Welland Canal (-)
Ontario (ONT)	Niagara River	St. Lawrence River	Welland Canal (+)

In addition, because connecting channel flows and diversions (which we hereafter represent as the set $\zeta \epsilon [Q, D]$) are measured and modelled in units of m^3/s (see section 3), we convert their values from units of m^3/s ($\zeta' \epsilon [Q', D']$) to mm over the respective lake surface in equation 1 such that:

$$\zeta = \frac{\zeta'}{A_l} (1000*86400*d_t)$$

where A_l is the respective lake's surface area, derived from NOAA GLERL's 1-km digital maps (table 3, Schwab and Sellers, 1996).

Table 3: Surface areas of each lake in the analysis as derived from NOAA GLERL's 1-kilometer resolution digital maps. For perspective, we provide average flow in a 30-day month required to change the respective lake's water level by 1 mm, given its surface area.

Lake	Surface Area (m^2)	Average flow in 30-day month (m^3/s) required for 1 mm of level change
Superior	8.1925×10^{10}	31.61
Michigan-Huron	1.1685×10^{11}	45.08
St. Clair	1.1090×10^{9}	0.43
Erie	2.5404×10^{10}	9.80
Ontario	1.9121×10^{10}	7.38

3 – Data and the Bayesian network

3.1 – Data

Table 4: Summary of data sets used to develop water balance component prior probability distributions and as a basis for likelihood functions.

Variable	Data source description	Year range	Units
$y_{l,\Delta H,t,w}$	CCGLBHHD	1950-2015	mm
$y_{l,P,1,t}$	GLM-HMD (Thiessen Weighting)	1950-2015	mm
$y_{l,P,2,t}$	USACE AHPS	1950-2015	mm
$y_{l,P,3,t}$	ECCC-CaPA	2006-2015	mm
$y_{l,P,4,t}$	Historical Coordinated	1950-2015	mm
$y_{l,P,5,t}$	GEM-MESH w/CaPA (*Prototype*)	June 2004-2014	mm
$y_{l,E,1,t}$	GLM-HMD (LLTM)	1950-2015	mm
$y_{l,E,2,t}$	USACE AHPS	1950-2015	mm
$y_{l,E,3,t}$	GEM-MESH (*Prototype*)	June 2004-2014	mm
$y_{l,R,1,t}$	GLM-HMD (ARM)	1950-2015	mm
$y_{l,R,2,t}$	USACE AHPS	1950-2015	mm
$y_{l,R,3,t}$	GEM-MESH (*Prototype*)	June 2004-2009	mm
$y'_{l,Q,1,t}$	CCGLBHHD	1950-2015	m^3/s
$y'_{l,Q,2,t}$	IGS	Oct. 2008-2015	m^3/s
$y'_{l,D,1,t}$	CCGLBHHD	1950-2015	m^3/s
$y'_{STC,NBS,1,t}$	GLM-HMD	1950-2015	m^3/s
$y'_{STC,NBS,2,t}$	USACE AHPS	1950-2015	m^3/s
$y'_{STC,NBS,3,t}$	CaPA, GEM-MESH (*Prototype*)	June 2004-2012	m^3/s
$y'_{STC,NBS,4,t}$	CCGLBHHD	1950-2015	m^3/s

To estimate parameters for water balance component prior probability distributions and likelihood functions in the L2SWBM, we aggregated data from a variety of sources (table 4), including NOAA-GLERL's Great Lakes Monthly Hydrometeorological Database (GLM-HMD, Hunter et al. 2015), the United States Army Corps of Engineers (USACE) – Detroit District's implementation of NOAA-GLERL's Advanced Hydrologic Prediction System (AHPS, Gronewold et al. 2011), as well as legacy data sets of lakewide average water levels, channel flows, diversions, and residual NBS for Lake St. Clair ($y'_{STC,NBS,4,t} = y'_{STC,\Delta H,t} - y'_{MHU,Q,1,t} + y'_{STC,Q,1,t}$) from the Coordinating Committee on Great Lakes Basic Hydraulic and Hydrologic Data (CCGLBHHD, 1977; hereafter referred to as the Coordinating Committee). Datasets developed by the Coordinating Committee are referred to as "coordinated" through the rest of this report. We also include newer data sets either developed by Environment and Climate Change Canada (ECCC) — the Global Environmental Multiscale (GEM), Modélisation Environmentale–Surface et Hydrologie (MESH), and Canadian Precipitation Analysis (CaPA) regional model output (Deacu et al. 2012, Lespinas et al. 2015) — or (e.g. for connecting channel flows) adapted from gauging stations maintained through a binational partnership

between the United States and Canada (international gauging stations, or IGS). Data sets with '*Prototype*' in their description were employed in the prototype L2SWBM (Gronewold 2016).

3.2 – Bayesian network

We produce new estimates of Great Lakes water balance components using a Bayesian network, a type of statistical model that links parameters, and updates them using a process known as Bayesian inference. Bayesian inference is based on formulating a posterior distribution for each model parameter that is proportional to the product of a prior probability distribution and a likelihood function. The posterior distributions then serve as our new water balance component estimates.

We used the sampling program JAGS (Just Another Gibbs Sampler, Plummer et al., 2003), discussed in section 4, to compute and sample from the posterior distributions using Markov chain Monte Carlo (MCMC) methods. We describe our development of priors and likelihoods in the subsections below. For more on Bayesian analysis and MCMC, see Bishop 2011 and Gelman et al. 2013.

3.2.1 – Prior distributions

We develop a distinct prior probability distribution, or simply a prior ($\pi(\theta_{l,t})$, $\pi(\zeta'_{l,t})$), for each water balance component ($\theta \epsilon [P, E, R]$, $\zeta' \epsilon [Q', D']$) and each month of the year — 12 per component and per lake — to capture any seasonality. These prior distributions describe the range of quantities we expect for water balance components in a given calendar month. Prior probability density functions were fit to historical (1950-2015) water balance data from the NOAA-GLERL GLM-HMD for P, E, and R, and the CCGLBHHD for Q' and D' (due to their longer records and overall consistent methodology). The following distributions were fitted:

$$\pi(P_{l,t}) \sim \mathrm{Ga}(\psi_{1,l,c(t)}, \psi_{2,l,c(t)}) \quad (5)$$

$$\pi(E_{l,t}) \sim \mathrm{N}(\hat{\mu}_{l,E,c(t)}, 0.5\hat{\tau}_{l,E,c(t)}) \quad (6)$$

$$\pi(R_{l,t}) \sim \mathrm{LN}(\hat{\mu}_{l,\ln(R),c(t)}, \hat{\tau}_{l,\ln(R),c(t)}) \quad (7)$$

$$\pi(Q'_{l,t}) \sim \mathrm{N}(\hat{\mu}'_{l,Q,c(t)}, 0.5\hat{\tau}_{l,Q',c(t)}) \quad (8)$$

$$\pi(D'_{l,t}) \sim \mathrm{N}(\hat{\mu}'_{l,D,c(t)}, \hat{\tau}_{l,D',c(t)}) \quad (9)$$

where for equations 6, 8, and 9, $\hat{\mu}_{l,*,c(t)}$ is the calendar month mean for the respective parameter and $\hat{\tau}_{l,*,c(t)}$ is the calendar month precision of historical estimates for the respective parameter. As variation in the historical data is fairly small for E and Q', we allowed room for climate change and physical changes to connecting channels within the analysis by halving the calculated prior precisions ($\hat{\tau}_{l,E,c(t)}$ and $\hat{\tau}_{l,Q',c(t)}$). To develop the parameters for equation 7, we took the natural logarithms of the historical data and calculated the resulting means ($\hat{\mu}_{l,\ln(R),c(t)}$) and precisions ($\hat{\tau}_{l,\ln(R),c(t)}$).

Lastly, for equation 5, following Thom (1958) and Husak et al. (2007), we calculated maximum likelihood estimates of shape ($\psi_{1,l,c(t)}$) and rate ($\psi_{2,l,c(t)}$) parameters as:

$$\psi_{1,l,c(t)} = \frac{1}{4\phi_{l,c(t)}}\left(1 + \sqrt{1 + \frac{4\phi_{l,c(t)}}{3}}\right) \quad (10)$$

$$\phi_{l,c(t)} = \ln\left(\hat{\mu}_{l,P,c(t)}\right) - \hat{\mu}_{l,\ln(P),c(t)}$$

$$\psi_{2,l,c(t)} = \psi_{1,l,c(t)}/\hat{\mu}_{l,P,c(t)} \quad (11)$$

where $\hat{\mu}_{l,P,c(t)}$ and $\hat{\mu}_{l,\ln(P),c(t)}$ are the means of the historical precipitation observations for a given calendar month and natural logarithms thereof, respectively.

Graphical summaries of prior distributions are provided in Appendix C.

3.2.2 – Likelihood functions

For each component of the water balance, we linked true, but unobserved monthly values $\theta_{l,t}$ and $\zeta'_{l,t}$ to monthly observations $y_{l,\theta,n,t}$ and $y'_{l,\zeta,n,t}$ from source n for lake l with the following likelihood functions:

$$y_{l,\theta,n,t} \sim \mathrm{N}(\theta_{l,t} + \eta_{l,\theta,n,c(t)}, \tau_{l,\theta,n}) \quad (12)$$

$$y'_{l,\zeta,n,t} \sim \mathrm{N}(\zeta'_{l,t} + \eta'_{l,\zeta,n,c(t)}, \tau_{l,\zeta',n}) \quad (13)$$

where η represents the mean bias of each data source, for each water balance component, for each of the 12 months of the year. We define a vague $\mathrm{Ga}(0.1, 0.1)$ prior for likelihood precisions $\tau_{l,\theta,n}$ and $\tau_{l,\zeta',n}$. While called likelihood functions, these distributions additionally act as a reference to specific calendar months' water balances, in contrast to priors, which reference the historical record. Bias terms for precipitation, evaporation, and runoff from all data sources are given vague, zero-mean, normal priors:

$$\pi(\eta_{l,\theta,n,c(t)}) \sim \mathrm{N}(0, 0.01) \quad (14)$$

where the precision 0.01 equates to a standard deviation of 10 mm.

Bias terms for channel flows and diversions, are given prior means of zero, while the precisions are informed from a combination of a previous uncertainty analysis on Lake Erie's water balance (Bruxer 2010) and informally acquired expert opinion:

$$\pi(\eta'_{l,\zeta,n,c(t)}) \sim \mathrm{N}(0, \tau_{l,\zeta',n,c(t)}) \quad (15)$$

Each $\tau_{l,\zeta',n,c(t)}$ is derived from a percentage (measure of uncertainty) of the seasonal average flow (λ, table 5) derived from historical data ($\hat{\mu}'_{l,\zeta,c(t)}$):

$$\tau_{l,\zeta',n,c(t)} = 1/\left(\hat{\sigma}'_{l,\zeta,c(t)}\right)^2, \hat{\sigma}'_{l,\zeta,c(t)} = \lambda\, x\, \hat{\mu}'_{l,\zeta,c(t)} \quad (16)$$

Table 5: λ for equation 17 by lake and channel flow or diversion

Lake, Channel Flow or Diversion	$\boldsymbol{\lambda}$
Superior Outflow	0.02
Superior Diversion	0.04
Michigan-Huron Outflow	0.03
Michigan-Huron Diversion	0.04
St. Clair Outflow	0.03
Erie Outflow	0.02
Erie Diversion	0.04
Ontario Outflow	0.02

With respect to St. Clair NBS estimates, the prior precisions for their biases are equivalent to the prior precision for process error (equation 4):

$$\pi(\eta'_{STC,NBS,n,c(t)}) \sim \mathrm{N}(0, 0.053) \quad (17)$$

4 – Inference software

We use MCMC methods to simulate the Bayesian Networks and obtain inferences for parameter values from their posterior distributions with JAGS, and the 'rjags' package in the R statistical software environment (R Core Team, 2013). We run JAGS for each model alternative, generating 1,000,000 samples across three, parallel MCMC chains, and thin the last 500,000 samples of each chain (omitting the first 500,000 iterations as a burn-in period) at even intervals such that the resulting 'thinned' chains each have 1,000 values. The resulting 3,000 MCMC samples for each parameter then serve as the basis for our inferences and overall performance assessment. Our models require 1-2 weeks computer time to complete sampling. In previous research, we found that a 2-lake model run over a 10-year period converged after 250,000 iterations. In this study, we found that while it was difficult to assess convergence given the complexity of a 5-lake model extending back to 1950, the uncertainty in model parameter estimates was consistent across the different model configurations and across results from previous versions of the model (see section 5.2).

5 – Results

A graphical summary of all newly-derived water balance component estimates from selected model 12F (along with a comparison to historical observations) is included in Appendix D. Corresponding data sets (in spreadsheets) are available via the project web-site at

https://www.glerl.noaa.gov/data/WaterBalanceModel/. In the following subsections, we present four representative analyses of those results that cater specifically to stakeholder interests.

5.1 – Water balance closure assessment

To be of practical use in water resource management decisions, L2SWBM-derived water balance component estimates should "close" the water balance across a range of different time periods. In other words, the sum of inferred precipitation, evaporation, runoff, incoming and outgoing channel flows, and diversions (including associated expressions of uncertainty) should include the observed change in storage. We therefore assessed water balance closure by simulating the posterior predictive distribution of measured changes in lake storage across all 1, 12 (1-year), and 60-month (5-year) periods from 1950 through 2015, and then calculating the frequency with which corresponding observed changes in lake storage fell within those 95% posterior predictive intervals (tables 6 to 8).

Table 6: 1-month water balance closure rates for the experimental L2SWBMs.

Lake	**06N**	**06F**	**12N**	**12F**
Superior	97	99	90	96
Michigan-Huron	96	98	73	83
St. Clair	67	88	92	75
Erie	75	85	93	97
Ontario	81	67	59	92

Table 7: 12-month (1-year) water balance closure rates for the experimental L2SWBMs.

Lake	**06N**	**06F**	**12N**	**12F**
Superior	98	99	99	99
Michigan-Huron	98	98	99	99
St. Clair	100	100	100	100
Erie	100	100	100	100
Ontario	100	100	100	100

Table 8: 60-month (5-year) water balance closure rates for the experimental L2SWBMs.

Lake	**06N**	**06F**	**12N**	**12F**
Superior	99	99	97	97
Michigan-Huron	95	97	98	98
St. Clair	100	100	100	100
Erie	100	100	98	99
Ontario	100	100	100	100

5.2 – Intercomparison of L2SWBM configurations

Table 9: Inferred cumulative (over 792-months) median value of water balance components (in meters, except for St. Clair NBS, which is in thousands of cubic meters per second) for our four L2SWBMs.

Lake	θ, ζ	Cumulative median			
		6N	6F	12N	12F
Superior (m)	P	49.49	50.58	49.92	50.64
	E	36.91	36.33	37.01	36.31
	R	38.20	38.5	37.99	38.39
	Q	54.57	54.95	54.73	54.97
	D	3.93	3.94	3.93	3.93
Michigan-Huron (m)	P	51.24	54.28	51.86	54.35
	E	38.39	35.15	37.40	35.08
	R	46.72	47.46	45.38	47.29
	Q	95.73	95.32	95.86	95.08
	D	1.62	1.62	1.62	1.62
Erie (m)	P	58.19	58.32	58.18	58.39
	E	58.05	57.74	57.78	57.63
	R	56.95	56.21	56.06	56.36
	I	453.06	451.22	453.62	450.03
	Q	490.26	490.79	491.24	490.95
	D	18.35	18.37	18.37	18.37
Ontario (m)	P	57.82	57.85	57.85	58.11
	E	43.95	43.78	44.13	44.12
	R	111.72	111.42	110.69	111.81
	Q	801.00	797.62	801.71	799.18
St. Clair (m^3/1000/s)	NBS	123.67	123.54	123.74	123.68

We compared the cumulative median of each inferred water balance component for the four intermediate models across the 792-month analysis period (table 9). Differences between models are negligible.

5.3 – Verification of channel flow estimates

Due to our unique approach to modeling channel flow estimates, we present here a cursory analysis of our new estimates derived from the L2SWBM. We found that 95% credible intervals for our inferred channel flow estimates (from all four model configurations) were consistent with 95% confidence intervals for corresponding coordinated estimates ($y'_{l,Q,n,t}$). We calculated 95% confidence intervals for coordinating estimates as the mean coordinated value plus or minus $2\hat{\sigma}'_{l,\zeta,c(t)}$ (from equation 16). However, we did observe some differences in central tendency between the two sets of estimates; the most significant were for Niagara and St. Lawrence River flows.

5.4 – Comparison of residual and component net basin supplies

We compared median cumulative sums of component and residual net basin supplies for all lakes using estimates from L2SWBM 12F, where component NBS is the sum of precipitation, evaporation, and runoff, while residual NBS is the approximation of component NBS by calculating the net amount of water in a lake given change in storage, channel inflows, channel outflows, and diversions. If the L2SWBM effectively closes the water balance, we expect there to be little to no gap between component and residual NBS estimates derived from L2SWBM inferences, despite the existence of process error.

We found differences between component and residual NBS to be small, on average, compared to the measurement precision of monthly water level estimates (10 mm). The median cumulative difference between NBS estimates for Lake Superior over the 792-month analysis period totaled 1,562 mm, or an average 1.97 mm per month — the smallest among the Great Lakes. For Lake Michigan-Huron, the total difference was found to be 7,807 mm or 9.86 mm per month — the largest among the Great Lakes. Average monthly differences for Lakes Erie and Ontario were 3.33 and 3.82 mm. The gap between residual and component NBS for Lake St. Clair totaled 0.47 m^3/s or about 1.09 mm per month.

6. Acknowledgments

Funding for this project was provided by the International Joint Commission's International Watersheds Initiative through a NOAA Cooperative Agreement with the University of Michigan (NA12OAR4320071).

We would like to thank Song Qian, Yves Atchade, Kerby Shedden, Edward Ionides, Vincent Fortin, Bryan Tolson, David Holtschlag, and Craig Stow for initial, helpful discussions on Bayesian inference and alternative formulations of our water balance model. Jacob Bruxer, Frank Seglenieks, Tim Hunter, and Lauren Fry provided expert opinions and water balance data. Nicole Rice provided graphical and editorial support. Additionally, we appreciate the efforts of Wendy Leger and Mike Shantz for securing funding for this project.

References

Ahrestani, F.S., Hebblewhite, M., Post, E., 2013. The importance of observation versus process error in analyses of global ungulate populations. *Scientific reports* 3, 3125.

Bishop, C.M., 2011. *Pattern Recognition and Machine Learning*. Springer New York.

Bruxer, J., ENG, B., ENG, P. 2010. Uncertainty Analysis of Lake Erie Net Basin Supplies as Computed Using the Residual Method. Thesis Submittal, McMaster University, Hamilton, Ontario, Canada. http://hdl.handle.net/11375/9907

CCGLBHHD, 1977. Coordinated Great Lakes physical data. Tech. Rep., Coordinating Committee on Great Lakes Basic Hydraulic and Hydrologic Data. www.lre.usace.army.mil/

Changnon, S.A. and Changnon, J.M., 1996. History of the Chicago diversion and future implications. *Journal of Great Lakes Research*, *22*(1), pp.100-118.

Day, J.C., Bridger, K.C., Peet, S.E. and Friesen, B.F., 1982. Northwestern Ontario river dimensions. *JAWRA Journal of the American Water Resources Association*, *18*(2), pp.297-305.

Deacu, D., Fortin, V., Klyszejko, E., Spence, C., Blanken, P.D., 2012. Predicting the net basin supply to the Great Lakes with a hydrometeorological model. *Journal of Hydrometeorology* 13(6), pp.1739–1759.

Gelman, A., Carlin, J.B., Stern, H.S., Dunson, D.B., Vehtari, A. and Rubin, D.B., 2013. *Bayesian data analysis*. CRC press.

Gronewold, A.D., Bruxer, J., Durnford, D., Smith, J.P., Clites, A.H., Seglenieks, F., Qian, S.S., Hunter, T.S. and Fortin, V., 2016. Hydrological drivers of record-setting water level rise on Earth's largest lake system. *Water Resources Research*, *52*(5), pp.4026-4042.

Gronewold, A.D., Clites, A.H., Hunter, T.S. and Stow, C.A., 2011. An appraisal of the Great Lakes advanced hydrologic prediction system. *Journal of Great Lakes Research*, 37(3), pp.577–583.

Gronewold, A.D., Fortin, V., Caldwell, R. and Noel, J., 2018. Resolving hydrometeorological data discontinuities along an international border. *Bulletin of the American Meteorological Society*, 99(5), pp.899-910.

Hunter, T.S., Clites, A.H., Campbell, K.B., Gronewold, A.D., 2015. Development and application of a North American Great Lakes hydrometeorological database — Part I: Precipitation, evaporation, runoff, and air temperature. *Journal of Great Lakes Research* 41(1), pp.65–77.

Husak, G.J., Michaelsen, J. and Funk, C., 2007. Use of the gamma distribution to represent monthly rainfall in Africa for drought monitoring applications. *International Journal of Climatology*, *27*(7), pp.935-944.

Lespinas, F., Fortin, V., Roy, G., Rasmussen, P., Stadnyk, T., 2015. Performance evaluation of the Canadian Precipitation Analysis (CaPA). *Journal of Hydrometeorology* 16(5), pp.2045–2064.

Montgomery, D.C., 2017. *Design and analysis of experiments*. John Wiley & Sons, Inc.

Plummer, M. et al. 2003. JAGS: A program for analysis of Bayesian graphical models using Gibbs sampling. In *Proceedings of the 3rd international workshop on distributed statistical computing* (Vol. 124, p. 125).

R Core Team, 2013. R: A language and environment for statistical computing.

Schwab, D. and Sellers, D., 1996. Computerized bathymetry and shorelines of the Great Lakes. Great Lakes Environmental Research Laboratory. Ann Arbor, Mich., NOAA Data Report ERL GLERL-16.

Smith, J.P. and Gronewold, A.D., 2018. Development and analysis of a Bayesian water balance model for large lake systems. *arXiv preprint arXiv:1710.10161*. https://arxiv.org/abs/1710.10161

Thom, H.C., 1958. A note on the gamma distribution. *Monthly Weather Review*, *86*(4), pp.117-122.

Appendix

A. Stakeholder input

We held two workshops during the course of the project, coinciding with the spring 2016 and 2017 meetings of the Coordinating Committee for Great Lakes Basic Hydrologic and Hydraulic Data (CCGLBHHD). This section contains a list of requests obtained during those workshops and other correspondence, some with references, along with how the model was configured, if at all, to satisfy those requests.

- Bill Werick (GLAM) recommended more explicit bias terms, potentially with biases learned in a prior run. He also suggested using priors and posteriors to infer a conveyance change in the St. Clair River.
    - Regarding priors, tentatively the plan is to use the historical record run chosen here to calculate new prior distributions for biases in nearer term model runs. Coincidentally there was a suggestion to use biases inferred in the near-term model runs in the historical record generating runs. Near-term inferences, however, are likely more volatile due to the provisional and in some cases experimental nature of near-term data.
    - Regarding connecting channel flows, the model incorporates fairly broad, data-driven prior distributions that could accommodate phenomena such as conveyance changes that are possibly reflected in the input data. Bias priors for the coordinated and IGS flow estimates are based off of a previous uncertainty study. The combination of priors and overall model structure has, in our opinion, inferred new values for channel flows and quantified their uncertainty in an acceptable manner.
    - A phone call focusing on connecting channels developed more ideas, which we believe are addressed by the robust model structure detailed above:
        - Developing priors for historical flows that relate to historical water levels.
        - Incorporating the concept of transfer factors between the St. Clair and Detroit rivers.
        - Have the inflow for Lake Erie be the Fort Wayne IGS, and bias the coordinated flow ‘downward’ to not double count the Detroit River watershed. Similar situation for Michigan-Huron coordinated outflow and the IGS at Port Huron.
        - Establish independence from stage-fall discharge estimates.
        - Eliminating priors for outflows (dismissed).

- Werick additionally recommended using priors more reflective of climate change.
    - We believe the priors incorporated in the model are broad enough to allow for changes in climate. Ultimately, the model will be informed by data, which should reflect changes in the components of the water balance due to climate change.
- Questions were asked about how improvements in the model are to be tested for and confirmed. We believe that the experimental framework in Smith and Gronewold (2018) addresses those questions.
- John Allis (USACE – Detroit District) suggested running the model without any prior information and see if results change, seeing if inferences are invariant to priors. He also suggested running with boundary conditions.
    - Informally, we ran versions of the model with uniform prior distributions on select variables, where the minimums and maximums were well beyond the expected lower and upper limits of the variables. Minimums were zero if the variables' values were expected to be greater than or equal to zero. Inferences from these models, for the tested variables, tended to have wider than acceptable uncertainty, and in some cases were well outside the range of input data.
    - Additionally, academic literature offer no rigorous solution to the desire of a 'flat', non-informative prior in Bayesian MCMC modelling/Bayesian networks. The JAGS framework expects some prior, or will throw an error.
- There was a question to how long do we need to run the cumulative storage term (see Gronewold et al. 2016). A suggestion, instead of 50, 65 years, was a rolling 12 year window. There was a more general suggestion to run on different time frames. Dorothy Durnford (ECCC) recommended running the model with a different analysis period: 1980-2010, to represent climate change, or use a rolling x-year period.
    - We found that a 12 month rolling window, even a 6 month, was sufficient to close the water balance.
    - We anticipate the rolling window will help facilitate proper inference given new data and possible signals of climate change.
- There was a suggestion to allow the model to explicitly calculate NBS.
    - Modelling NBS in the model would be redundant as we model the individual NBS components. We can supply scripts to calculate the NBS from the MCMC samples and provide uncertainty information.
- Many suggested assessing spatial and temporal auto-correlation, cross correlation between components, such as precipitation and runoff, water levels (changes in storage) and flows. This may be a future focus of analyzing inferences from the model.
- There was a suggestion to declare physically impossible values and monitor for invalid inferences. We believe that the model structure adequately ensures inferences are proper, with few errors. Specifically, for example, priors for precipitation and runoff are greater than or equal to zero. However, priors for channel flows and diversion could be negative, yet data generally do not support negative inferences of those variables, and the probability of a negative inference is small.
- Deborah Lee (NOAA GLERL) suggested finding a way to isolate thermal expansion, perhaps as an explicit water balance term, even seasonal, seeing if the term leads to an

improvement. Someone suggested finding a way to get the direction of thermal expansion in warming and cooling months, possibly through a bias term for change in storage. We believe this may be captured in the process error term.

- There was a suggestion for using the Derecki method for evaporation over Lake St. Clair, but that was dismissed in favor of the modelling procedure using NBS in units of cubic meters per second.
- There was a suggestion to put National Weather Service (NWS) Precipitation estimates at a higher level of confidence, and Area Ratio Method (ARM) runoff estimates at a higher level of confidence than estimates from the Large Basin Runoff Model (LBRM). While we did not explicitly use LBRM nor NWS estimates in the generation of the new historical record, previously utilized, shorter term (10 year) models tend to favor ARM over LBRM without any explicit expression of confidence. We believe this is due to MCMC and the Bayesian Network generating estimates of runoff with consideration of not only runoff data, but all other data on the water balance. ARM estimates appear to help close the balance better. NWS estimates would be submitted to the same analysis — that is, the Bayesian Network would see how well precipitation values around NWS estimates help close the water balance with consideration of all other data.
- There was a suggestion to implement a seasonal precision, which we believe is best incorporated through the seasonal process error and bias terms.
- There was a suggestion to incorporate the land/lake precipitation ratio into the model. Informally there were attempts to incorporate a linear relationship between water levels and channel flows into the model. We found that convergence was difficult to achieve through that model. Thus, incorporating a linear relationship such as the land/lake precipitation ratio will probably be detrimental to model performance. Incorporating lag variables as David Holtschlag (United States Geological Survey) recommended would likely be detrimental in a similar way.
- Andrew Gronewold suggested using the National Aeronautics and Space Administration's (NASA) Gravity Recovery and Climate Experiment (GRACE) Satellite data in addition to coordinated water level estimates and gauge estimates. The model uses estimates of change in storage based off of the coordinated beginning of month water levels. Beginning of month levels may not be available for a given month in GRACE data. The data could be extrapolated to fill in missing days to produce a GRACE based beginning-of-month water level record. GRACE data could be a focus of a future iteration of the model.
- John Allis requested more formal training on how to use the model for interested parties, particularly if we use JAGS. Over the model development process, versions of the model have been given to prospective operators (Frank Seglenieks, Lauren Fry, Heather Lucier) and have been ran by them. A system has been developed involving a configuration file (similar to what Dorothy Durnford recommended) and a 'main' R script to run the model as desired. Data are being assimilated such that updates can be easily made on a monthly basis for monthly communications. The configuration file enables users to select individual component estimates for Bayesian Network analysis.

- There was a suggestion to break up the model into individual lakes. Preliminary model runs with the lakes separated inferred differing values for the connecting channel flows, indicating that an ‘all-lakes’, fully connected model is ideal.

B. Implications of uncertainty in coordinated channel flows and diversions

The L2SWBM assumes that inflows, outflows, and diversions contribute to a lake's water balance where the flow meets the edge of the lake or lake basin (outlet or inlet) – an approximate point in space, not over a broad area. Here, we document details of the measurement of coordinated channel flows and diversions, primary inputs of the model, which can inform interpretation of inferences derived from MCMC sampling.

B.1: Ogoki, Long Lac Diversion into Lake Superior

Figure 2: Maps of the Ogoki and Long Lac Diversions (reproduced with permission from Peter Annin, University of Waterloo — Department of Geography).

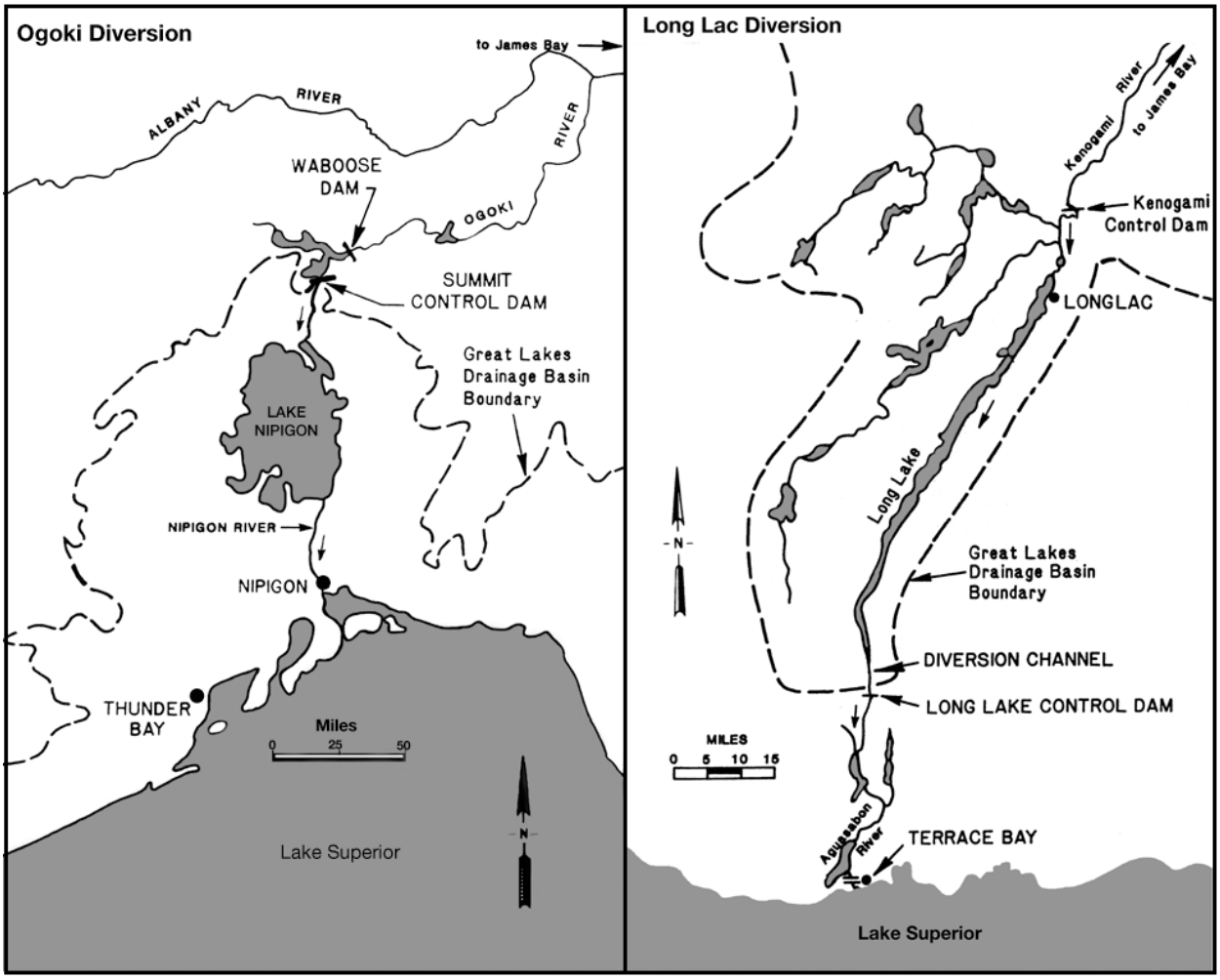

The coordinated flow estimates for the Ogoki River and Long Lac diversion that we used in the development of the L2SWBM are derived from flow measurements through the Summit

Control Dam north of Lake Nipigon, and respectively, Long Lake Control Dam along Long Lake just north of Lake Superior and Terrace Bay, ON, Canada (figure 2). Despite the fact that diverted water first flows through, respectively, Lake Nipigon (a relatively large lake with variable residence time) and the Aguasabon river and power dam, we do not explicitly model the implied uncertainties because we assume they are negligible relative to the overall water balance of Lake Superior and associated uncertainties. (Bruxer, formal correspondence)

B.2: St. Marys River

Figure 3: Photo (credit USACE), looking downstream from Lake Superior, with labels (via Bruxer) of measurement points for coordinated St. Marys River flows.

St. Marys River coordinated flows are measured by the International Lake Superior Board of Control via a series of control and hydropower structures near Sault Ste. Marie. This includes 3 power plants, gated flow structures, and the locks beneath the Sault Ste. Marie International Bridge. The combination of flows from these sources accounts for the St. Marys coordinated outflow (Sidick and Bruxer, formal correspondence). These measurements are performed close enough to the Superior outlet that any uncertainties in terms of the water balance are assumed negligible and are not explicitly modelled.

B.3: Chicago Diversion

The Chicago Diversion is physically regulated via the Chicago Harbor Lock. Regulation is enforced by the Great Lakes Commission, and the maximum flow of water (91 m^3/s) that can be allowed through the gates was set by decisions of the Supreme Court of the United States in

1967, 1980, and 1997. No significant uncertainties with respect to the Michigan-Huron water balance apply here.

B.4: St. Clair River

Coordinated flows through the St. Clair River are measured by an Acoustic Doppler Velocity Meter (ADVM) at an IGS nearby Fort Gratiot in Port Huron, MI, USA, which is near or on the assumed outlet and basin boundary of Lake Michigan-Huron. If the ADVM is not working, the water level gauge data at NOAA Gauge 9014098 (Fort Gratiot) and nearby NOAA Gauge 9014080 (called the St. Clair State Police Gauge) are used, along with Stage Fall Discharge (SFD) equations and an estimated ratio of ADVM flows to SFD flows computed with data from 2009-2016 to estimate the outflow of Lake Michigan-Huron (Calappi, formal correspondence).

B.5: Detroit River

With respect to the Detroit River, coordinated flow estimates are derived from ADVM measurements at an IGS near Historic Fort Wayne, which is near the basin boundary of Lake St. Clair and Erie, yet downstream from the outlet of Lake St. Clair, assumed to be near Windmill Pointe. In the case that the ADVM is not working, tentatively the plan is to use a level gauge near Wyandotte and an estimated ratio between there and Fort Wayne (or Windmill Point, to be determined) in Stage Fall Discharge equations to compute flow (Calappi, formal correspondence).

B.6: Niagara River and Welland Canal

Figure 4: Map of the Niagara River (Bruxer 2010)

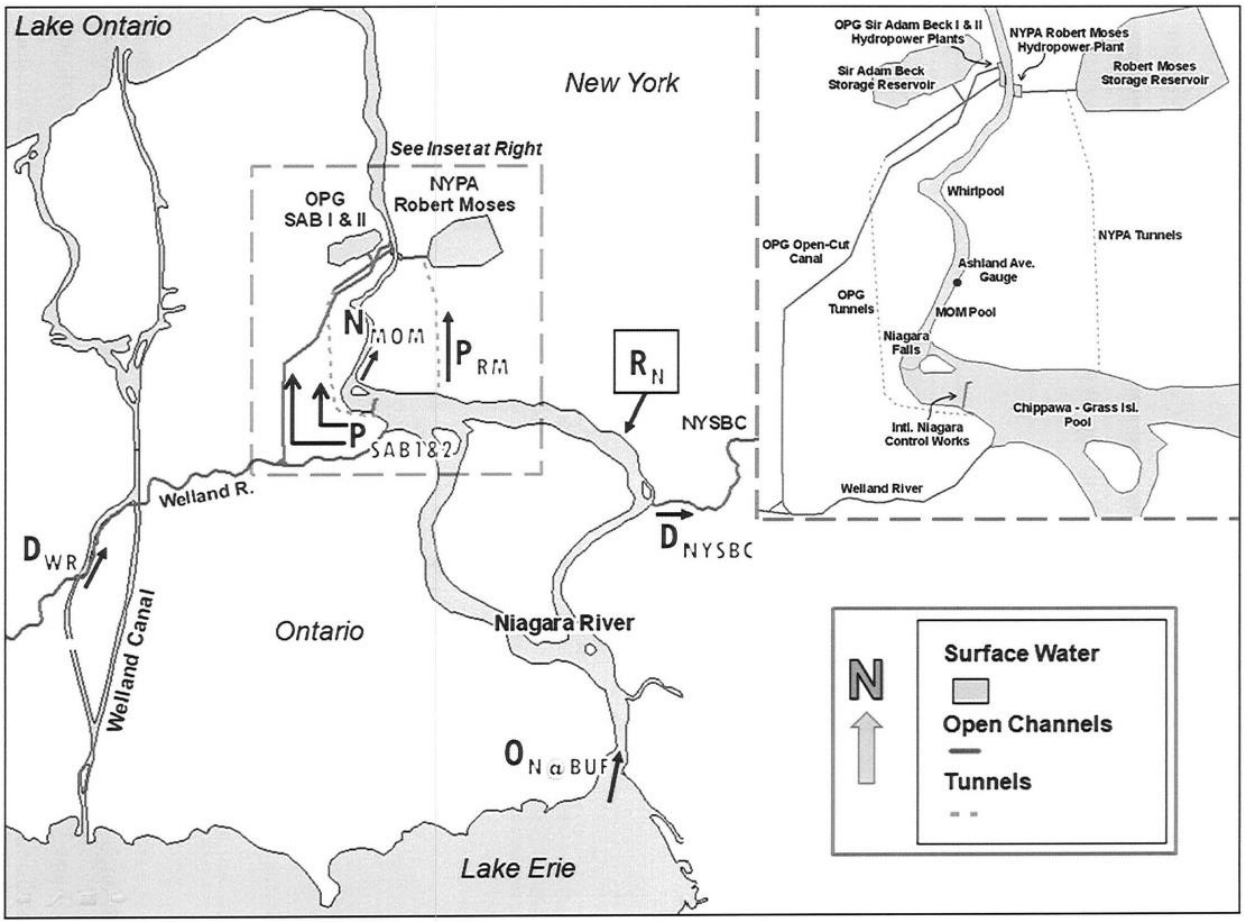

For the Niagara River, six points or areas of measurement are between the outlet of Lake Erie at Buffalo, NY, USA, and the mouth of the Niagara into Lake Ontario to calculate the river's flow ($O_{N\ @\ BUF}$, figure 4, Bruxer 2010). These are:

- Maid-of-the-Mist pool outflow near Niagara Falls (N_{MOM})
- Ontario Power Generation's Sir Adam Beck No. 1 and No. 2 hydropower plants (SAB I & II)
- Diverted water for New York Power Authority's (NYPA's) Robert Moses hydropower plant
- Water diverted into the New York State Barge Canal (D_{NYSBC})
- Local runoff into the Niagara River (R_N, subtracted term)
- Water diverted into the Niagara via the Welland River (D_{WR}, subtracted term)

Figure 5: Maps detailing the Welland Canal (Bruxer 2010)

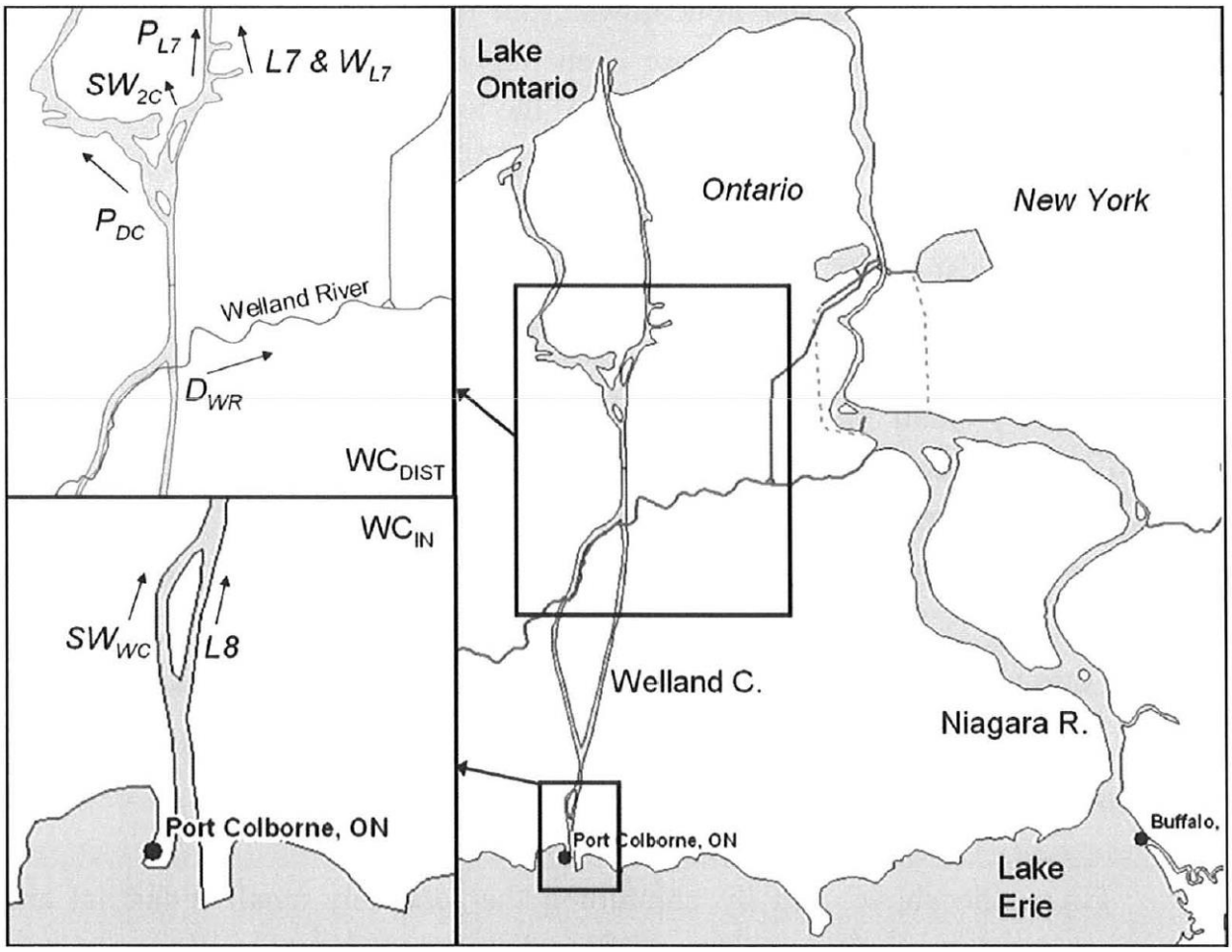

Welland canal flow data also come in from multiple sources and are managed by the St. Lawrence Seaway Management Corporation (SLSMC). Sources of data include local municipal and industrial users (Bruxer 2010). Points of measurement include:

- Welland Canal supply weirs (points labelled SW in figure 5)
- Welland Canal lock 8, nearest Lake Erie (L8)
- Points of diversion into the Welland River (D_{WR}, Welland Water Works, syphon culvert roof drains)
- Diversions to the OPG De Cew generating station (P_{DC})
- Flows through Lock 7 (L7), its weir (W_{L7}), and SLSMC powerhouse (P_{L7})
- Other municipal and industrial withdrawal measurements available

We assume that, while the multiple measurement points conceivably increase uncertainty in the estimates of Niagara and Welland Canal flows, the net impact of that uncertainty on the model and water balance is minimal.

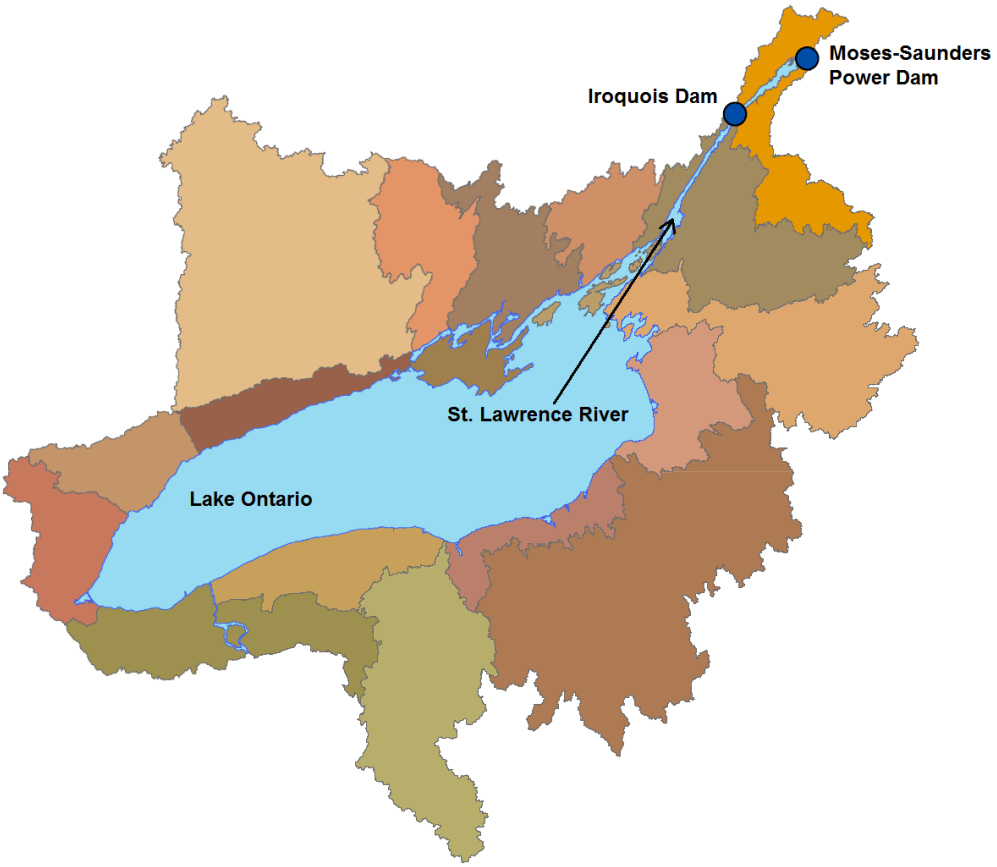

Figure 6: Lake Ontario basin map, outlining the lake and surrounding sub-basins, the St. Lawrence River, Iroquois Dam, and Moses-Saunders Power Dam, the latter two of which control flow through the St. Lawrence River. Courtesy Tim Hunter, NOAA-GLERL

B.7: St. Lawrence River

St. Lawrence River flows are measured at the Moses-Saunders Power Dam in Cornwall, ON, Canada, near the Lake Ontario basin boundary. The distance from the assumed outlet of Ontario – near Kingston, ON, Canada – challenges the assumption that lake outflow is through the outlet of the lake, yet we assume minimal model error. In terms of water balance computation, there may be some interference due to runoff that enters between the Iroquois and Moses-Saunders dams, yet is not accounted for in the GLM-HMD or other runoff estimates, nor is subtracted from the estimate at the Moses-Saunders Dam.

C. Water balance component prior distributions

Plots in the following pages illustrate prior distributions for the components of the water balance. Each of the 12 calendar months are represented by rows, and each of the Great Lakes (and St. Clair if applicable) are represented by columns. The gray vertical bars form histograms of the historical distribution of a component mentioned in the title above the plots, and the dotted, blue lines represent the probability density fit to those historical data. Vertical axes represent probability density, while the horizontal axes represent values for the components in units noted in the title above the plots.

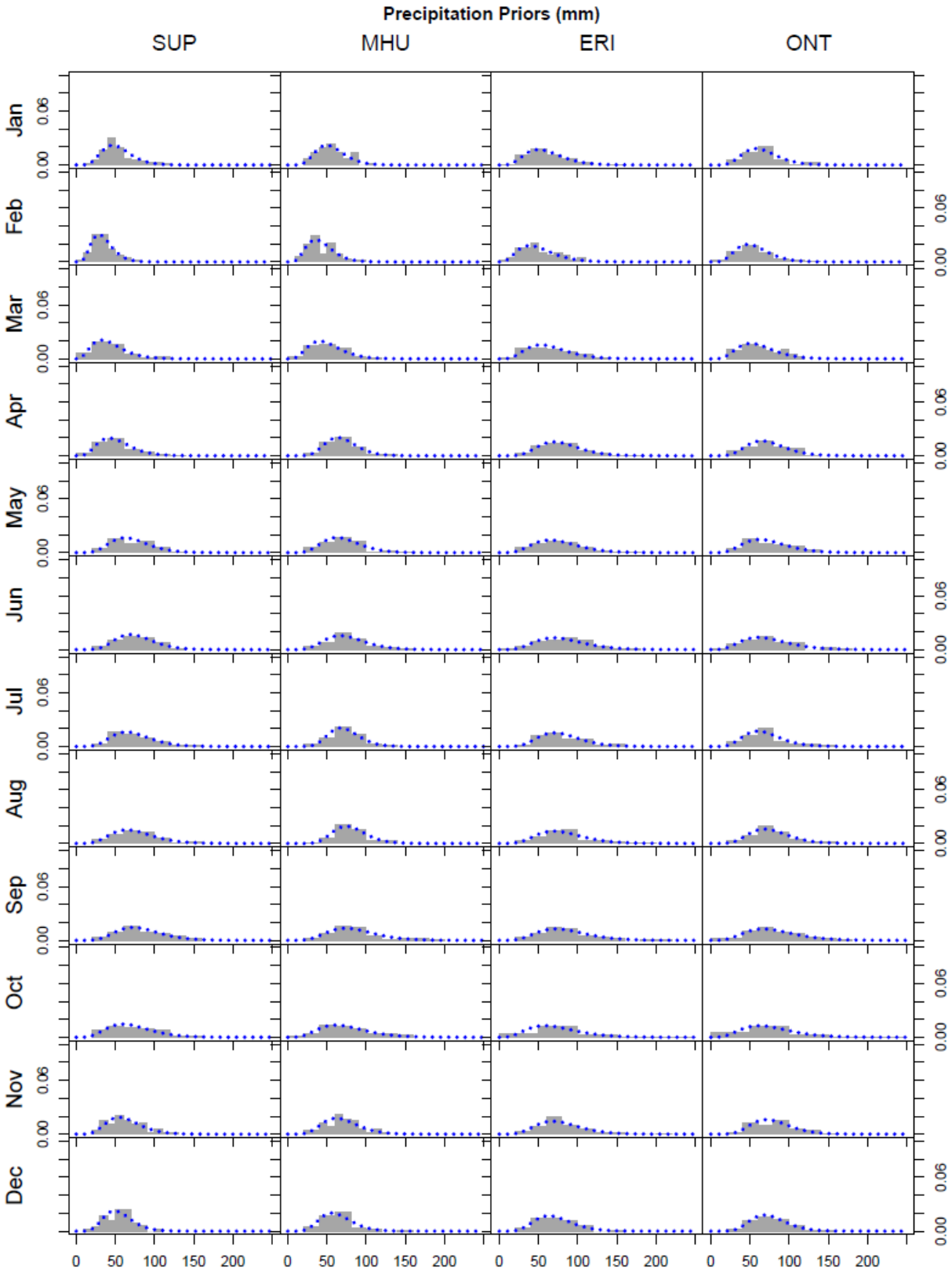
Precipitation Priors (mm)
SUP
MHU
ERI
ONT
Jan
Feb
Mar
Apr
May
Jun
Jul
Aug
Sep
Oct
Nov
Dec
0.00
0.06
0
50
100
150
200

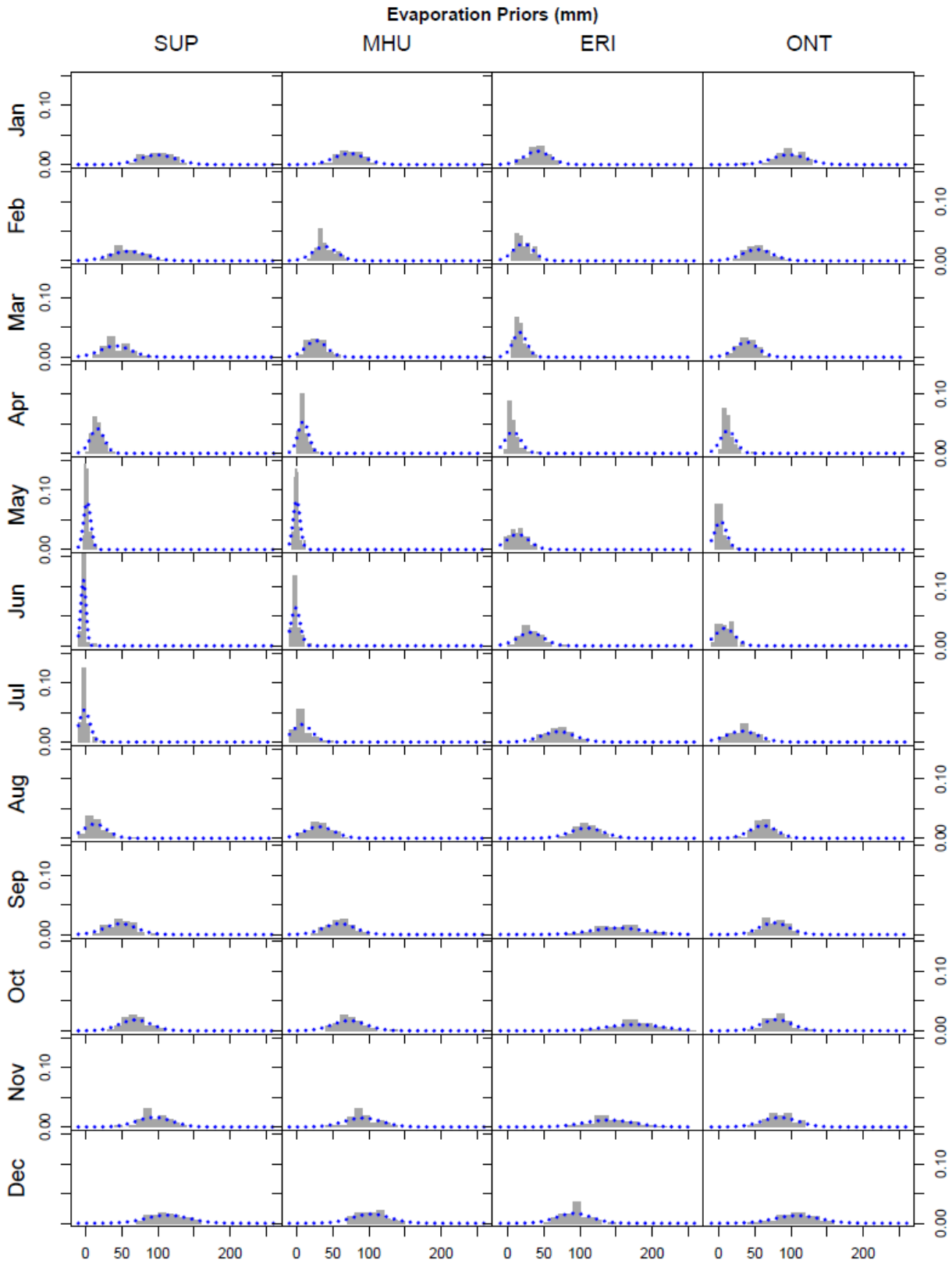
Evaporation Priors (mm)
SUP
MHU
ERI
ONT
Jan
Feb
Mar
Apr
May
Jun
Jul
Aug
Sep
Oct
Nov
Dec
0.00
0.10
0
50
100
200

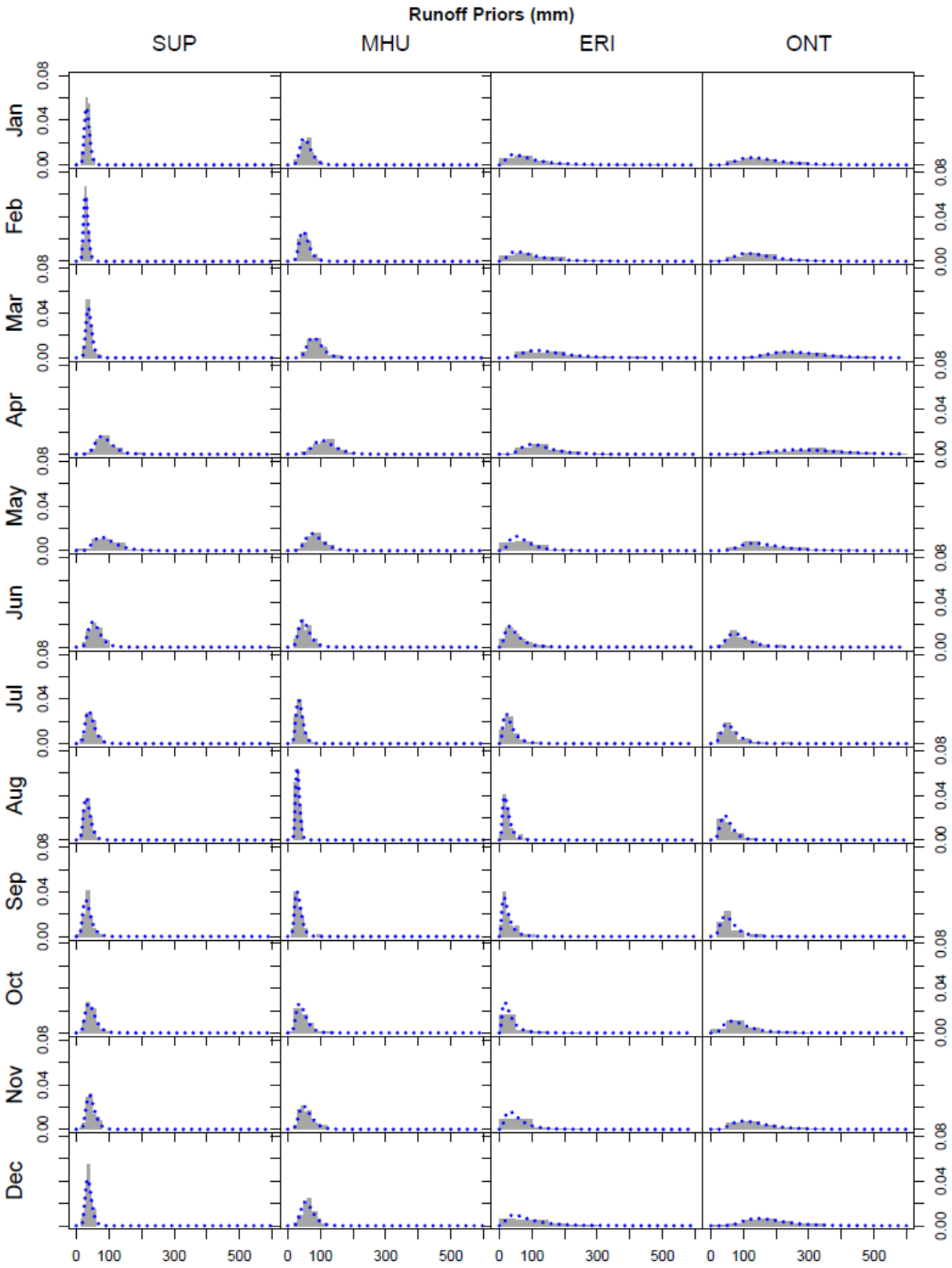
Runoff Priors (mm)
SUP
MHU
ERI
ONT
Jan
Feb
Mar
Apr
May
Jun
Jul
Aug
Sep
Oct
Nov
Dec
0.00
0.04
0.08
0
100
300
500

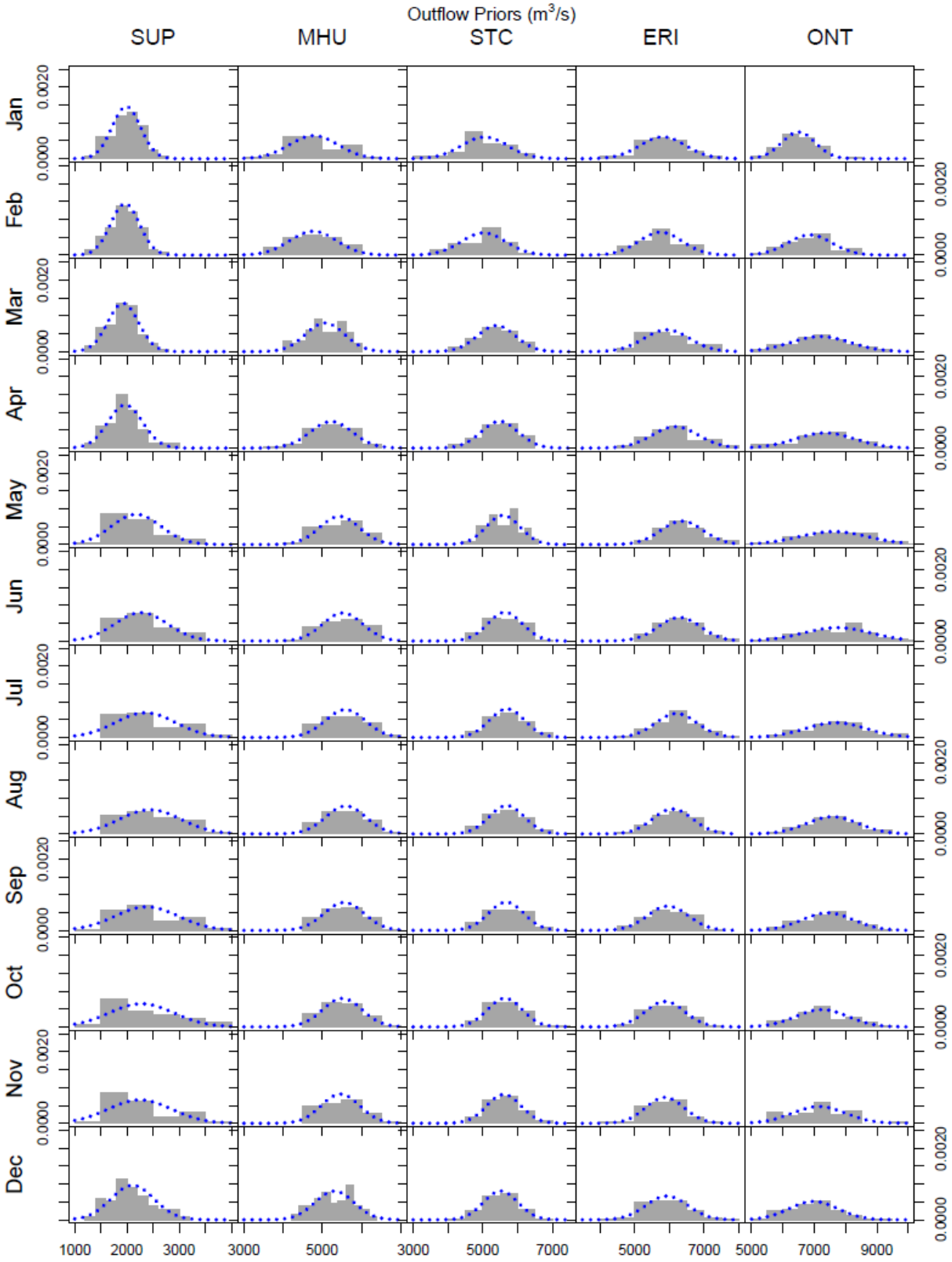
Outflow Priors (m³/s)
SUP
MHU
STC
ERI
ONT
Jan
Feb
Mar
Apr
May
Jun
Jul
Aug
Sep
Oct
Nov
Dec
0.0000
0.0020
1000
2000
3000
3000
5000
3000
5000
7000
5000
7000
5000
7000
9000

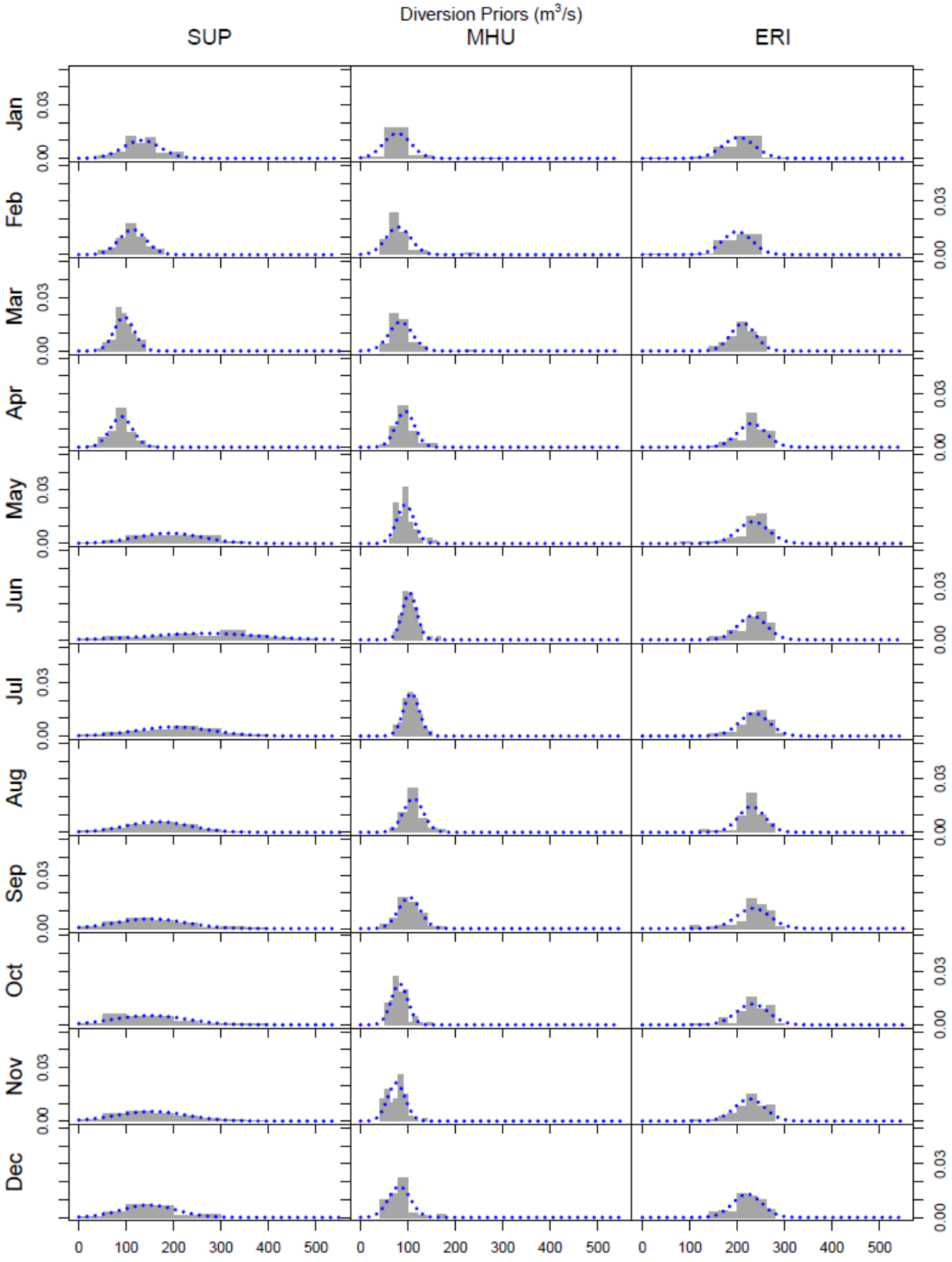
Diversion Priors (m3/s)
SUP
MHU
ERI
Jan
Feb
Mar
Apr
May
Jun
Jul
Aug
Sep
Oct
Nov
Dec
0.00
0.03
0
100
200
300
400
500

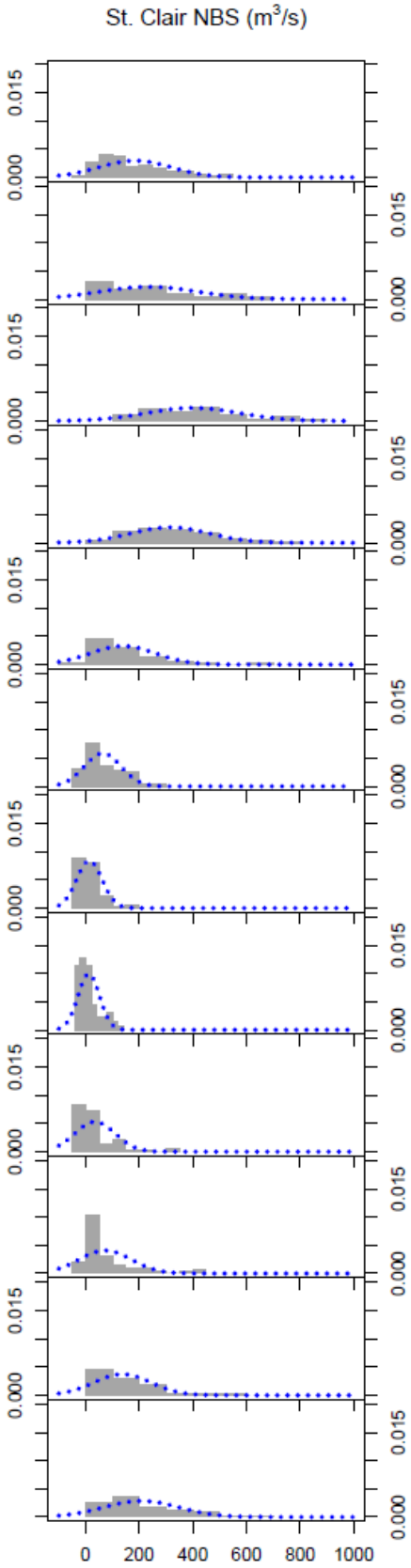
St. Clair NBS (m3/s)
0.000
0.015
0
200
400
600
800
1000

D. Graphical summary of new historical record

The following pages contain plots of time series of the Laurentian Great Lakes water balance historical record generated from model 12F. For each Great Lake and Lake St. Clair, the historical record has one page per decade covered. Thus, as the historical record spans 66 years, each lake has seven pages of time series plots.

Each page has a series of plots, one per component of the water balance. Vertical axes illustrate the range of values a component may have in a month, horizontal axes represent time. Inflows are not plotted as they are plotted as outflows for the upstream lake. Change in storage (ΔH) is always the bottom plot on a page. Within each plot, line segments represent an independent model input into the L2SWBM. Gray bars represent the 95% Bayesian credible interval inferred from the L2SWBM. Additional symbols may be included, and are labeled in the legend at the top of each individual plot (more than one per page).

We begin with Lake Superior's water balance, and proceed downstream, with the last set of plots to be for Lake Ontario's water balance.

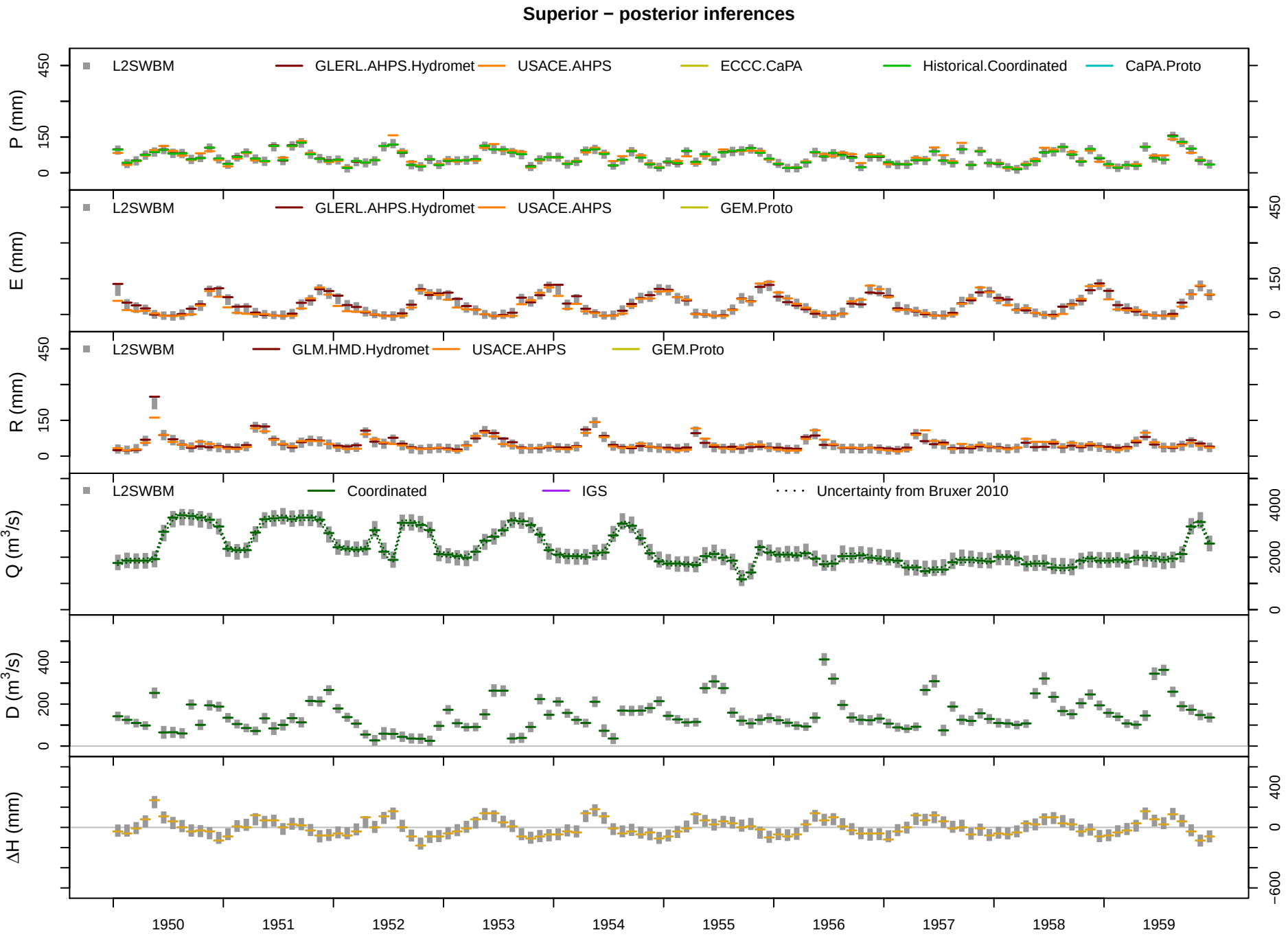
Superior − posterior inferences
P (mm)
L2SWBM
GLERL.AHPS.Hydromet
USACE.AHPS
ECCC.CaPA
Historical.Coordinated
CaPA.Proto
E (mm)
L2SWBM
GLERL.AHPS.Hydromet
USACE.AHPS
GEM.Proto
R (mm)
L2SWBM
GLM.HMD.Hydromet
USACE.AHPS
GEM.Proto
Q (m3/s)
L2SWBM
Coordinated
IGS
Uncertainty from Bruxer 2010
D (m3/s)
ΔH (mm)
1950
1951
1952
1953
1954
1955
1956
1957
1958
1959

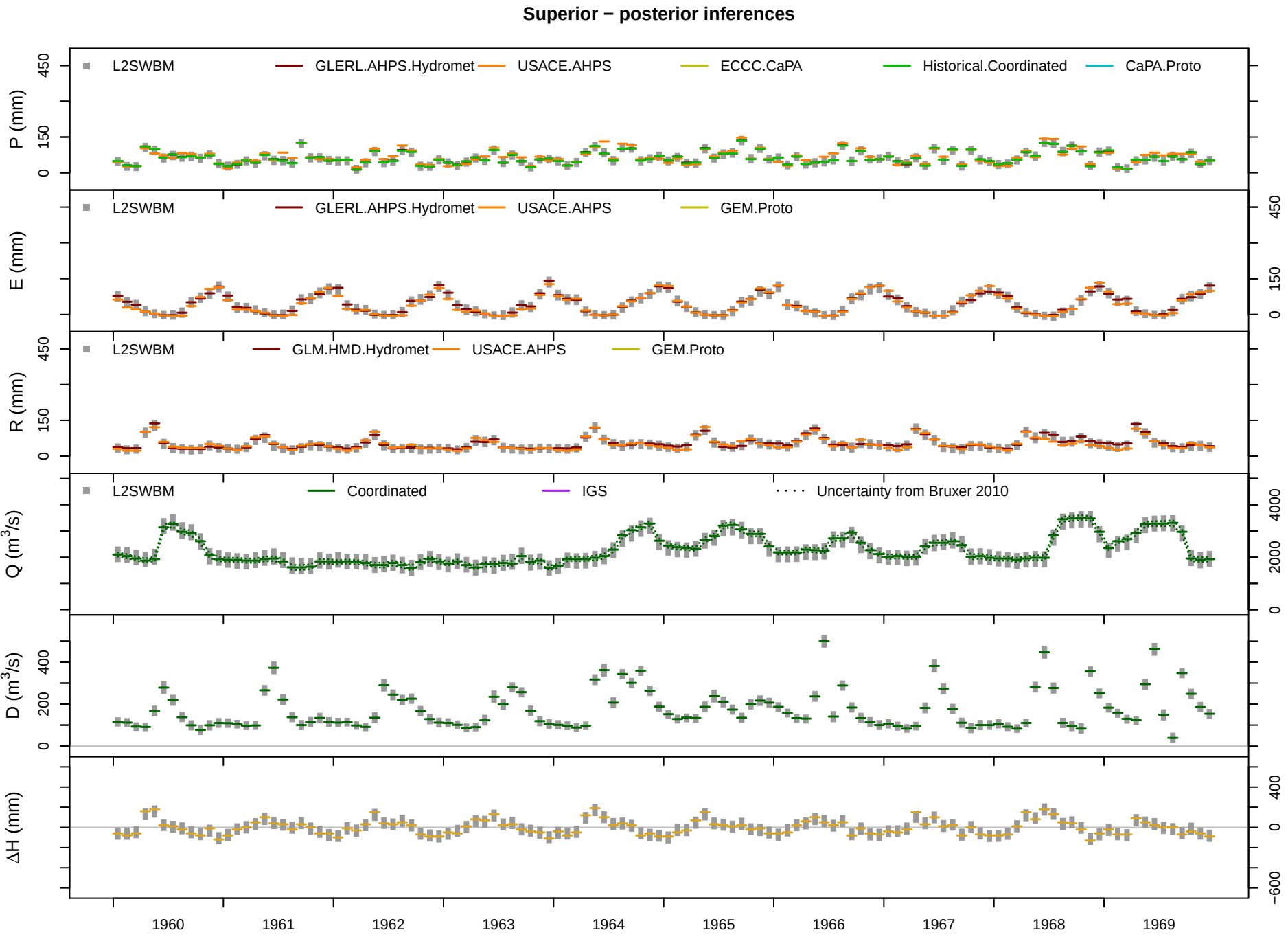
Superior − posterior inferences
P (mm)
L2SWBM
GLERL.AHPS.Hydromet
USACE.AHPS
ECCC.CaPA
Historical.Coordinated
CaPA.Proto
E (mm)
L2SWBM
GLERL.AHPS.Hydromet
USACE.AHPS
GEM.Proto
R (mm)
L2SWBM
GLM.HMD.Hydromet
USACE.AHPS
GEM.Proto
Q (m3/s)
L2SWBM
Coordinated
IGS
Uncertainty from Bruxer 2010
D (m3/s)
ΔH (mm)
1960
1961
1962
1963
1964
1965
1966
1967
1968
1969

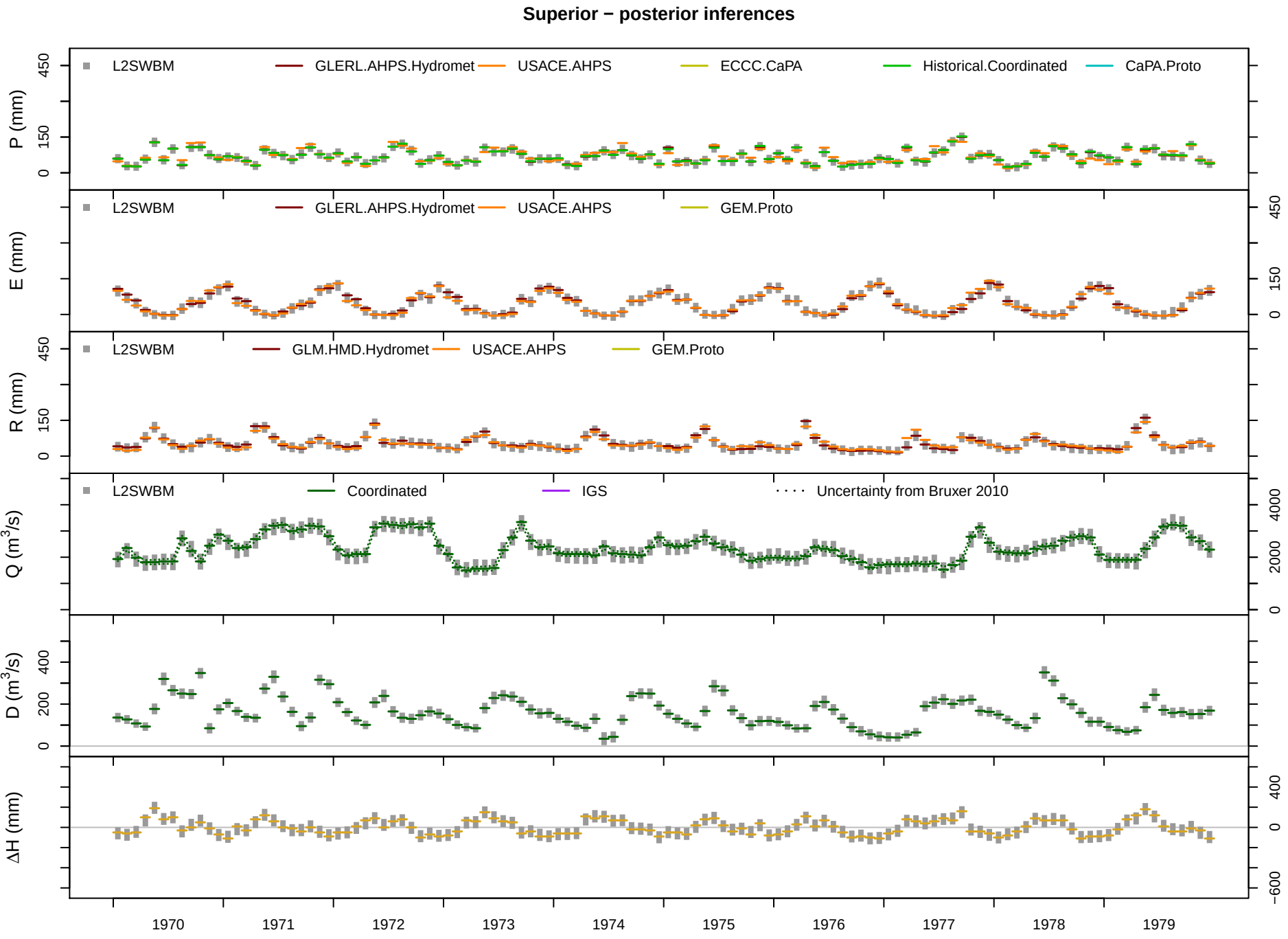
Superior − posterior inferences
P (mm)
L2SWBM
GLERL.AHPS.Hydromet
USACE.AHPS
ECCC.CaPA
Historical.Coordinated
CaPA.Proto
E (mm)
L2SWBM
GLERL.AHPS.Hydromet
USACE.AHPS
GEM.Proto
R (mm)
L2SWBM
GLM.HMD.Hydromet
USACE.AHPS
GEM.Proto
Q (m3/s)
L2SWBM
Coordinated
IGS
Uncertainty from Bruxer 2010
D (m3/s)
ΔH (mm)
1970
1971
1972
1973
1974
1975
1976
1977
1978
1979

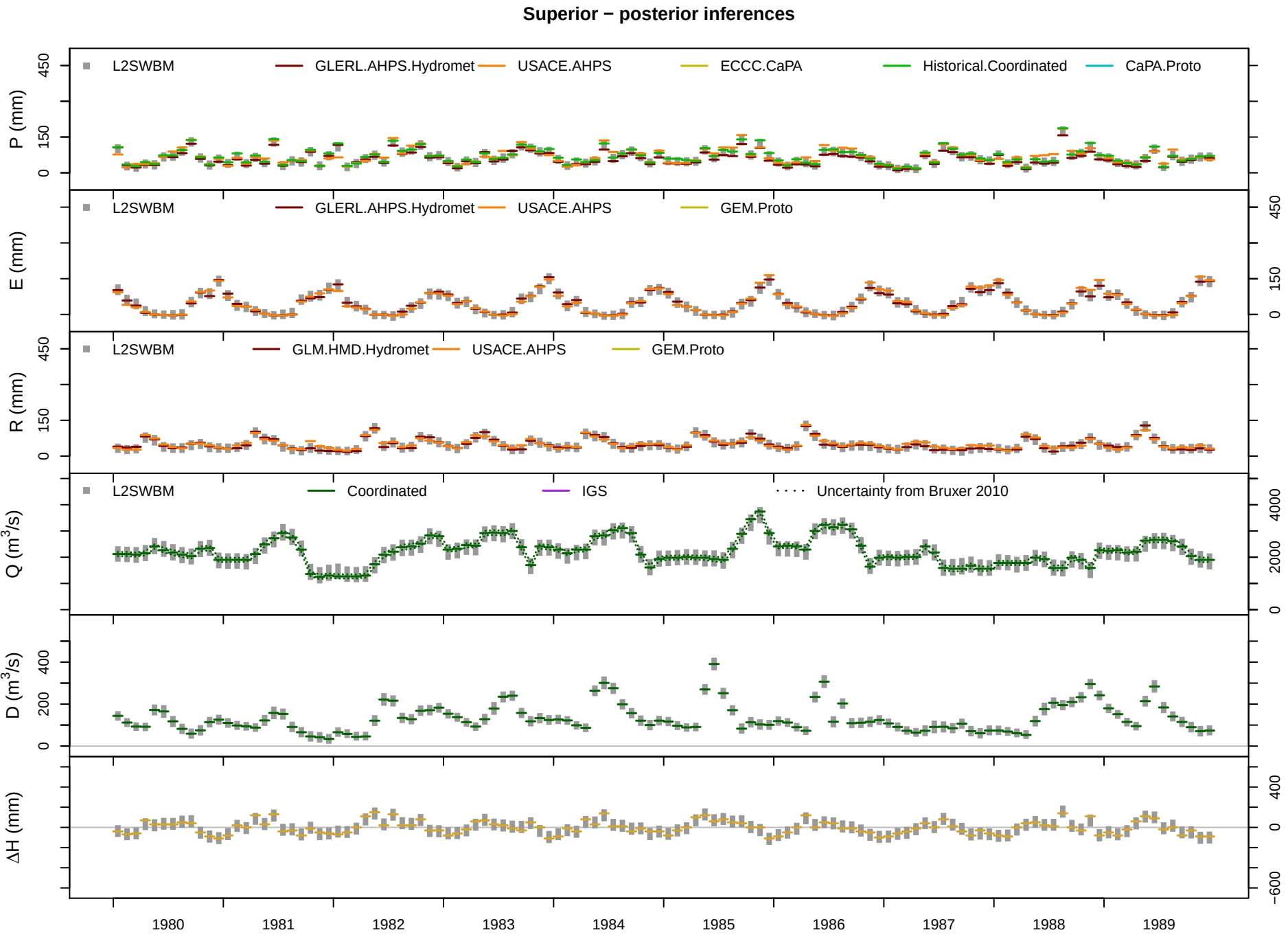
Superior − posterior inferences
P (mm)
L2SWBM
GLERL.AHPS.Hydromet
USACE.AHPS
ECCC.CaPA
Historical.Coordinated
CaPA.Proto
E (mm)
L2SWBM
GLERL.AHPS.Hydromet
USACE.AHPS
GEM.Proto
R (mm)
L2SWBM
GLM.HMD.Hydromet
USACE.AHPS
GEM.Proto
Q (m3/s)
L2SWBM
Coordinated
IGS
Uncertainty from Bruxer 2010
D (m3/s)
ΔH (mm)
1980
1981
1982
1983
1984
1985
1986
1987
1988
1989

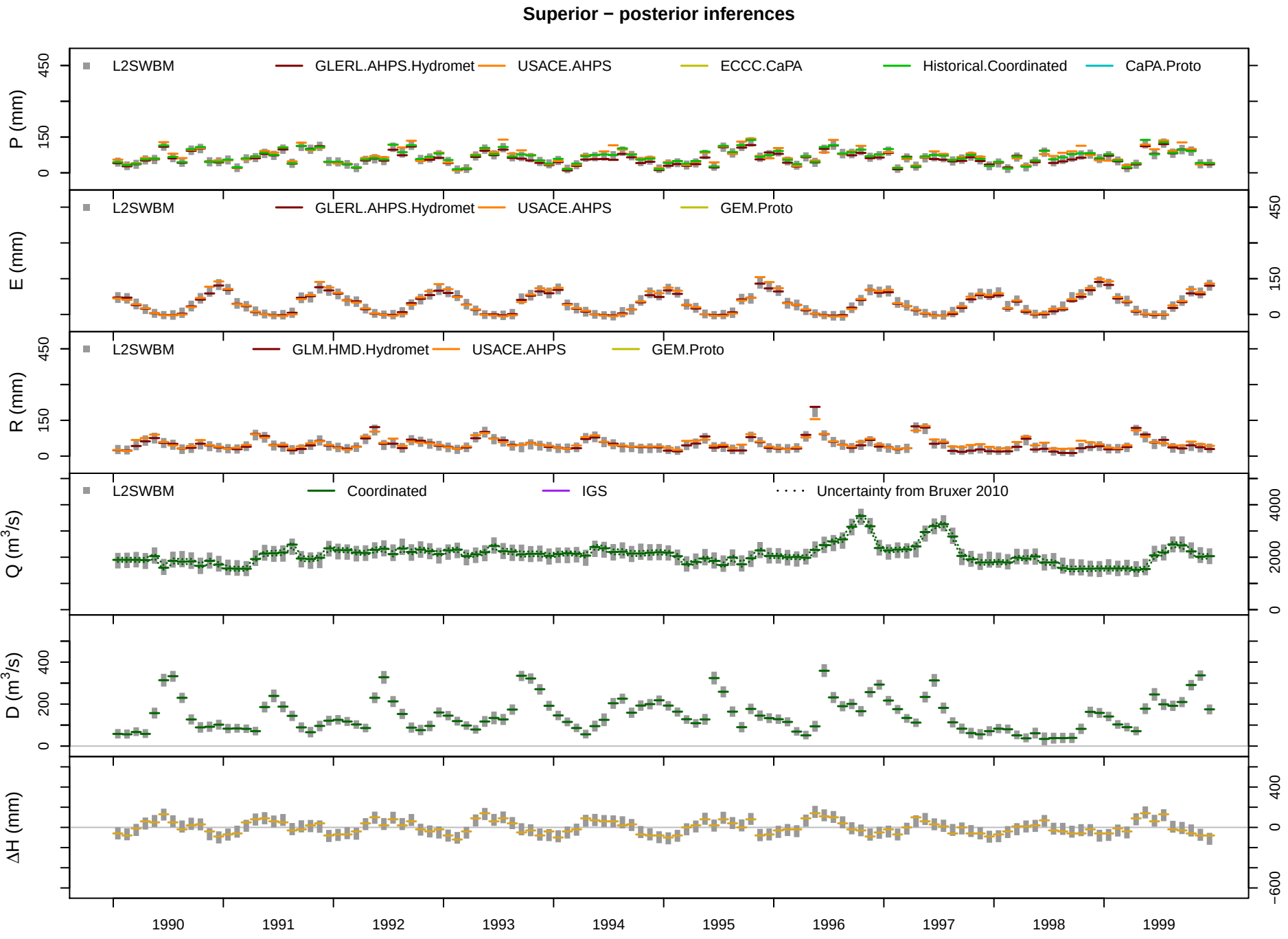
Superior − posterior inferences
P (mm)
L2SWBM
GLERL.AHPS.Hydromet
USACE.AHPS
ECCC.CaPA
Historical.Coordinated
CaPA.Proto
E (mm)
L2SWBM
GLERL.AHPS.Hydromet
USACE.AHPS
GEM.Proto
R (mm)
L2SWBM
GLM.HMD.Hydromet
USACE.AHPS
GEM.Proto
Q (m3/s)
L2SWBM
Coordinated
IGS
Uncertainty from Bruxer 2010
D (m3/s)
ΔH (mm)
1990
1991
1992
1993
1994
1995
1996
1997
1998
1999

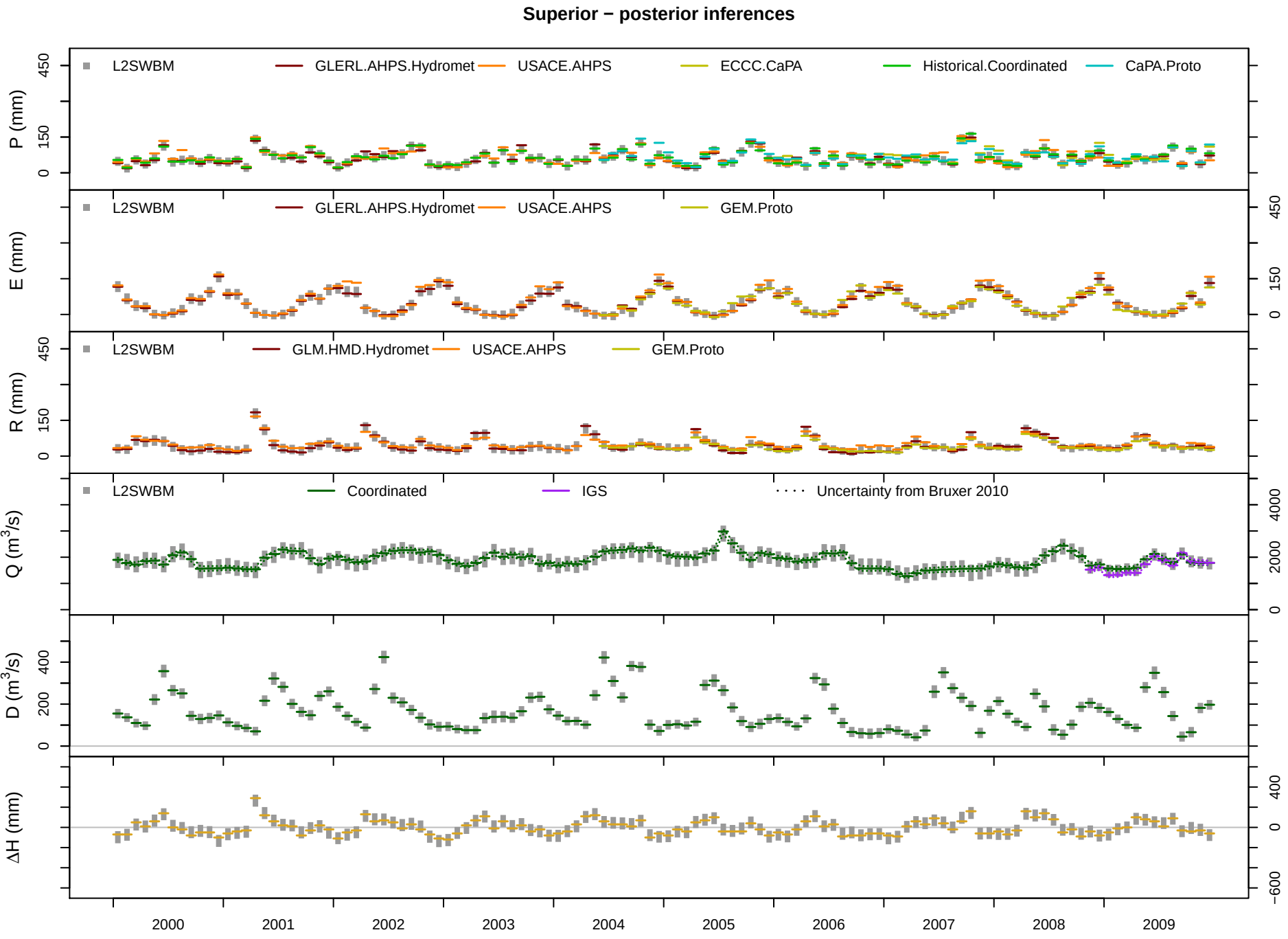
Superior − posterior inferences
P (mm)
L2SWBM
GLERL.AHPS.Hydromet
USACE.AHPS
ECCC.CaPA
Historical.Coordinated
CaPA.Proto
E (mm)
L2SWBM
GLERL.AHPS.Hydromet
USACE.AHPS
GEM.Proto
R (mm)
L2SWBM
GLM.HMD.Hydromet
USACE.AHPS
GEM.Proto
Q (m3/s)
L2SWBM
Coordinated
IGS
Uncertainty from Bruxer 2010
D (m3/s)
ΔH (mm)
2000
2001
2002
2003
2004
2005
2006
2007
2008
2009

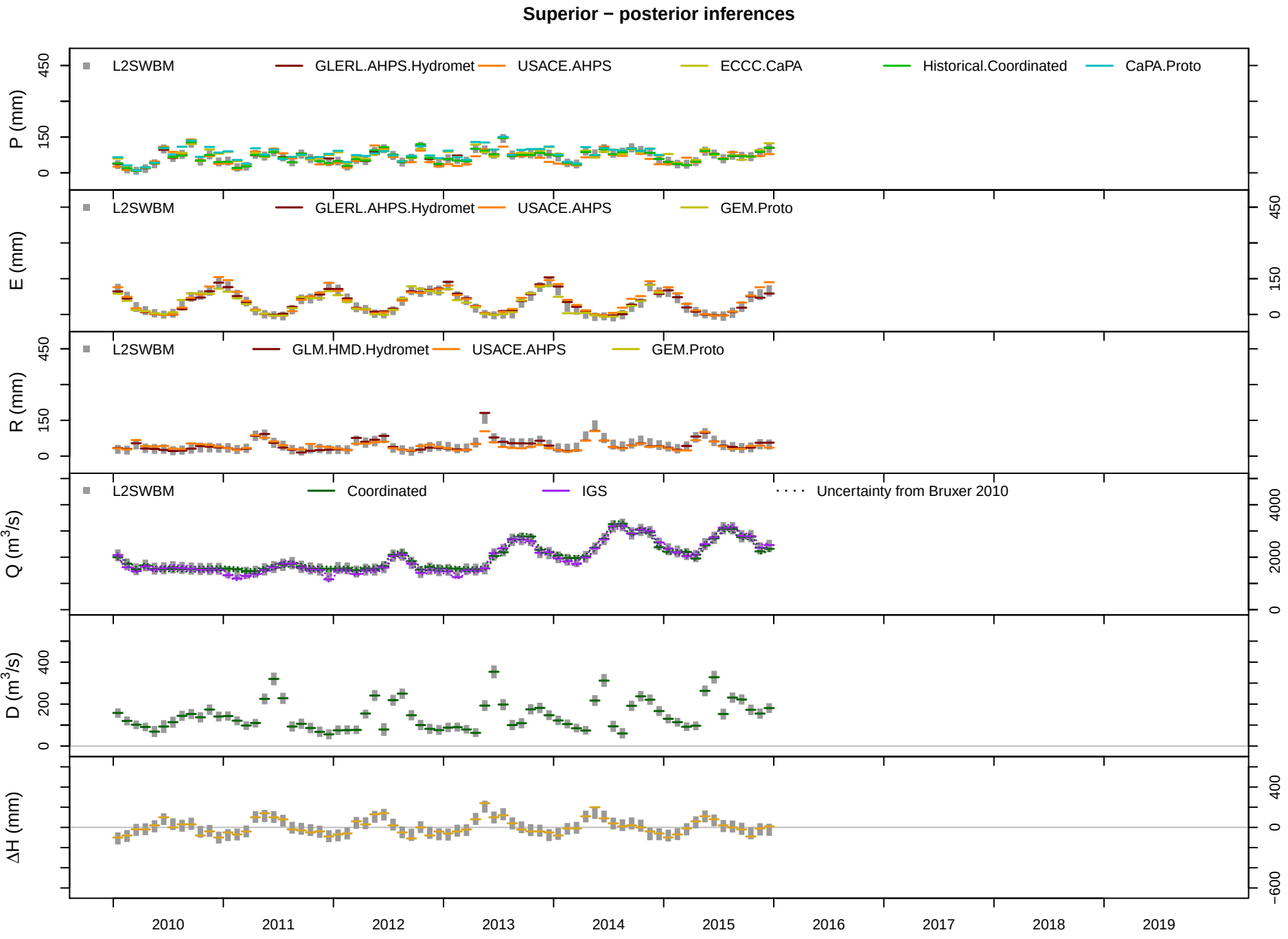
Superior − posterior inferences
P (mm)
L2SWBM
GLERL.AHPS.Hydromet
USACE.AHPS
ECCC.CaPA
Historical.Coordinated
CaPA.Proto
E (mm)
L2SWBM
GLERL.AHPS.Hydromet
USACE.AHPS
GEM.Proto
R (mm)
L2SWBM
GLM.HMD.Hydromet
USACE.AHPS
GEM.Proto
Q (m3/s)
L2SWBM
Coordinated
IGS
Uncertainty from Bruxer 2010
D (m3/s)
ΔH (mm)
2010
2011
2012
2013
2014
2015
2016
2017
2018
2019

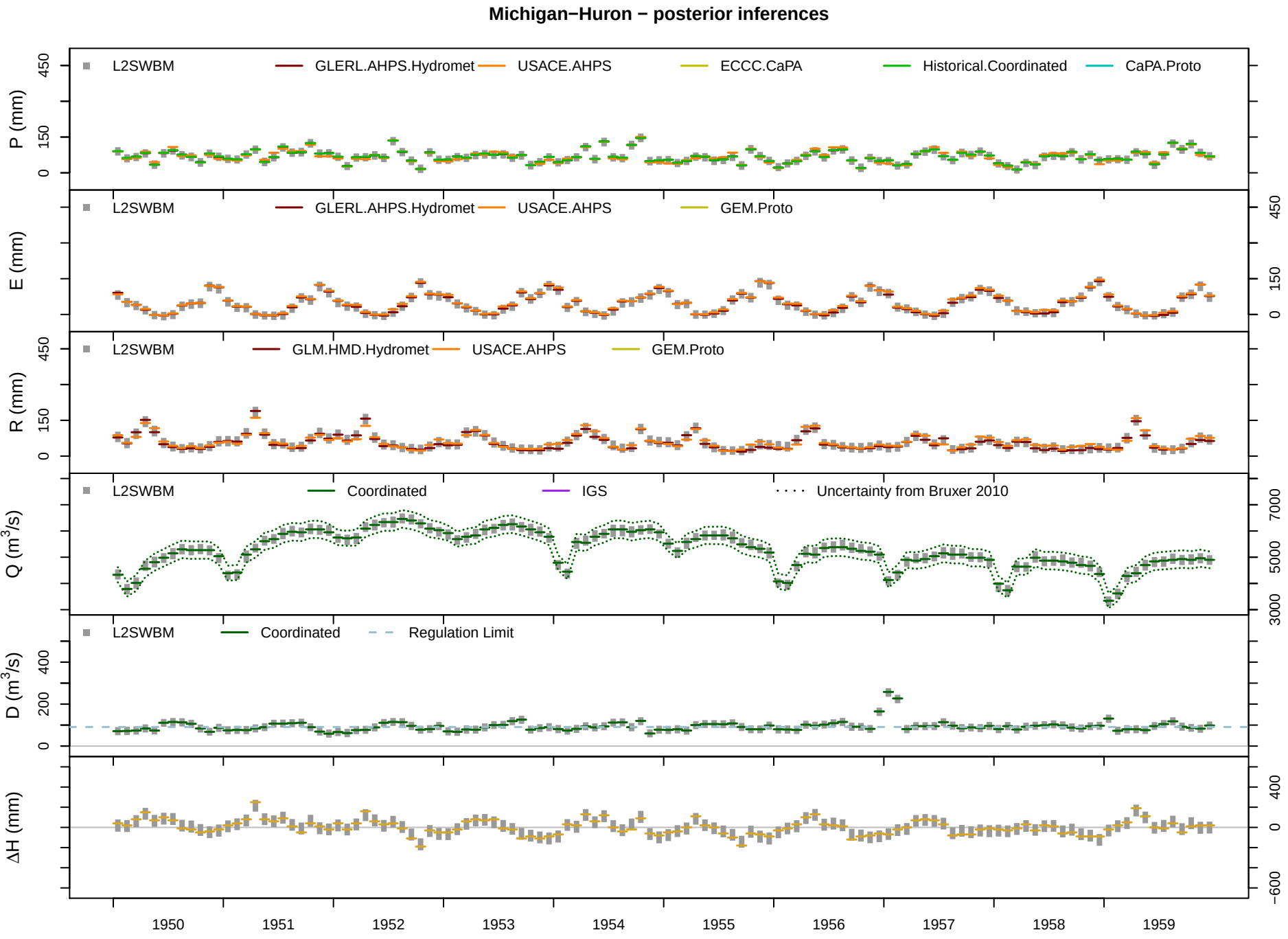
Michigan−Huron − posterior inferences
P (mm)
L2SWBM
GLERL.AHPS.Hydromet
USACE.AHPS
ECCC.CaPA
Historical.Coordinated
CaPA.Proto
E (mm)
L2SWBM
GLERL.AHPS.Hydromet
USACE.AHPS
GEM.Proto
R (mm)
L2SWBM
GLM.HMD.Hydromet
USACE.AHPS
GEM.Proto
Q (m3/s)
L2SWBM
Coordinated
IGS
Uncertainty from Bruxer 2010
D (m3/s)
L2SWBM
Coordinated
Regulation Limit
ΔH (mm)
1950
1951
1952
1953
1954
1955
1956
1957
1958
1959

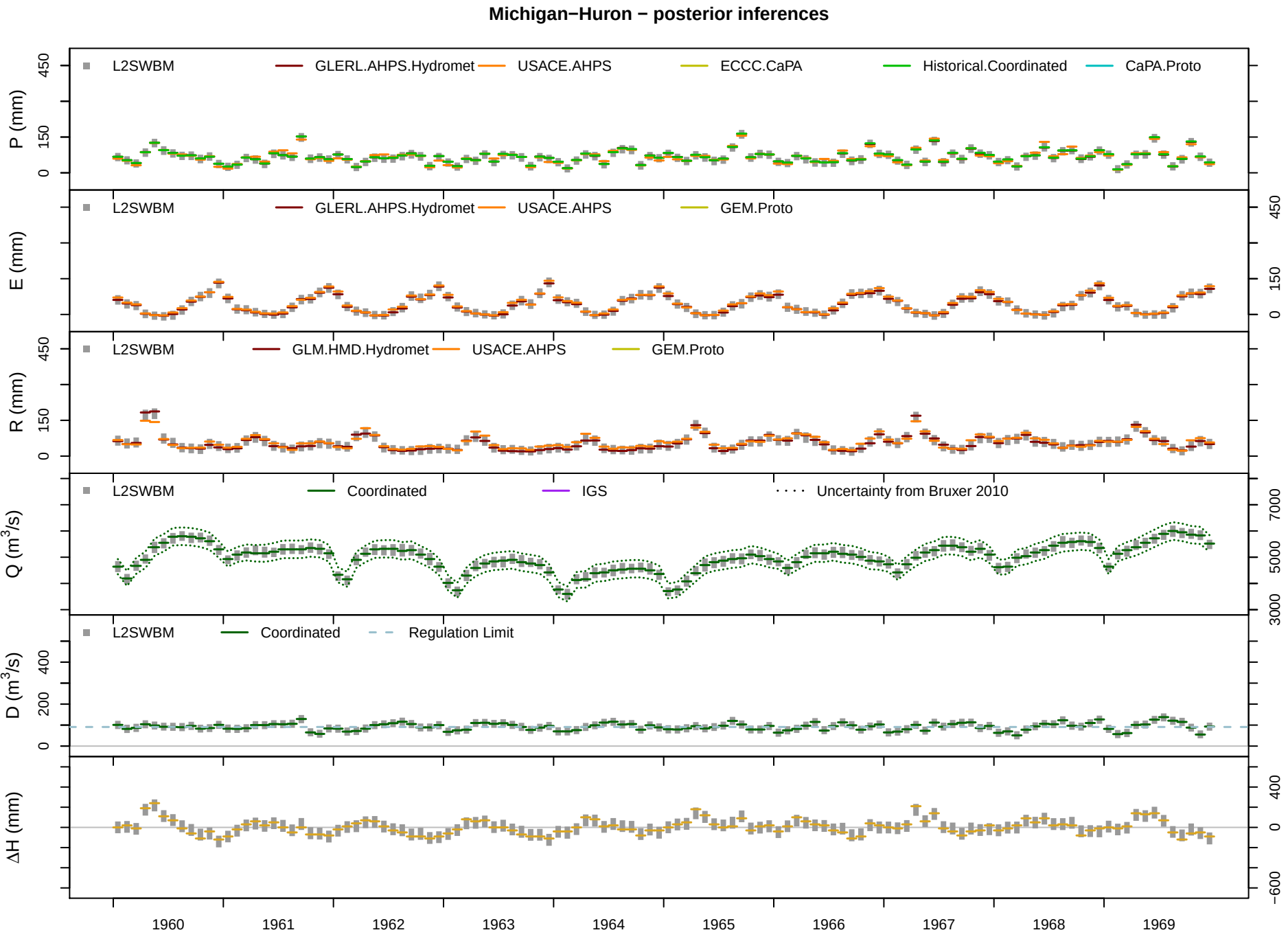
Michigan−Huron − posterior inferences
P (mm)
L2SWBM
GLERL.AHPS.Hydromet
USACE.AHPS
ECCC.CaPA
Historical.Coordinated
CaPA.Proto
E (mm)
L2SWBM
GLERL.AHPS.Hydromet
USACE.AHPS
GEM.Proto
R (mm)
L2SWBM
GLM.HMD.Hydromet
USACE.AHPS
GEM.Proto
Q (m3/s)
L2SWBM
Coordinated
IGS
Uncertainty from Bruxer 2010
D (m3/s)
L2SWBM
Coordinated
Regulation Limit
ΔH (mm)
1960
1961
1962
1963
1964
1965
1966
1967
1968
1969

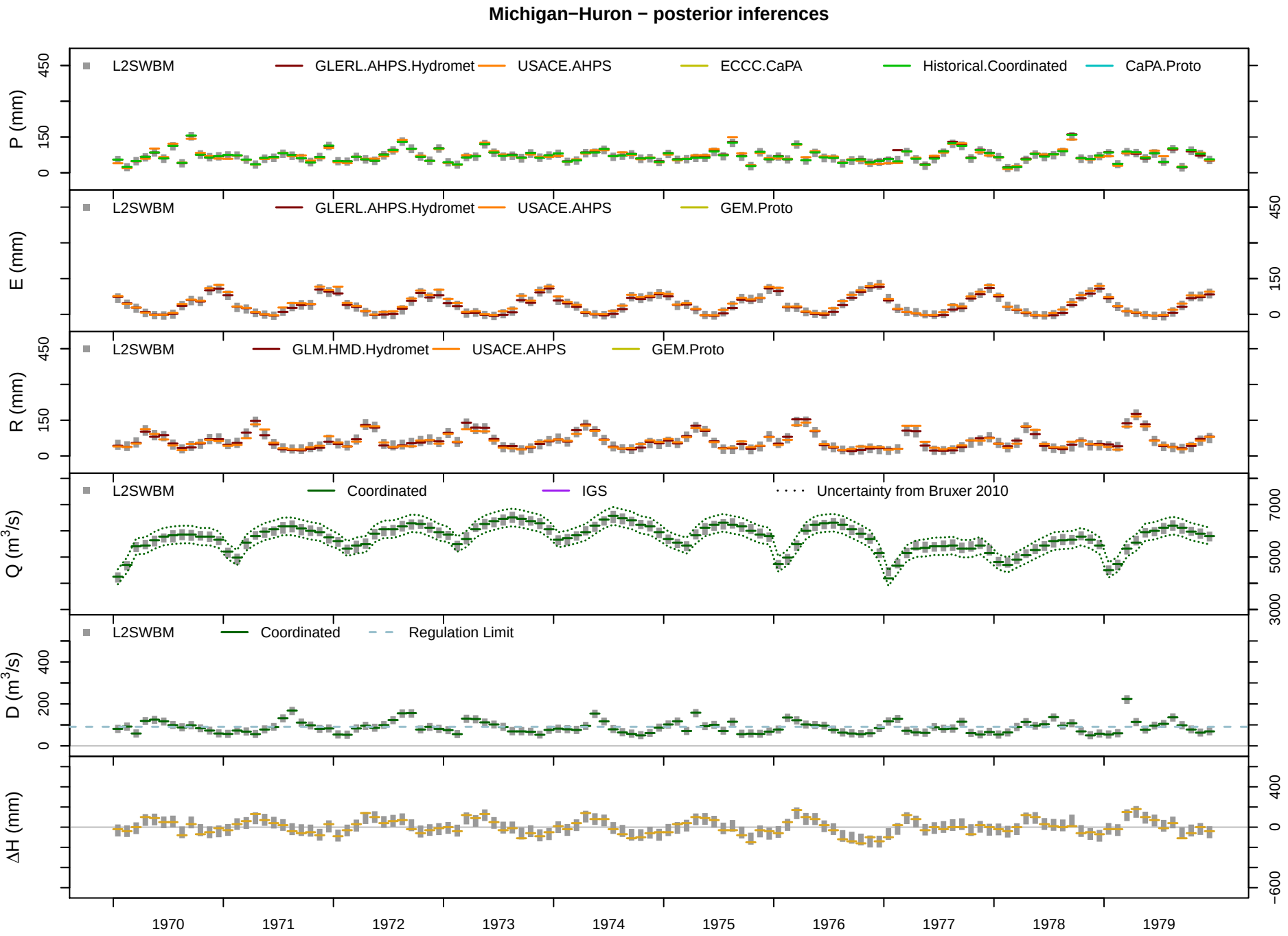
Michigan−Huron − posterior inferences
P (mm)
L2SWBM
GLERL.AHPS.Hydromet
USACE.AHPS
ECCC.CaPA
Historical.Coordinated
CaPA.Proto
E (mm)
L2SWBM
GLERL.AHPS.Hydromet
USACE.AHPS
GEM.Proto
R (mm)
L2SWBM
GLM.HMD.Hydromet
USACE.AHPS
GEM.Proto
Q (m3/s)
L2SWBM
Coordinated
IGS
Uncertainty from Bruxer 2010
D (m3/s)
L2SWBM
Coordinated
Regulation Limit
ΔH (mm)
1970
1971
1972
1973
1974
1975
1976
1977
1978
1979

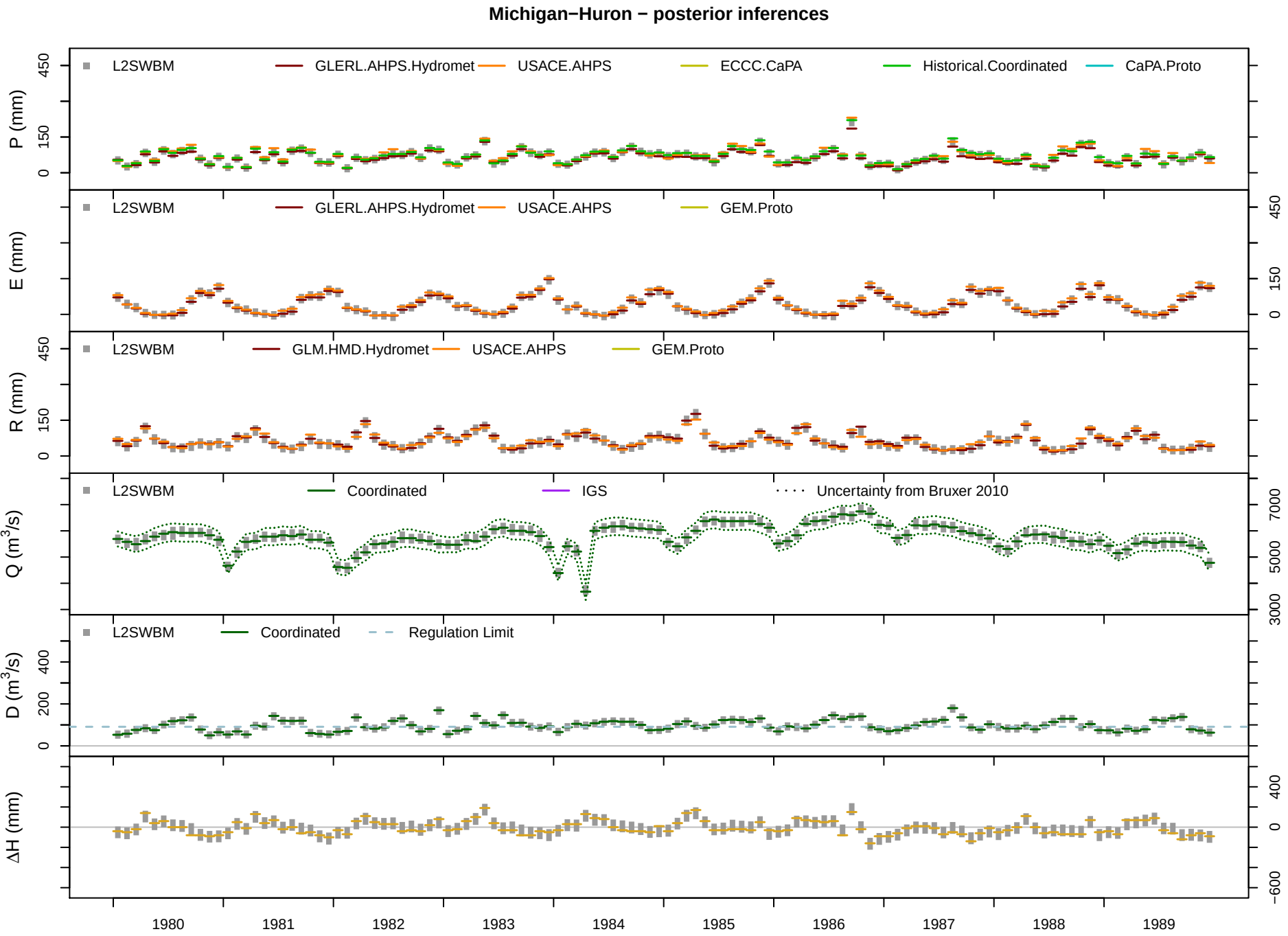
Michigan−Huron − posterior inferences
P (mm)
L2SWBM
GLERL.AHPS.Hydromet
USACE.AHPS
ECCC.CaPA
Historical.Coordinated
CaPA.Proto
E (mm)
L2SWBM
GLERL.AHPS.Hydromet
USACE.AHPS
GEM.Proto
R (mm)
L2SWBM
GLM.HMD.Hydromet
USACE.AHPS
GEM.Proto
Q (m3/s)
L2SWBM
Coordinated
IGS
Uncertainty from Bruxer 2010
D (m3/s)
L2SWBM
Coordinated
Regulation Limit
ΔH (mm)
1980
1981
1982
1983
1984
1985
1986
1987
1988
1989

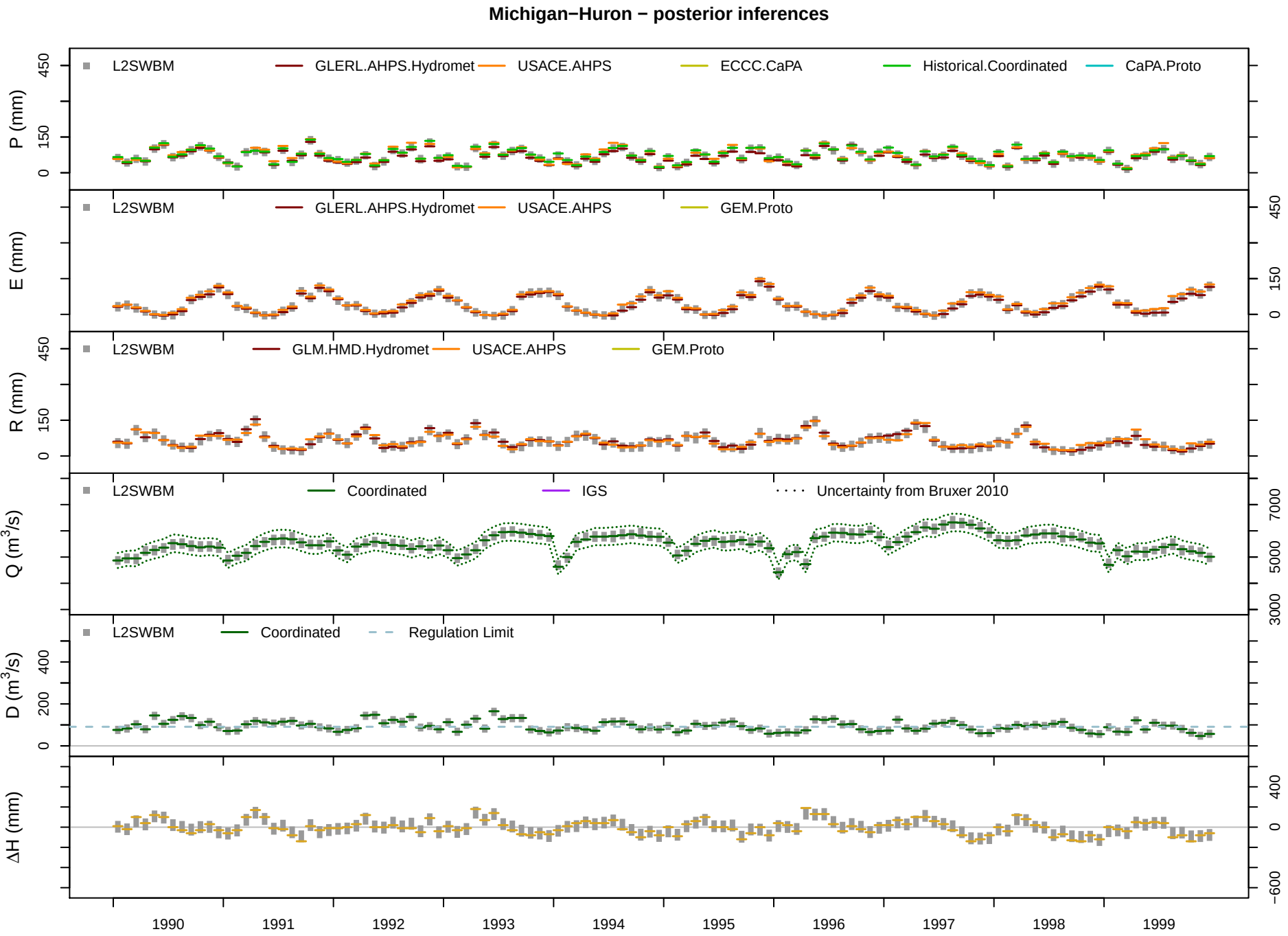
Michigan−Huron − posterior inferences
P (mm)
L2SWBM
GLERL.AHPS.Hydromet
USACE.AHPS
ECCC.CaPA
Historical.Coordinated
CaPA.Proto
E (mm)
L2SWBM
GLERL.AHPS.Hydromet
USACE.AHPS
GEM.Proto
R (mm)
L2SWBM
GLM.HMD.Hydromet
USACE.AHPS
GEM.Proto
Q (m3/s)
L2SWBM
Coordinated
IGS
Uncertainty from Bruxer 2010
D (m3/s)
L2SWBM
Coordinated
Regulation Limit
ΔH (mm)
1990
1991
1992
1993
1994
1995
1996
1997
1998
1999

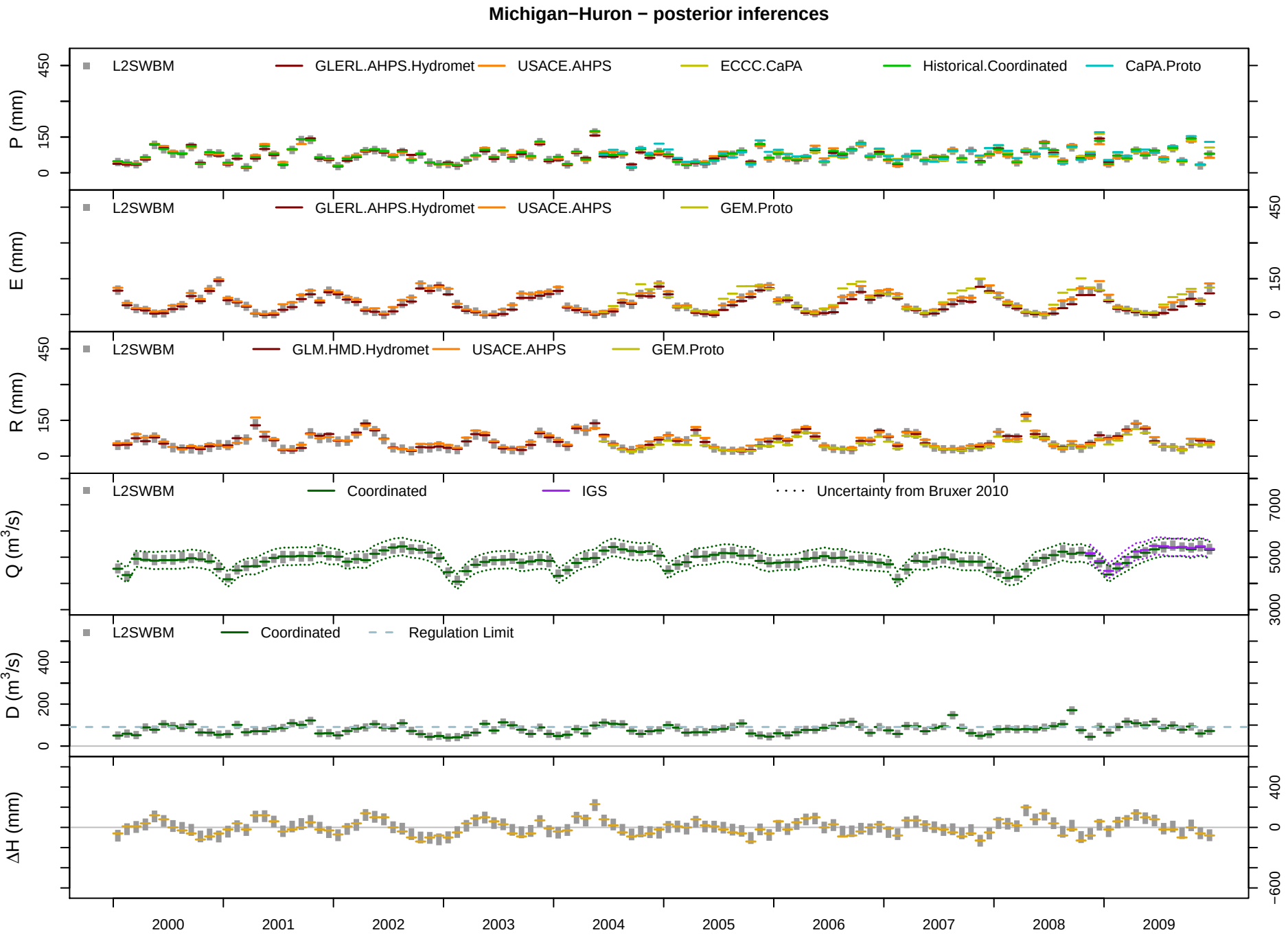
Michigan−Huron − posterior inferences
P (mm)
L2SWBM
GLERL.AHPS.Hydromet
USACE.AHPS
ECCC.CaPA
Historical.Coordinated
CaPA.Proto
E (mm)
L2SWBM
GLERL.AHPS.Hydromet
USACE.AHPS
GEM.Proto
R (mm)
L2SWBM
GLM.HMD.Hydromet
USACE.AHPS
GEM.Proto
Q (m3/s)
L2SWBM
Coordinated
IGS
Uncertainty from Bruxer 2010
D (m3/s)
L2SWBM
Coordinated
Regulation Limit
ΔH (mm)
2000
2001
2002
2003
2004
2005
2006
2007
2008
2009

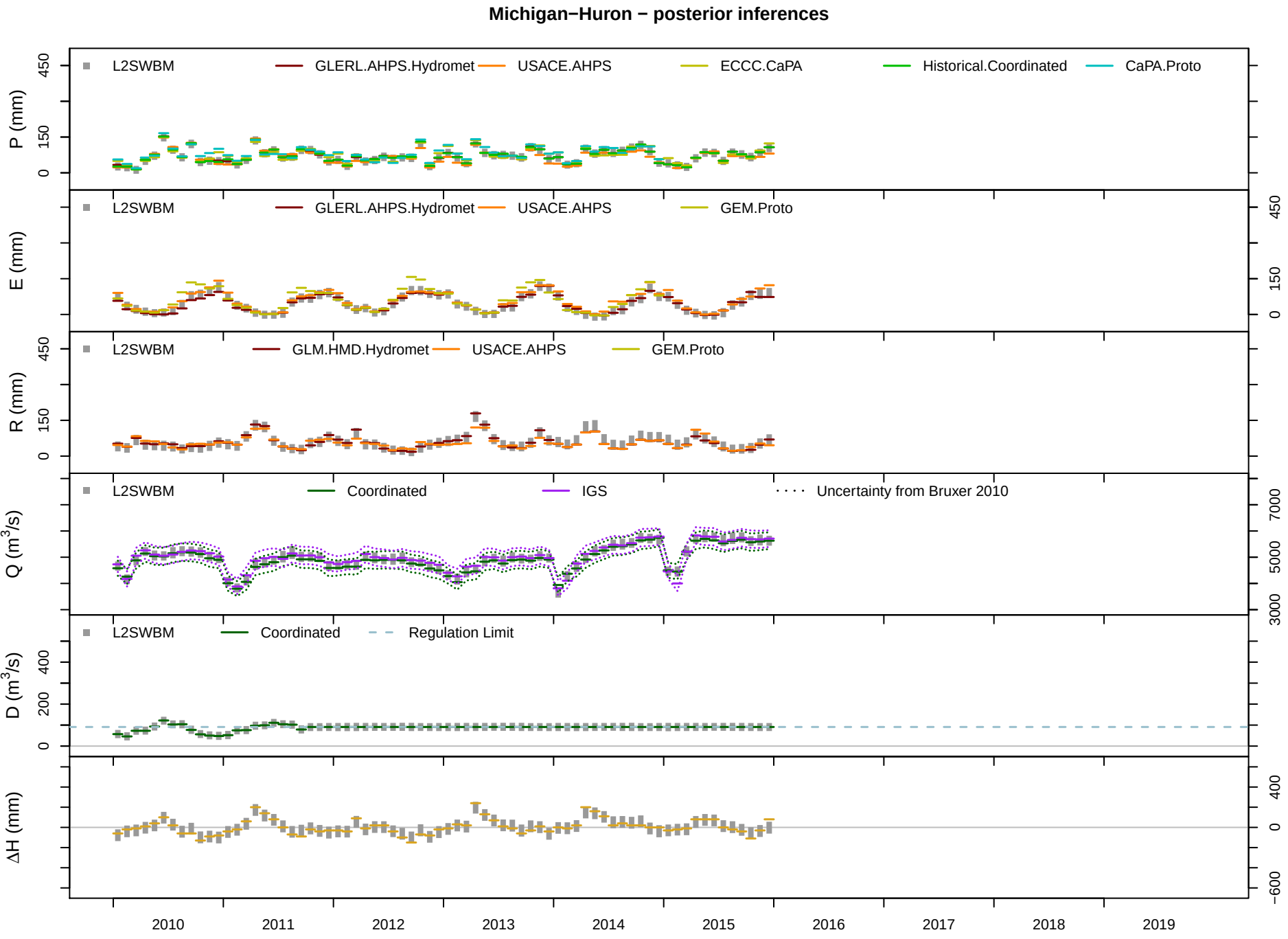
Michigan−Huron − posterior inferences
P (mm)
L2SWBM
GLERL.AHPS.Hydromet
USACE.AHPS
ECCC.CaPA
Historical.Coordinated
CaPA.Proto
E (mm)
L2SWBM
GLERL.AHPS.Hydromet
USACE.AHPS
GEM.Proto
R (mm)
L2SWBM
GLM.HMD.Hydromet
USACE.AHPS
GEM.Proto
Q (m3/s)
L2SWBM
Coordinated
IGS
Uncertainty from Bruxer 2010
D (m3/s)
L2SWBM
Coordinated
Regulation Limit
ΔH (mm)
2010
2011
2012
2013
2014
2015
2016
2017
2018
2019

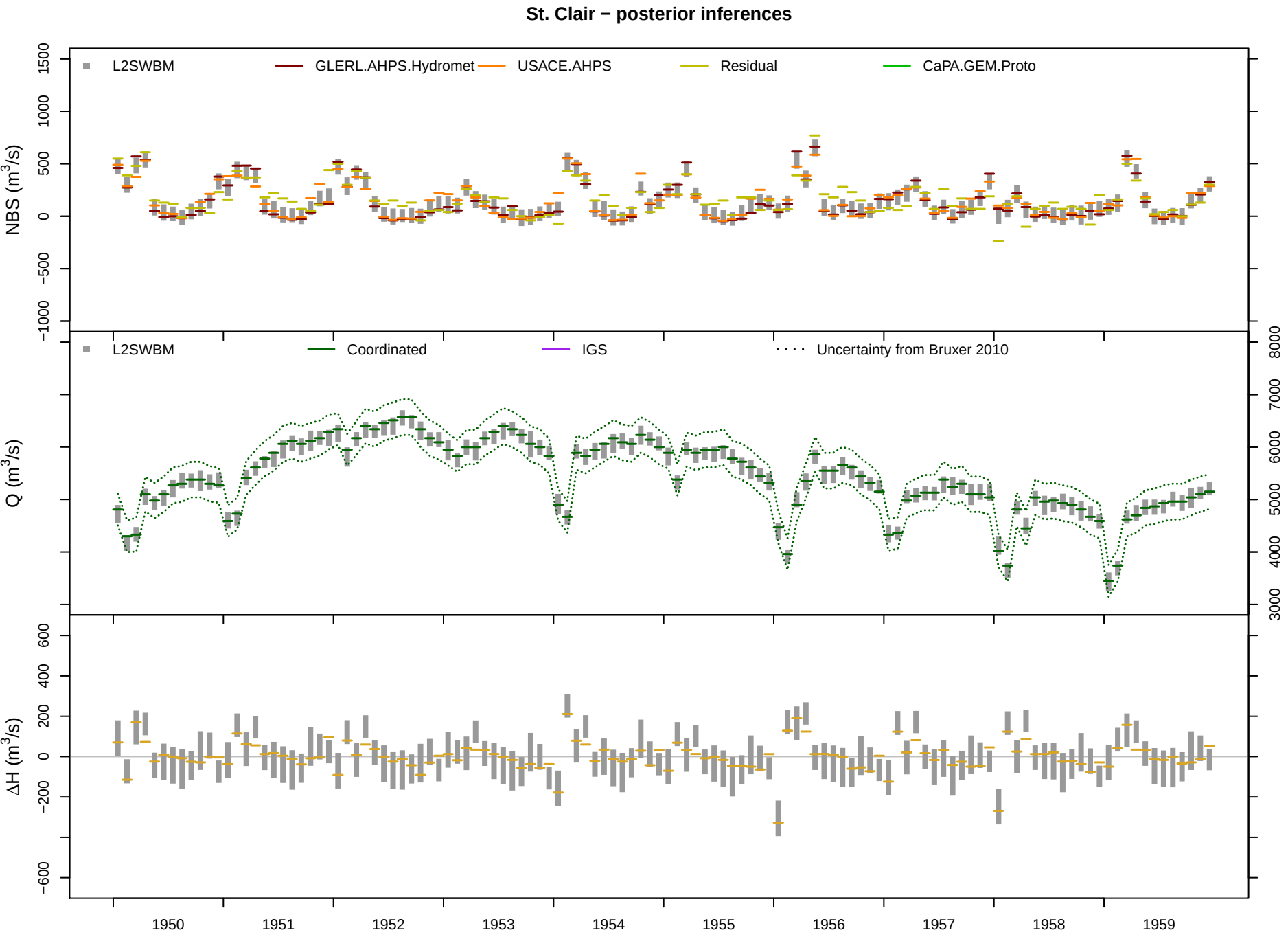
St. Clair − posterior inferences
L2SWBM
GLERL.AHPS.Hydromet
USACE.AHPS
Residual
CaPA.GEM.Proto
NBS (m3/s)
1500
1000
500
0
−500
−1000
L2SWBM
Coordinated
IGS
Uncertainty from Bruxer 2010
Q (m3/s)
8000
7000
6000
5000
4000
3000
ΔH (m3/s)
600
400
200
0
−200
−600
1950
1951
1952
1953
1954
1955
1956
1957
1958
1959

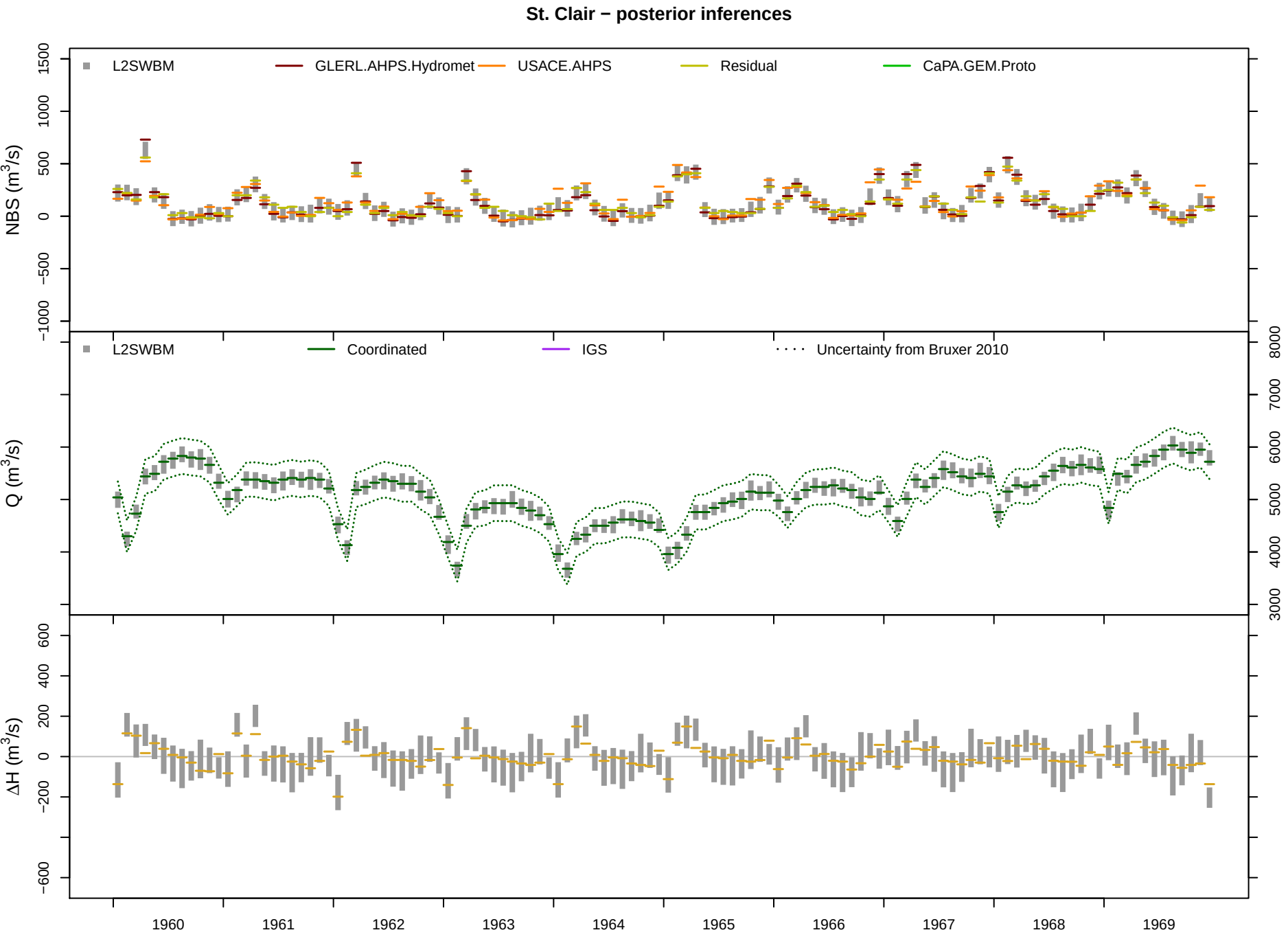
St. Clair − posterior inferences
L2SWBM
GLERL.AHPS.Hydromet
USACE.AHPS
Residual
CaPA.GEM.Proto
NBS (m3/s)
1500
1000
500
0
−500
−1000
L2SWBM
Coordinated
IGS
Uncertainty from Bruxer 2010
Q (m3/s)
8000
7000
6000
5000
4000
3000
ΔH (m3/s)
600
400
200
0
−200
−600
1960
1961
1962
1963
1964
1965
1966
1967
1968
1969

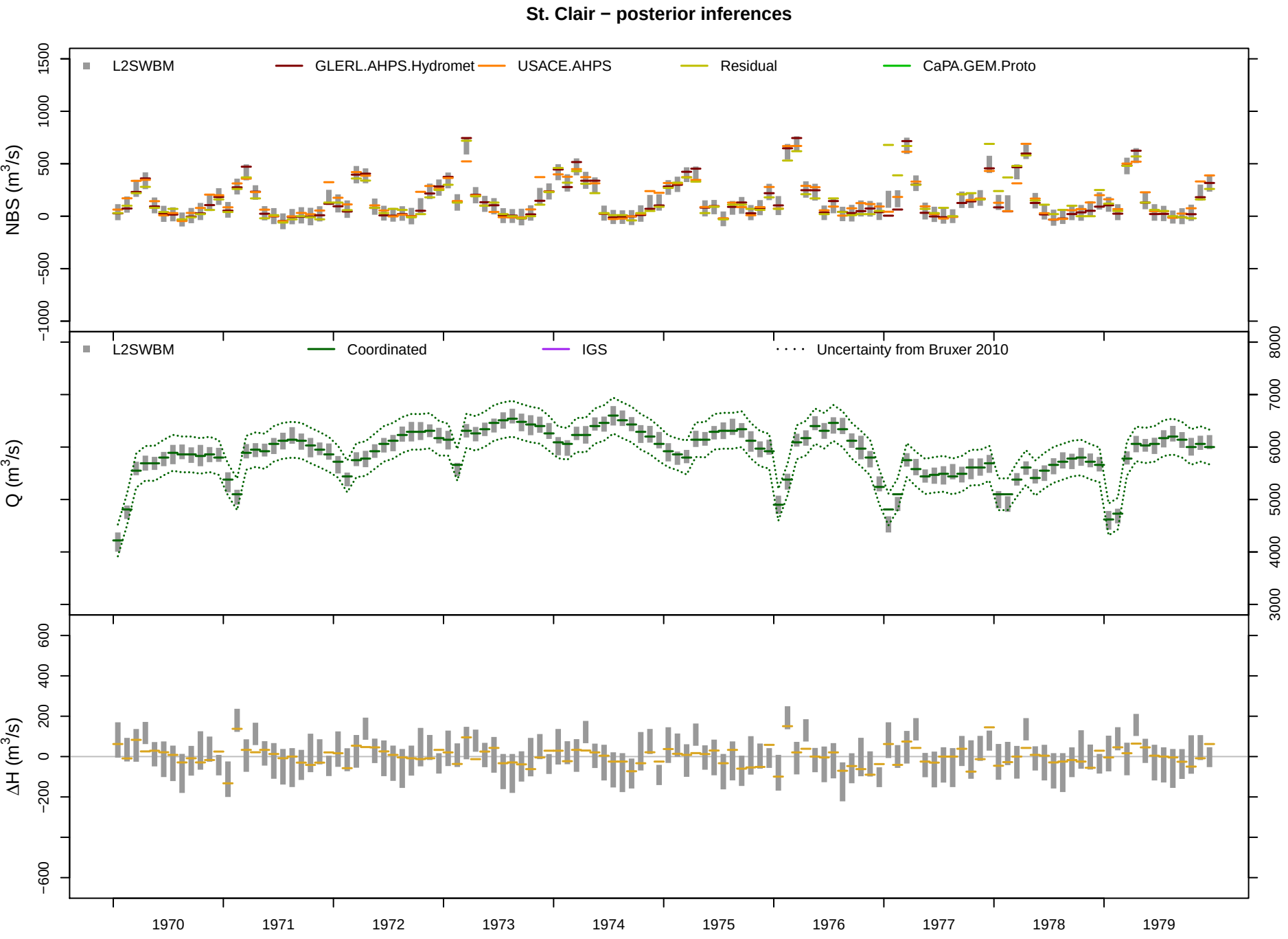
St. Clair − posterior inferences
L2SWBM
GLERL.AHPS.Hydromet
USACE.AHPS
Residual
CaPA.GEM.Proto
NBS (m3/s)
1500
1000
500
0
−500
−1000
L2SWBM
Coordinated
IGS
Uncertainty from Bruxer 2010
Q (m3/s)
8000
7000
6000
5000
4000
3000
ΔH (m3/s)
600
400
200
0
−200
−600
1970
1971
1972
1973
1974
1975
1976
1977
1978
1979

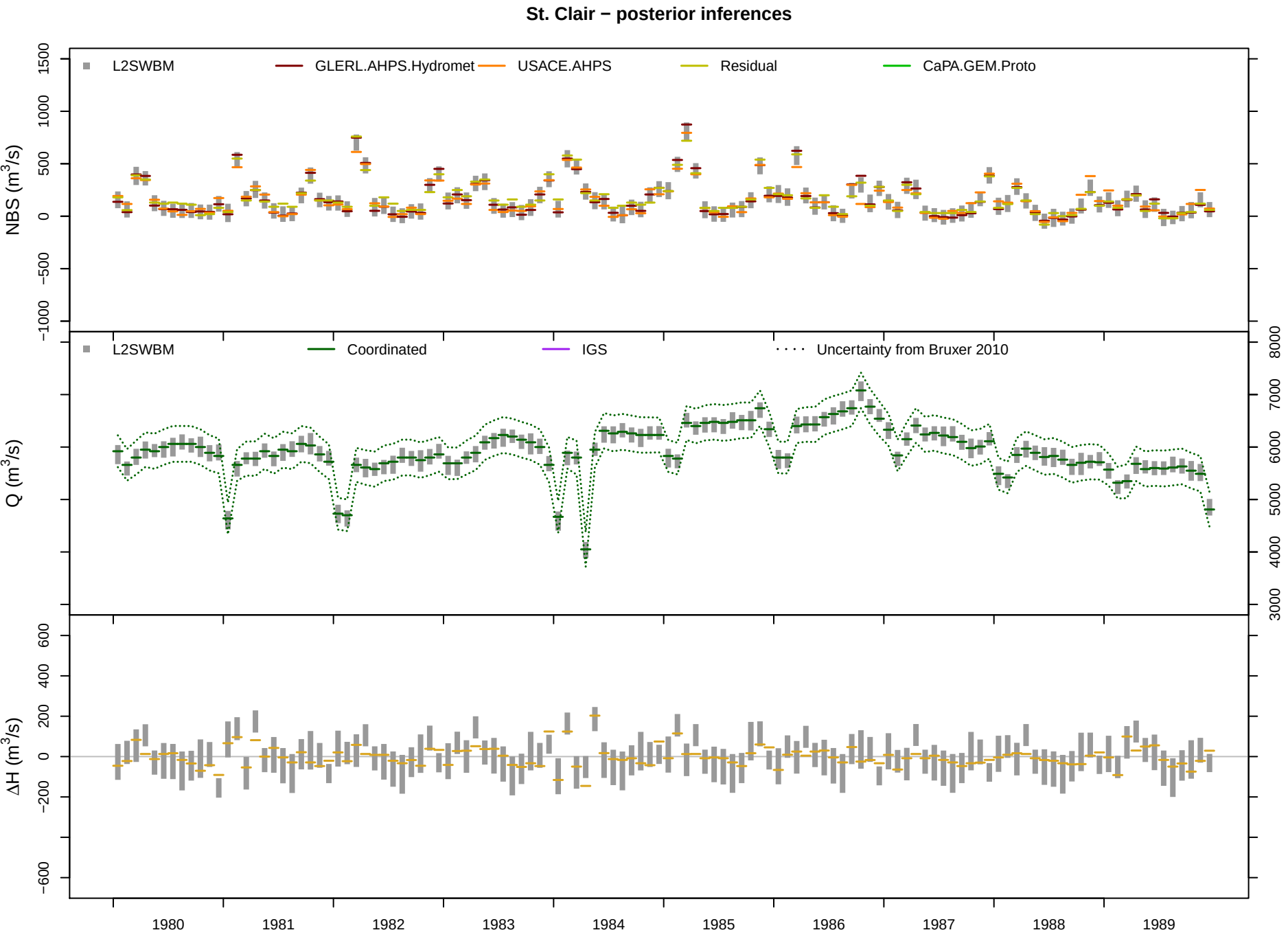
St. Clair − posterior inferences
L2SWBM
GLERL.AHPS.Hydromet
USACE.AHPS
Residual
CaPA.GEM.Proto
NBS (m3/s)
1500
1000
500
0
−500
−1000
L2SWBM
Coordinated
IGS
Uncertainty from Bruxer 2010
Q (m3/s)
8000
7000
6000
5000
4000
3000
ΔH (m3/s)
600
400
200
0
−200
−600
1980
1981
1982
1983
1984
1985
1986
1987
1988
1989

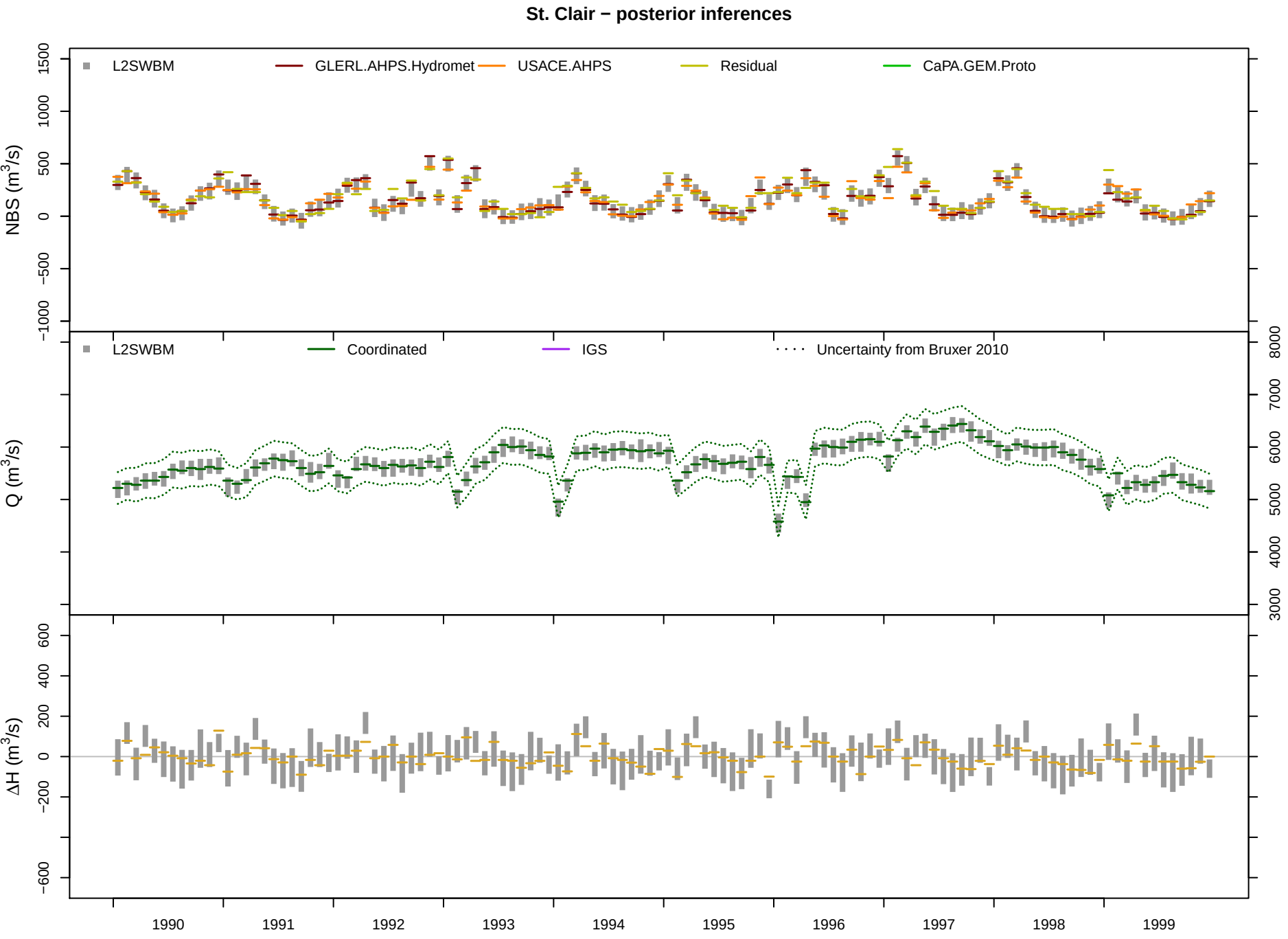
St. Clair − posterior inferences
L2SWBM
GLERL.AHPS.Hydromet
USACE.AHPS
Residual
CaPA.GEM.Proto
NBS (m3/s)
1500
1000
500
0
−500
−1000
L2SWBM
Coordinated
IGS
Uncertainty from Bruxer 2010
Q (m3/s)
8000
7000
6000
5000
4000
3000
ΔH (m3/s)
600
400
200
0
−200
−600
1990
1991
1992
1993
1994
1995
1996
1997
1998
1999

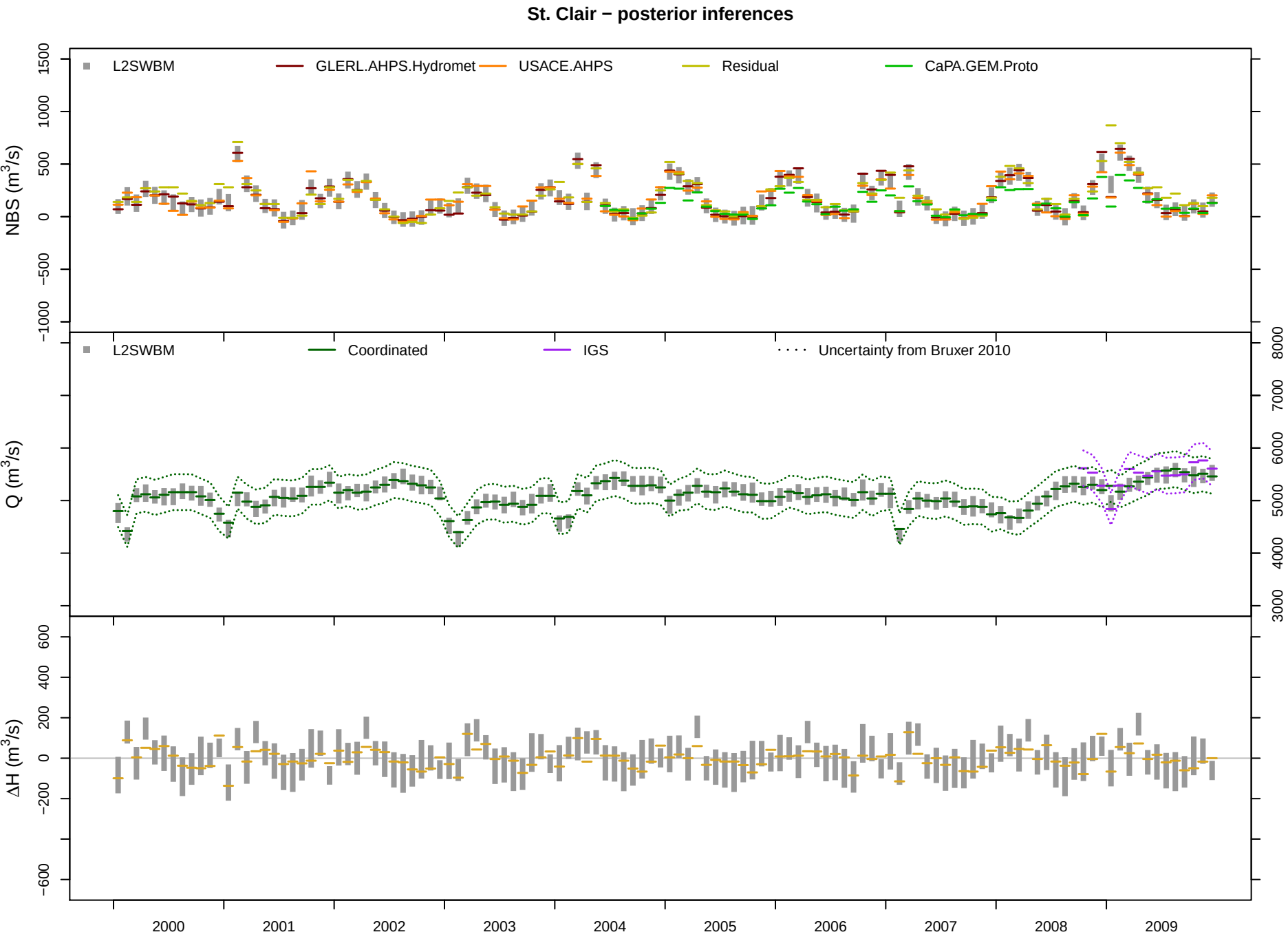
St. Clair − posterior inferences
L2SWBM
GLERL.AHPS.Hydromet
USACE.AHPS
Residual
CaPA.GEM.Proto
NBS (m3/s)
1500
1000
500
0
−500
−1000
L2SWBM
Coordinated
IGS
Uncertainty from Bruxer 2010
Q (m3/s)
8000
7000
6000
5000
4000
3000
ΔH (m3/s)
600
400
200
0
−200
−600
2000
2001
2002
2003
2004
2005
2006
2007
2008
2009

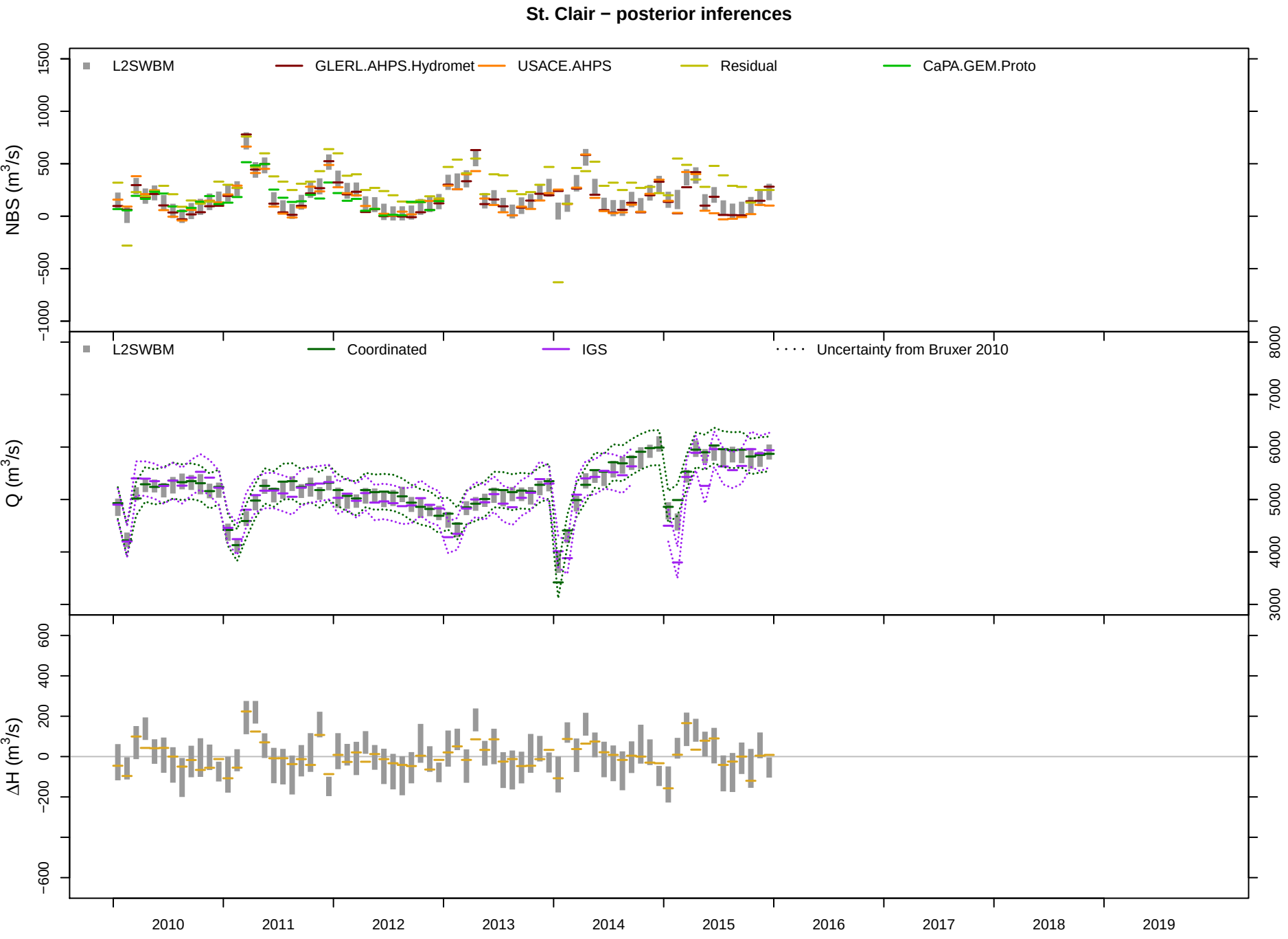
St. Clair − posterior inferences
L2SWBM
GLERL.AHPS.Hydromet
USACE.AHPS
Residual
CaPA.GEM.Proto
NBS (m3/s)
1500
1000
500
0
−500
−1000
L2SWBM
Coordinated
IGS
Uncertainty from Bruxer 2010
Q (m3/s)
8000
7000
6000
5000
4000
3000
ΔH (m3/s)
600
400
200
0
−200
−600
2010
2011
2012
2013
2014
2015
2016
2017
2018
2019

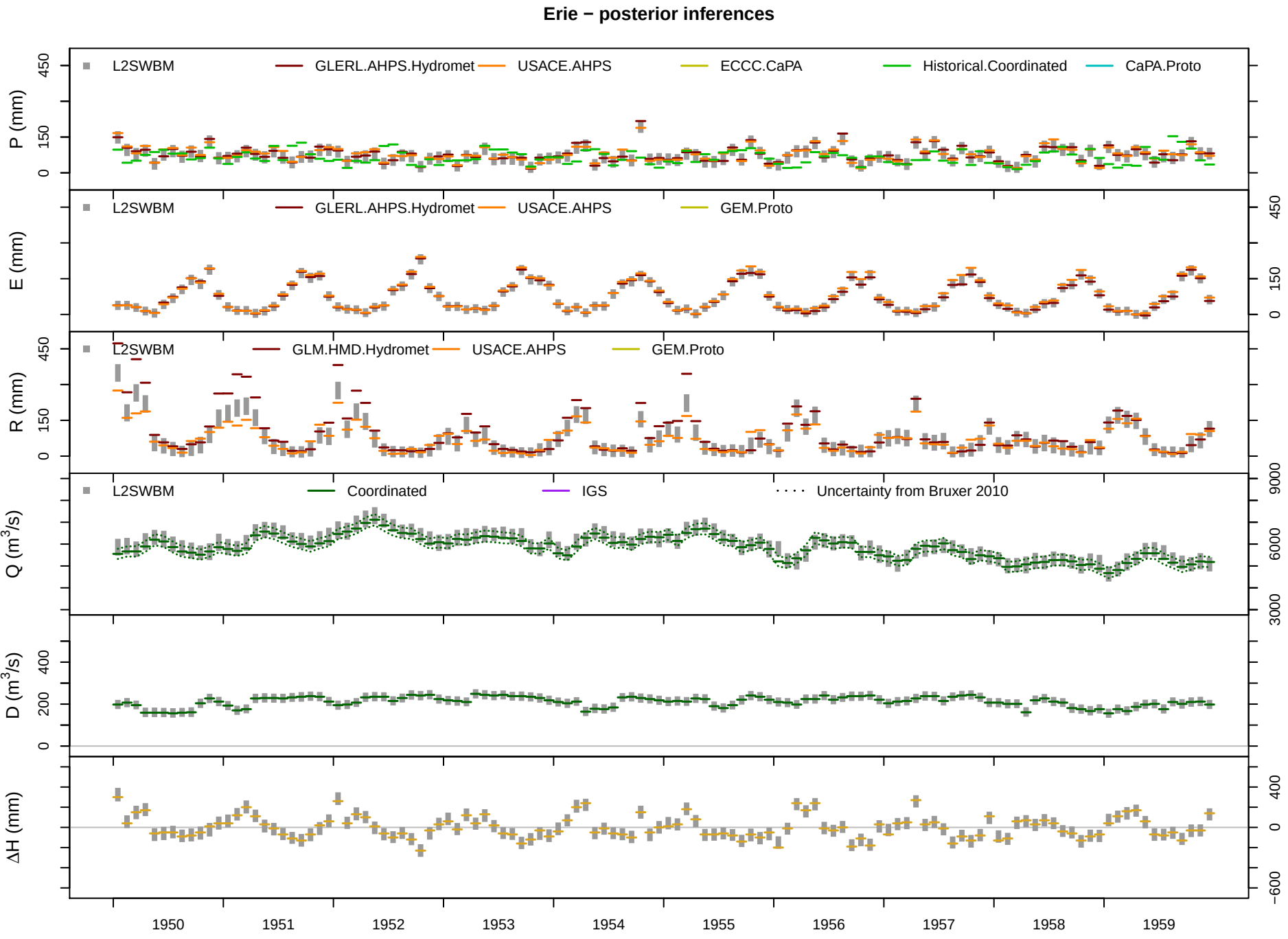
Erie − posterior inferences
P (mm)
L2SWBM
GLERL.AHPS.Hydromet
USACE.AHPS
ECCC.CaPA
Historical.Coordinated
CaPA.Proto
E (mm)
L2SWBM
GLERL.AHPS.Hydromet
USACE.AHPS
GEM.Proto
R (mm)
L2SWBM
GLM.HMD.Hydromet
USACE.AHPS
GEM.Proto
Q (m3/s)
L2SWBM
Coordinated
IGS
Uncertainty from Bruxer 2010
D (m3/s)
ΔH (mm)
1950
1951
1952
1953
1954
1955
1956
1957
1958
1959

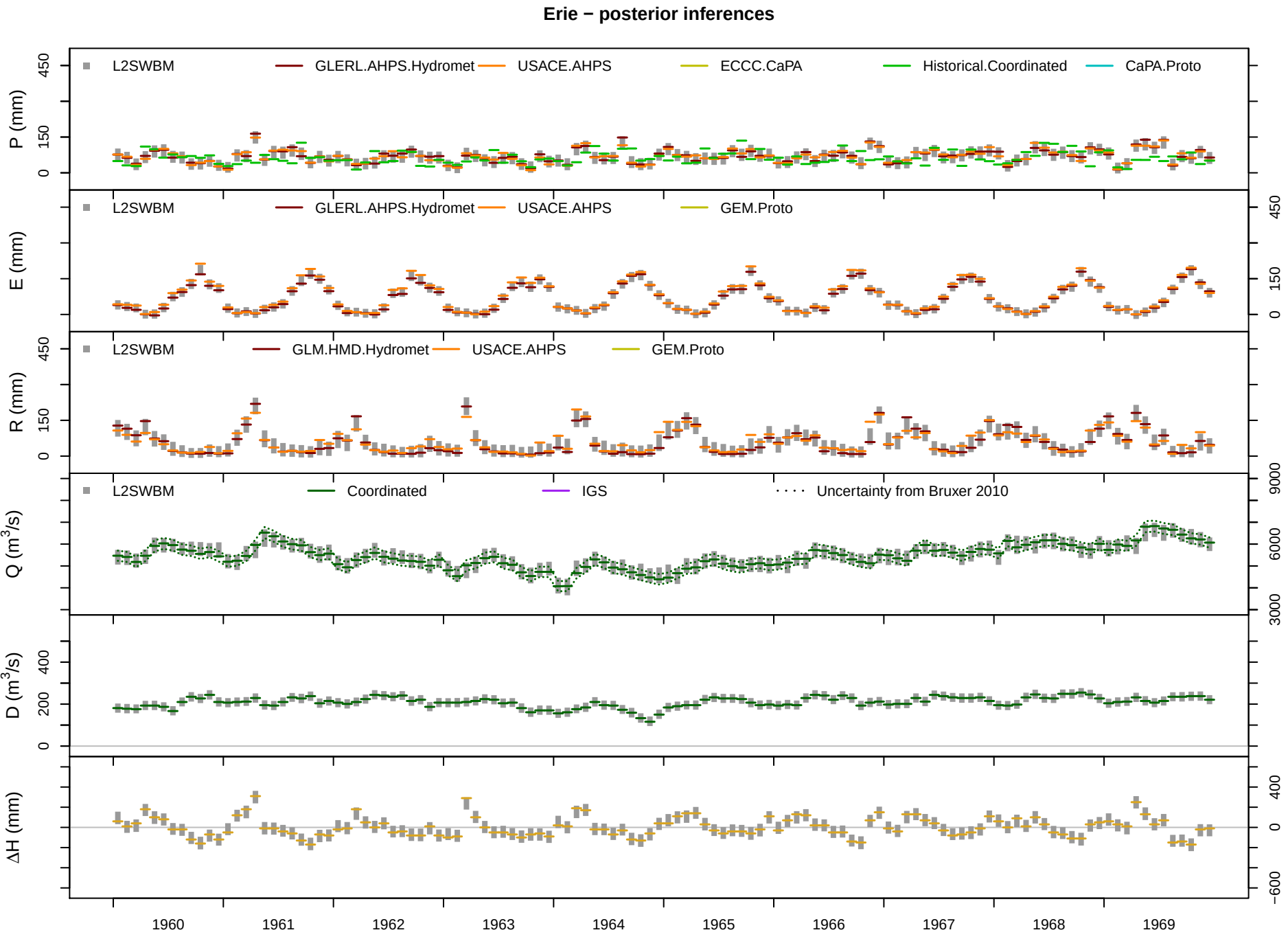
Erie − posterior inferences
P (mm)
L2SWBM
GLERL.AHPS.Hydromet
USACE.AHPS
ECCC.CaPA
Historical.Coordinated
CaPA.Proto
E (mm)
L2SWBM
GLERL.AHPS.Hydromet
USACE.AHPS
GEM.Proto
R (mm)
L2SWBM
GLM.HMD.Hydromet
USACE.AHPS
GEM.Proto
Q (m3/s)
L2SWBM
Coordinated
IGS
Uncertainty from Bruxer 2010
D (m3/s)
ΔH (mm)
1960
1961
1962
1963
1964
1965
1966
1967
1968
1969

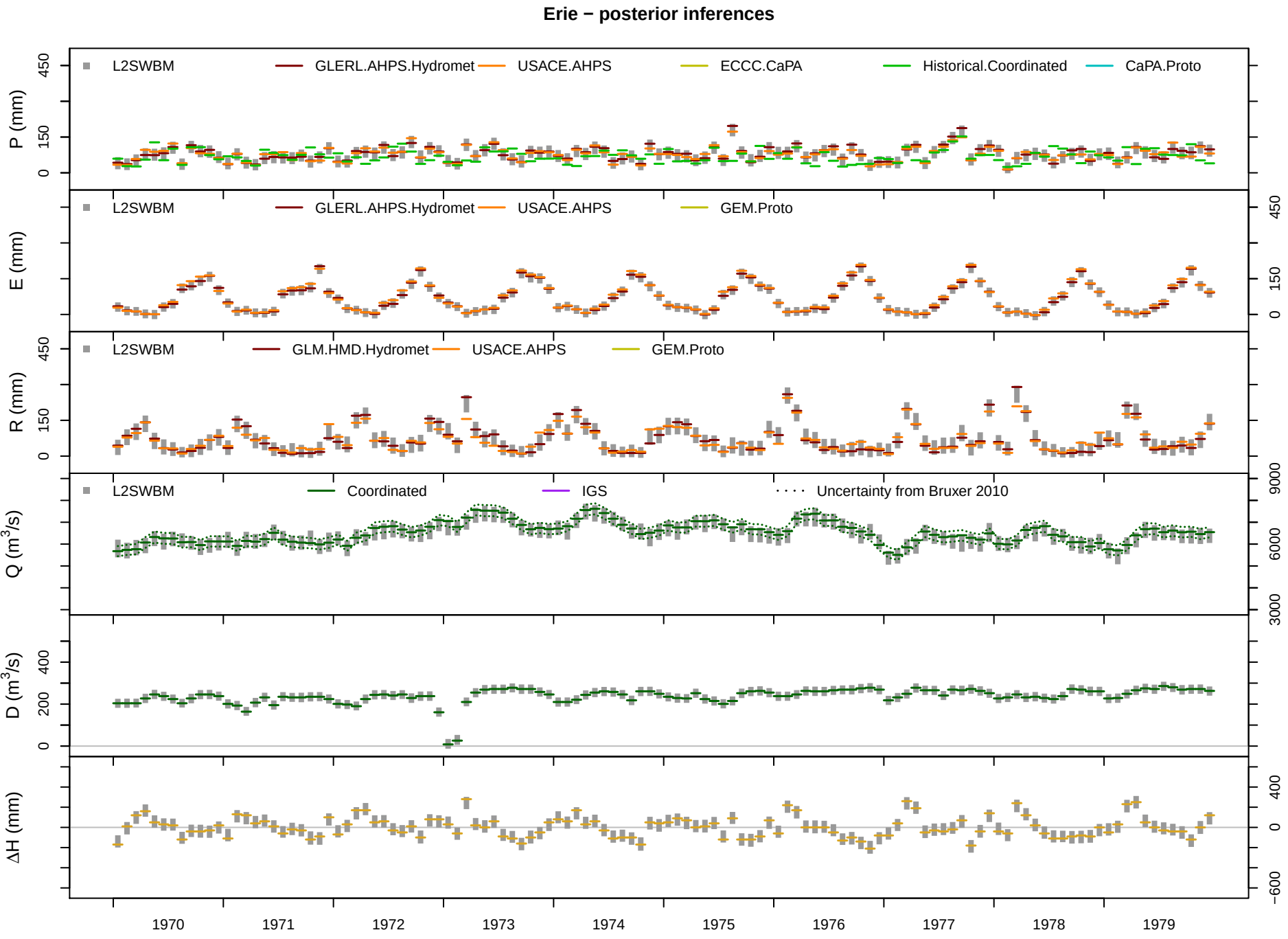
Erie − posterior inferences
P (mm)
L2SWBM
GLERL.AHPS.Hydromet
USACE.AHPS
ECCC.CaPA
Historical.Coordinated
CaPA.Proto
E (mm)
L2SWBM
GLERL.AHPS.Hydromet
USACE.AHPS
GEM.Proto
R (mm)
L2SWBM
GLM.HMD.Hydromet
USACE.AHPS
GEM.Proto
Q (m3/s)
L2SWBM
Coordinated
IGS
Uncertainty from Bruxer 2010
D (m3/s)
ΔH (mm)
1970
1971
1972
1973
1974
1975
1976
1977
1978
1979

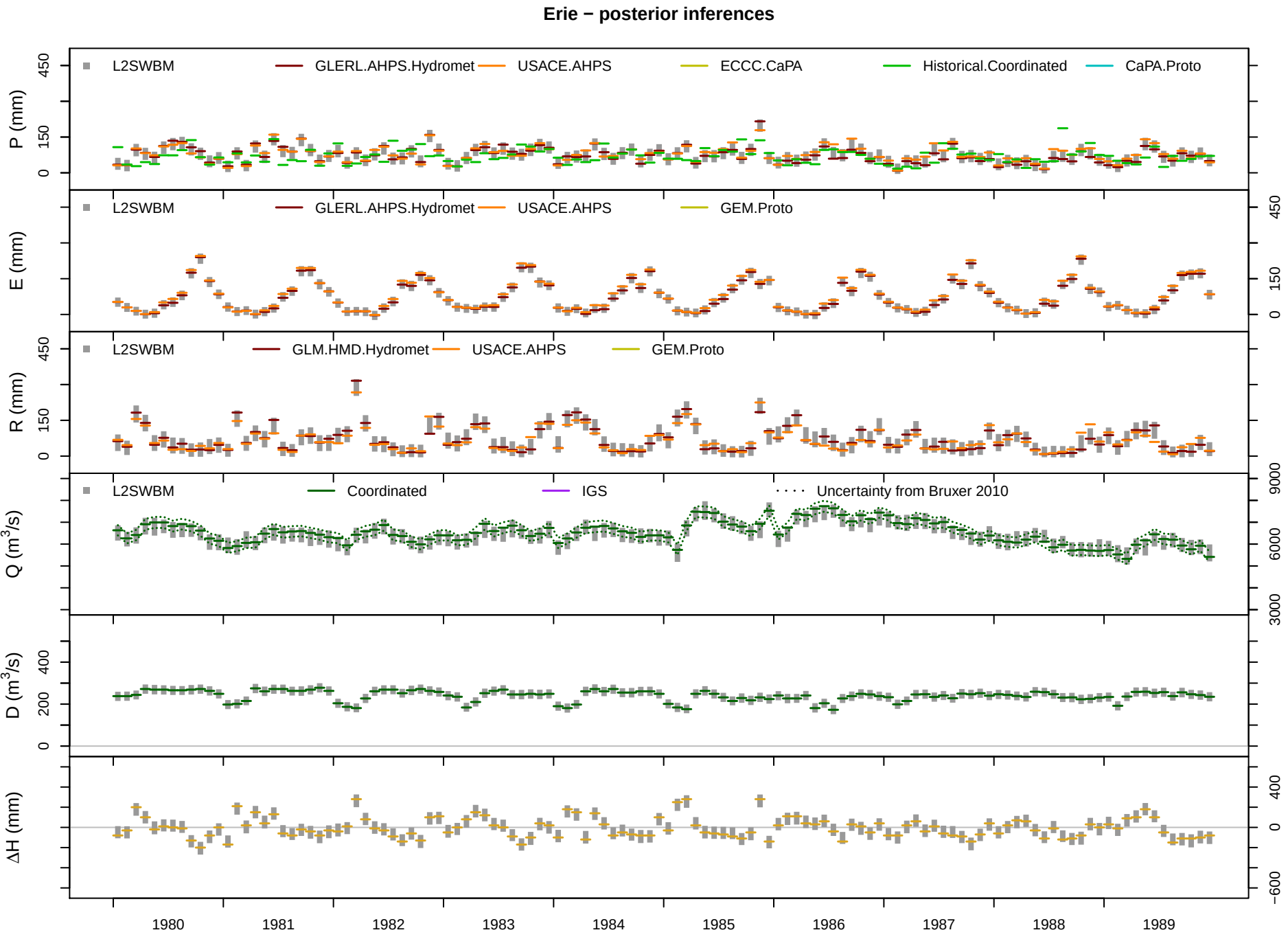
Erie − posterior inferences
P (mm)
L2SWBM
GLERL.AHPS.Hydromet
USACE.AHPS
ECCC.CaPA
Historical.Coordinated
CaPA.Proto
E (mm)
L2SWBM
GLERL.AHPS.Hydromet
USACE.AHPS
GEM.Proto
R (mm)
L2SWBM
GLM.HMD.Hydromet
USACE.AHPS
GEM.Proto
Q (m3/s)
L2SWBM
Coordinated
IGS
Uncertainty from Bruxer 2010
D (m3/s)
ΔH (mm)
1980
1981
1982
1983
1984
1985
1986
1987
1988
1989

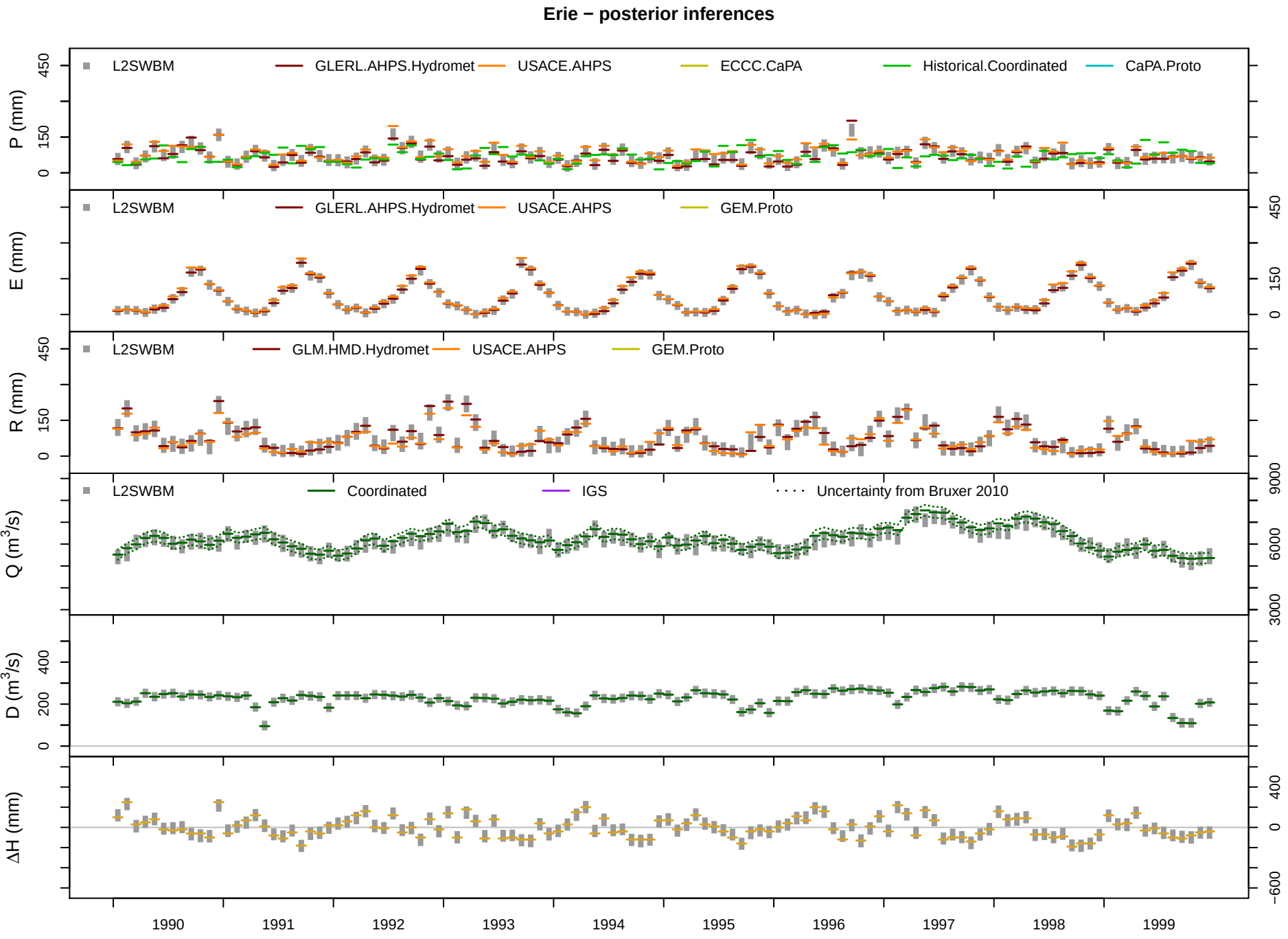
Erie − posterior inferences
P (mm)
L2SWBM
GLERL.AHPS.Hydromet
USACE.AHPS
ECCC.CaPA
Historical.Coordinated
CaPA.Proto
E (mm)
L2SWBM
GLERL.AHPS.Hydromet
USACE.AHPS
GEM.Proto
R (mm)
L2SWBM
GLM.HMD.Hydromet
USACE.AHPS
GEM.Proto
Q (m3/s)
L2SWBM
Coordinated
IGS
Uncertainty from Bruxer 2010
D (m3/s)
ΔH (mm)
1990
1991
1992
1993
1994
1995
1996
1997
1998
1999

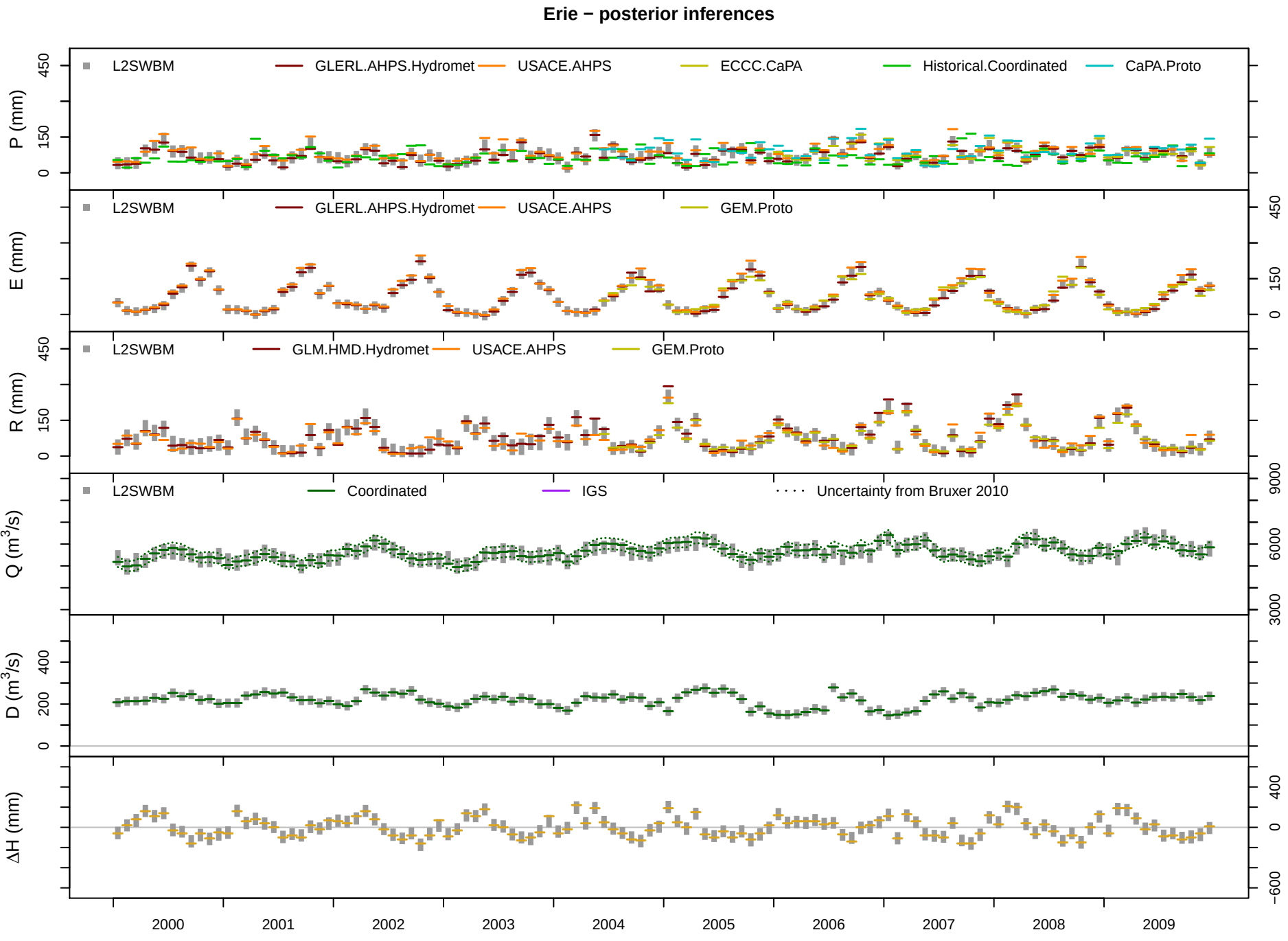
Erie − posterior inferences
P (mm)
L2SWBM
GLERL.AHPS.Hydromet
USACE.AHPS
ECCC.CaPA
Historical.Coordinated
CaPA.Proto
E (mm)
L2SWBM
GLERL.AHPS.Hydromet
USACE.AHPS
GEM.Proto
R (mm)
L2SWBM
GLM.HMD.Hydromet
USACE.AHPS
GEM.Proto
Q (m3/s)
L2SWBM
Coordinated
IGS
Uncertainty from Bruxer 2010
D (m3/s)
ΔH (mm)
2000
2001
2002
2003
2004
2005
2006
2007
2008
2009

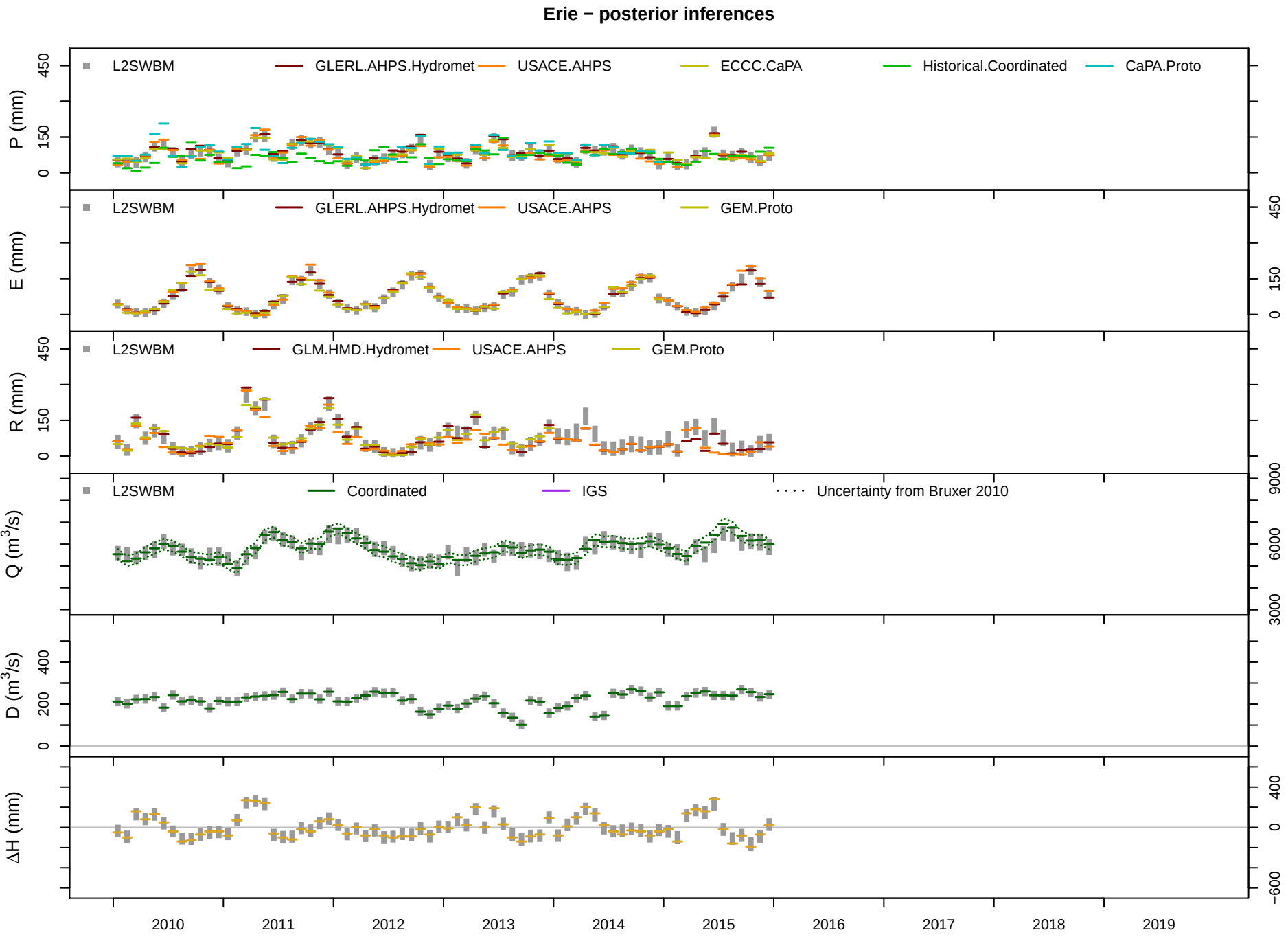
Erie − posterior inferences
P (mm)
L2SWBM
GLERL.AHPS.Hydromet
USACE.AHPS
ECCC.CaPA
Historical.Coordinated
CaPA.Proto
E (mm)
L2SWBM
GLERL.AHPS.Hydromet
USACE.AHPS
GEM.Proto
R (mm)
L2SWBM
GLM.HMD.Hydromet
USACE.AHPS
GEM.Proto
Q (m3/s)
L2SWBM
Coordinated
IGS
Uncertainty from Bruxer 2010
D (m3/s)
ΔH (mm)
2010
2011
2012
2013
2014
2015
2016
2017
2018
2019

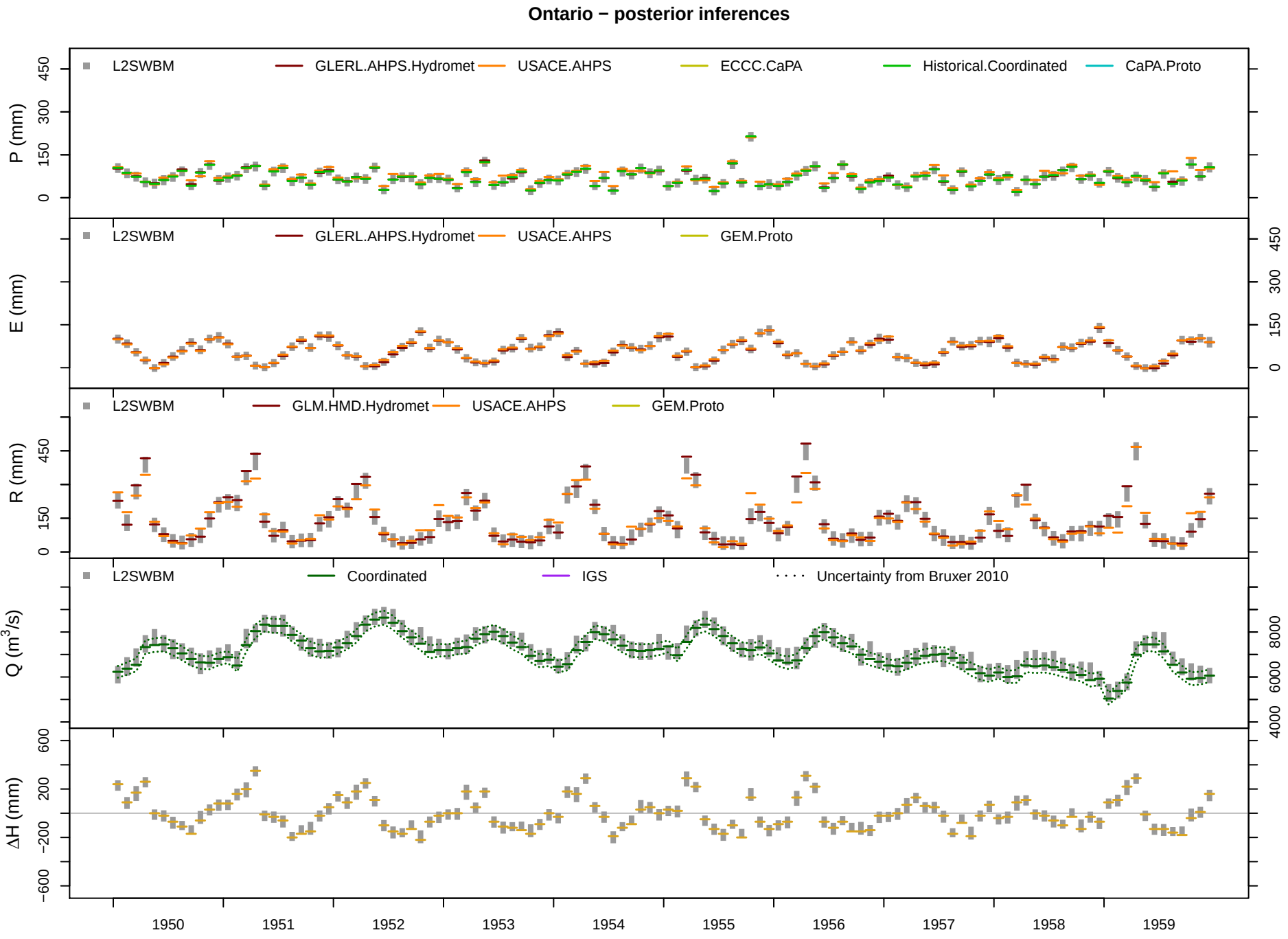
Ontario − posterior inferences
L2SWBM
GLERL.AHPS.Hydromet
USACE.AHPS
ECCC.CaPA
Historical.Coordinated
CaPA.Proto
P (mm)
L2SWBM
GLERL.AHPS.Hydromet
USACE.AHPS
GEM.Proto
E (mm)
L2SWBM
GLM.HMD.Hydromet
USACE.AHPS
GEM.Proto
R (mm)
L2SWBM
Coordinated
IGS
Uncertainty from Bruxer 2010
Q (m3/s)
ΔH (mm)
1950
1951
1952
1953
1954
1955
1956
1957
1958
1959

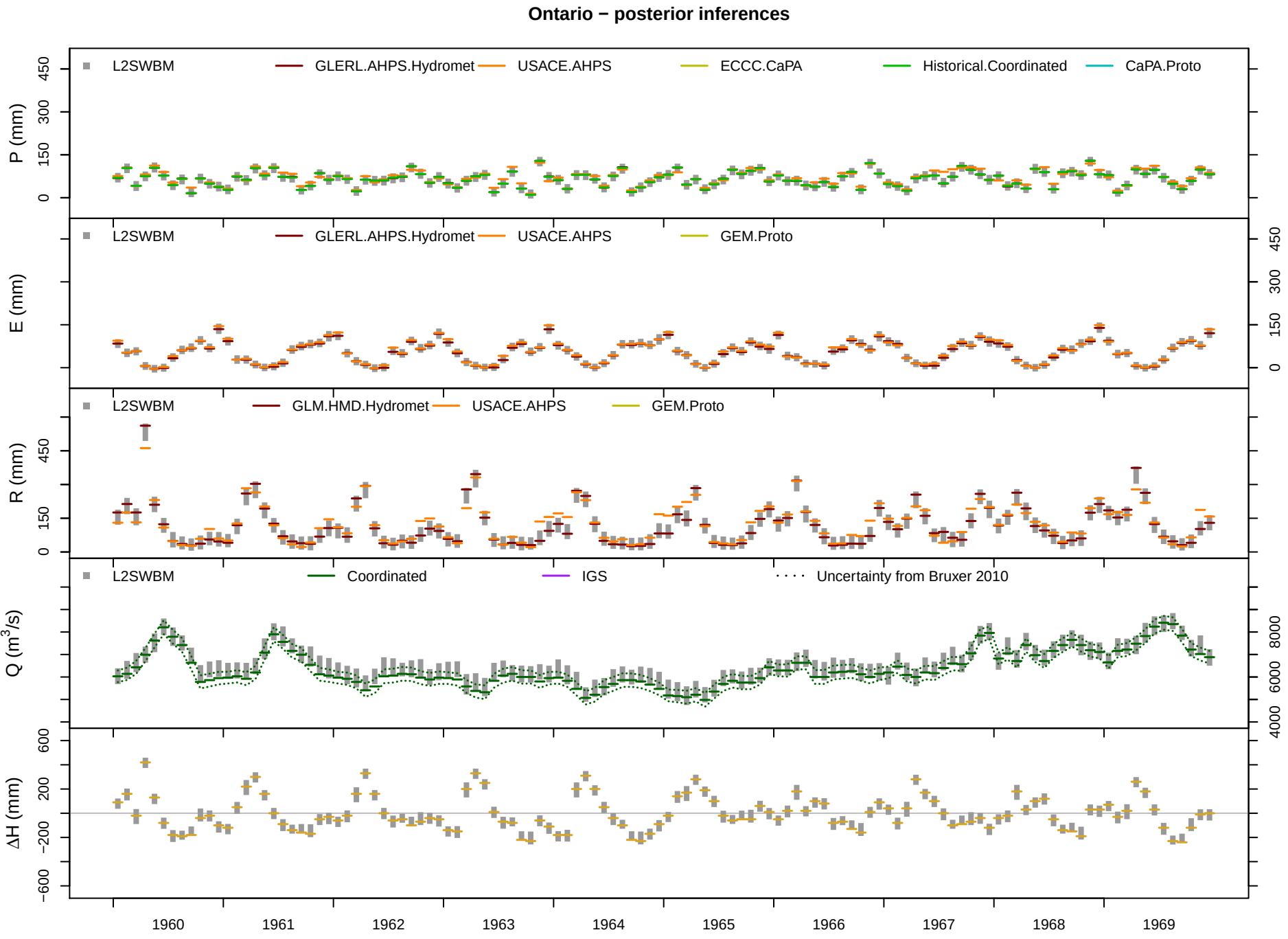
Ontario − posterior inferences
L2SWBM
GLERL.AHPS.Hydromet
USACE.AHPS
ECCC.CaPA
Historical.Coordinated
CaPA.Proto
P (mm)
0
150
300
450
L2SWBM
GLERL.AHPS.Hydromet
USACE.AHPS
GEM.Proto
E (mm)
0
150
300
450
L2SWBM
GLM.HMD.Hydromet
USACE.AHPS
GEM.Proto
R (mm)
0
150
450
L2SWBM
Coordinated
IGS
Uncertainty from Bruxer 2010
Q (m3/s)
4000
6000
8000
ΔH (mm)
−600
−200
200
600
1960
1961
1962
1963
1964
1965
1966
1967
1968
1969

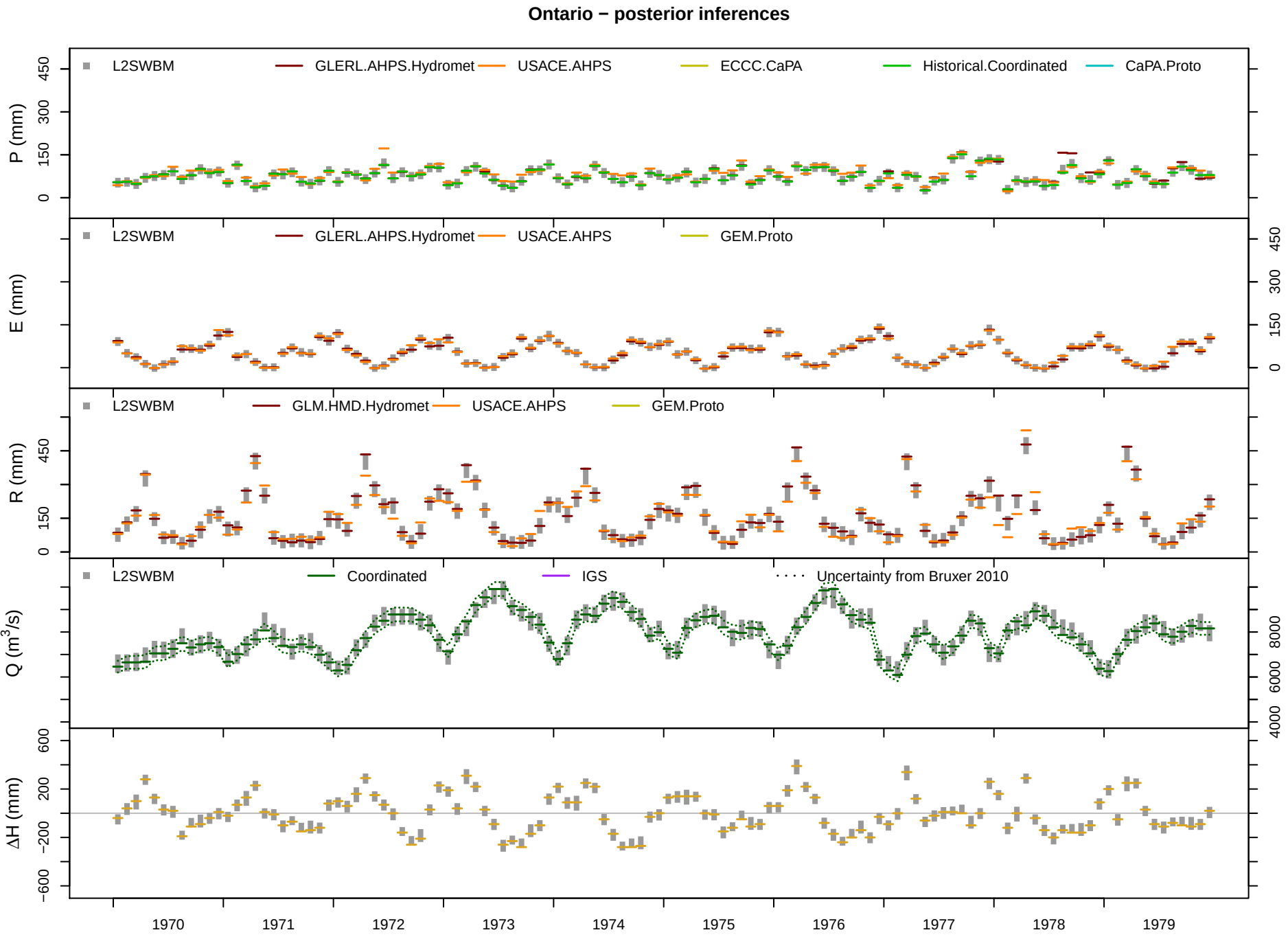
Ontario − posterior inferences
L2SWBM
GLERL.AHPS.Hydromet
USACE.AHPS
ECCC.CaPA
Historical.Coordinated
CaPA.Proto
P (mm)
0
150
300
450
L2SWBM
GLERL.AHPS.Hydromet
USACE.AHPS
GEM.Proto
E (mm)
0
150
300
450
L2SWBM
GLM.HMD.Hydromet
USACE.AHPS
GEM.Proto
R (mm)
0
150
450
L2SWBM
Coordinated
IGS
Uncertainty from Bruxer 2010
Q (m³/s)
4000
6000
8000
ΔH (mm)
−600
−200
200
600
1970
1971
1972
1973
1974
1975
1976
1977
1978
1979

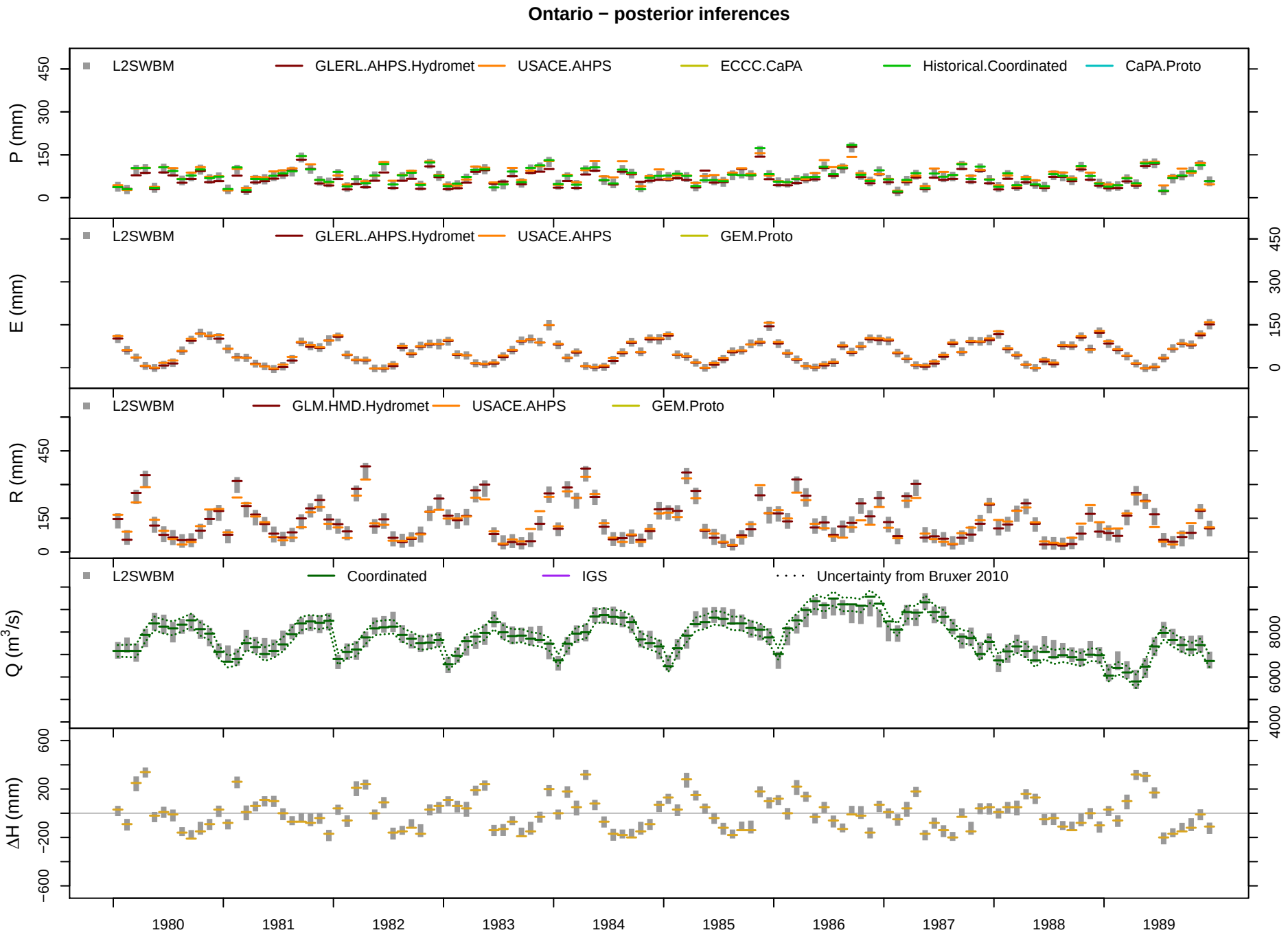
Ontario − posterior inferences
L2SWBM
GLERL.AHPS.Hydromet
USACE.AHPS
ECCC.CaPA
Historical.Coordinated
CaPA.Proto
P (mm)
L2SWBM
GLERL.AHPS.Hydromet
USACE.AHPS
GEM.Proto
E (mm)
L2SWBM
GLM.HMD.Hydromet
USACE.AHPS
GEM.Proto
R (mm)
L2SWBM
Coordinated
IGS
Uncertainty from Bruxer 2010
Q (m3/s)
ΔH (mm)
1980
1981
1982
1983
1984
1985
1986
1987
1988
1989

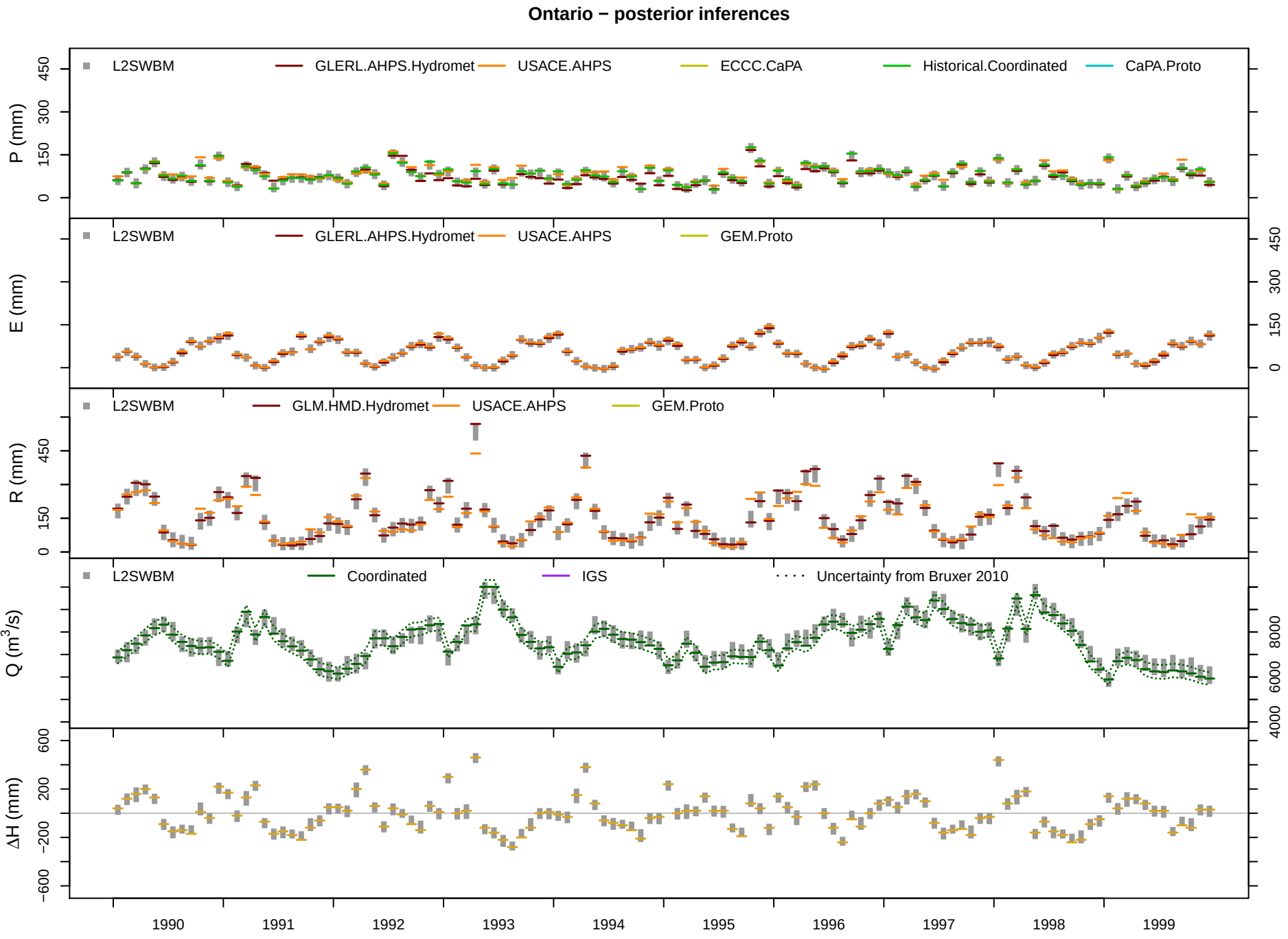
Ontario − posterior inferences
L2SWBM
GLERL.AHPS.Hydromet
USACE.AHPS
ECCC.CaPA
Historical.Coordinated
CaPA.Proto
P (mm)
L2SWBM
GLERL.AHPS.Hydromet
USACE.AHPS
GEM.Proto
E (mm)
L2SWBM
GLM.HMD.Hydromet
USACE.AHPS
GEM.Proto
R (mm)
L2SWBM
Coordinated
IGS
Uncertainty from Bruxer 2010
Q (m³/s)
ΔH (mm)
1990
1991
1992
1993
1994
1995
1996
1997
1998
1999

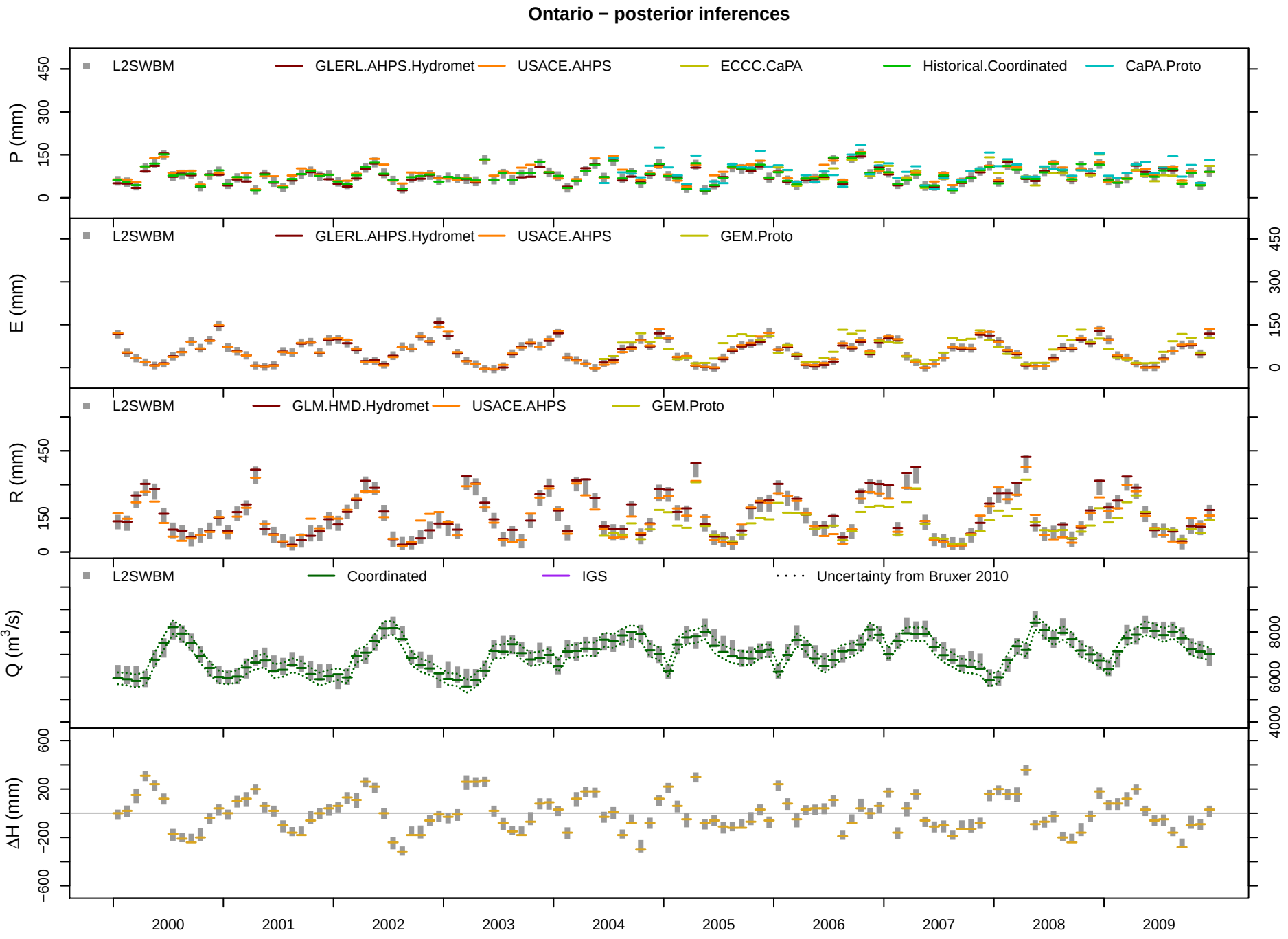
Ontario − posterior inferences
L2SWBM
GLERL.AHPS.Hydromet
USACE.AHPS
ECCC.CaPA
Historical.Coordinated
CaPA.Proto
P (mm)
GEM.Proto
E (mm)
GLM.HMD.Hydromet
R (mm)
Coordinated
IGS
Uncertainty from Bruxer 2010
Q (m³/s)
ΔH (mm)
2000
2001
2002
2003
2004
2005
2006
2007
2008
2009

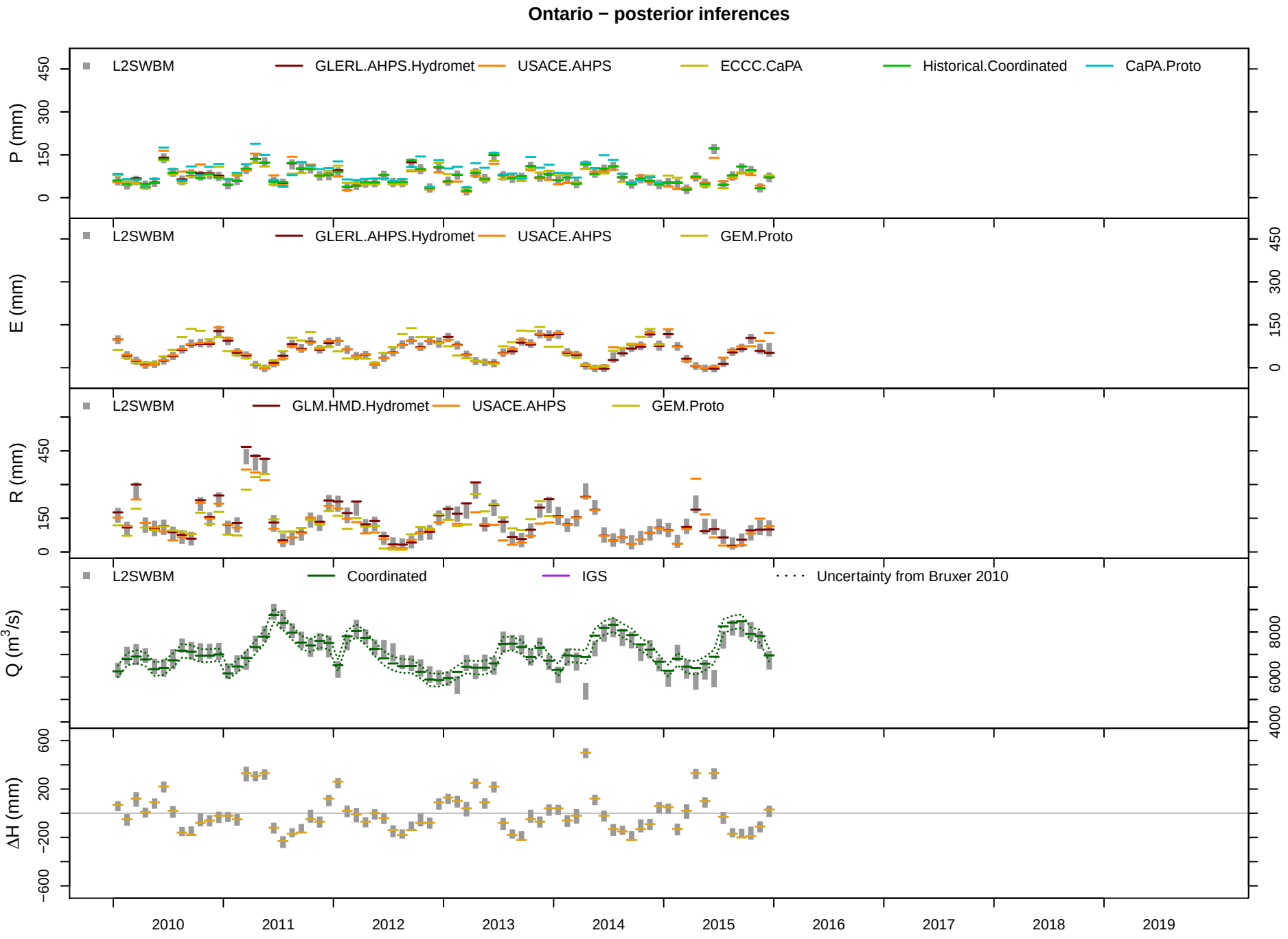
Ontario − posterior inferences
L2SWBM
GLERL.AHPS.Hydromet
USACE.AHPS
ECCC.CaPA
Historical.Coordinated
CaPA.Proto
P (mm)
L2SWBM
GLERL.AHPS.Hydromet
USACE.AHPS
GEM.Proto
E (mm)
L2SWBM
GLM.HMD.Hydromet
USACE.AHPS
GEM.Proto
R (mm)
L2SWBM
Coordinated
IGS
Uncertainty from Bruxer 2010
Q (m³/s)
ΔH (mm)
2010
2011
2012
2013
2014
2015
2016
2017
2018
2019